Review Article

Amende Sivanathan, Xi Guo, Ziyan Fu, and Mizi Fan*

Advances in phase change building materials: An overview

Abstract: Efficient and sustainable thermal management of buildings is critical since the building sector is considered as the largest energy contributor contributing around 40% of the total energy consumption which is responsible for about 38% of greenhouse gas emission. Utilisation of phase-change material (PCM) in building energy systems can enhance the overall energy performance of buildings, thereby making drastic reduction in greenhouse gas emissions. The major shortcoming of organic PCM is their leakage problem; however, this can be overcome through the employment of either encapsulation or shape stabilisation technology. Numerous papers have prepared unlimited number of form stable PCMs for various applications ranging from textiles to thermal energy storage (TES); however, the factors to consider when selecting PCM for an intended application are not clear and the influence of synthesis techniques and processing parameters on the performance of stabilised PCM is yet to be understood. Also, majority of the publications have focused mainly on the encapsulation of paraffins for TES by employing different encapsulation techniques. Therefore, selecting a suitable technique for the synthesis of form stable PCM is the most challenging. This review aims at providing a comprehensive database addressing these issues, focusing mainly on PCMs, processing techniques, performance of encapsulated and composite PCMs, and phase change building materials prepared in previous studies, since this is the most critical information required to widen the potential usage of PCM technology in building applications. A concise summary of environmentally friendly poly(ethylene glycol)-based composite PCMs is also included.

Abbreviations

BDO	1,4-butanediol
CNT	carbon nanotube
CHS	chemical heat storage
EG	expanded graphite
EP	expanded perlite
LA	lauric acid
LHS	latent heat storage
LHTES	latent heat thermal energy storage
MPCM	microencapsulated phase-change material
MA	myristic acid
MF	melamine formaldehyde
PA	palmitic acid
PCBM	phase change building material
PCM	phase-change material
PCMW	phase-change material wallboard
PEG	poly(ethylene glycol)
PGMA	poly(glycidyl methacrylate)
PGI	poly(glycerol-itaconic acid)
PMMA	poly(methyl methacrylate)
POM	polarised optical microscopy
PSt	polystyrene
PUU	poly(urea-urethane)
PVA	polyvinyl alcohol
PVC	polyvinyl chloride
SA	stearic acid
SHS	sensible heat storage
TDI	2,4-toluene diisocyanate
TES	thermal energy storage
UF	urea-formaldehyde

* **Corresponding author: Mizi Fan**, College of Transportation and Civil Engineering, Fujian Agriculture and Forestry University, Fuzhou, China; College of Engineering, Design and Physical Sciences, Brunel University London, London, United Kingdom, e-mail: mizi.fan@brunel.ac.uk
Amende Sivanathan, Ziyan Fu: College of Engineering, Design and Physical Sciences, Brunel University London, London, United Kingdom
Xi Guo: College of Engineering, Zhejiang Agricultural and Forestry University, Hangzhou, China

1 Introduction

The building sector is reported as the highest energy consumer worldwide due to the rapidly and continuously

growing population accompanied with rapid urbanisation [1,2]. The international energy agency reports that buildings contribute to 40% of total global energy consumption wherein the building envelope was responsible for 36% of the total energy consumed which was accountable for 39% of greenhouse gas emissions in 2018 [3,4]. Therefore, several studies and research projects have worked towards enhancing the thermal performance of buildings and/or building envelope by utilising the highly efficient, affordable, and high impact phase-change material (PCM) technology to make significant energy-saving and decarbonisation in the built environment [5]. Moreover, the application of PCMs is widely found in other fields such as thermal energy storage (TES), battery thermal management, electric and power peak regulation, and textiles for the fabrication of smart thermal fibres/clothing [6–8]. However, the building envelope is mainly comprised of building materials including bricks, cement, and concrete, which are sensible heat storage (SHS) materials. Utilisation of latent heat storage (LHS) materials *via* the application of advanced LHS materials like PCMs or incorporating stable PCMs in buildings is more effective, thus in the recent years, PCMs have become the hot topic among scientists and researchers.

PCMs can be embedded in bricks, wallboards, gypsum boards, and concrete slabs, to enhance the thermal mass of the building materials or components [9,10]. Integrating TES technologies in building energy systems or building envelopes is advantageous. It can overcome existing seasonal mismatch issues, increase the flexibility of energy usage, drastically reduce energy demand, and effectively utilise renewable energy like solar energy [11], and substantially enhance the overall performance and reliability of the energy systems, since no difference exists between the supply and demand, and heating and cooling loads will be reduced [12]. In addition, it reduces total premium fuel consumed and reduces the investment and running costs, overall it improves the cost effectiveness of the system [13]. The baseline concept of TES is that energy in the form of heat or cold can be stored in the designated storage medium for a particular duration and can be retrieved from the same location when required. Thermal performance of all TES methods is influenced strongly by the characteristics of the storage material. Hence, a material with high latent heat capacity along with good heat transfer characteristic (*e.g.* high thermal conductivity) will be desirable, since it will enhance the overall performance of the system [14]. Thermal energy can be stored by different methods, namely physical and chemical methods which are both differentiated based on their TES mechanisms; physical methods are commonly used in TES applications, and it involves using direct ways to store thermal energy, while the chemical methods use

chemical processes only in which advantages of endothermic and exothermic reactions take place indirectly [15]. TES is mainly classified by three different mechanisms: (1) SHS, (2) LHS, and (3) thermochemical heat storage [8]. Expected desirable characteristic of TES materials includes high energy storage density, thermal reliability, mechanical strength, chemical stability, and good chemical resistance [7].

This review first comprehensively summarises the different categories of PCMs available in market and the merits, which the PCMs are expected to exhibit for building applications since this will help choose the correct PCM for the intended building application. Second, the different approaches employed including encapsulation and shape stabilisation techniques to resolve the leakage problem of solid–liquid PCMs are discussed in detail and the properties of different PCMs and composite PCMs are investigated and summarised, mainly to help propose formulations that produce composite PCMs of optimum thermal performance. Third, the building application of PCMs are discussed and the properties of different phase changing building materials (PCBMs) prepared and investigated in previous literature are reported. Future recommendations are made to optimise the potential use of PCMs in buildings to enhance its thermal performance and thereby, work towards achieving carbon zero buildings.

2 PCBM through physical TES

The storage capacity of physical heat transfer processes, namely SHS and LHS depends mainly upon thermophysical properties including the thermal conductivity and specific heat capacity [16]. Previous literature states that LHS materials (*e.g.* PCMs) are more advantageous than SHS materials because they can store more energy in the form of both latent and sensible heat while the latter has relatively lower storage capacity; therefore, SHS systems require more space to store significant amount of energy [17]. LHS materials (*e.g.* PCMs) have TES capacity 5–14 times more than that of a conventional SHS material; therefore, less space and material will be required to store the same amount of energy [18,19]. Figure 1 shows the storage medium of different TES technologies, and the characteristics of both physical and chemical storage technologies are compared and summarised in Table 1.

2.1 PCBM working through SHS

SHS materials are intrinsically capable of storing or releasing thermal energy through conduction, convection or radiation
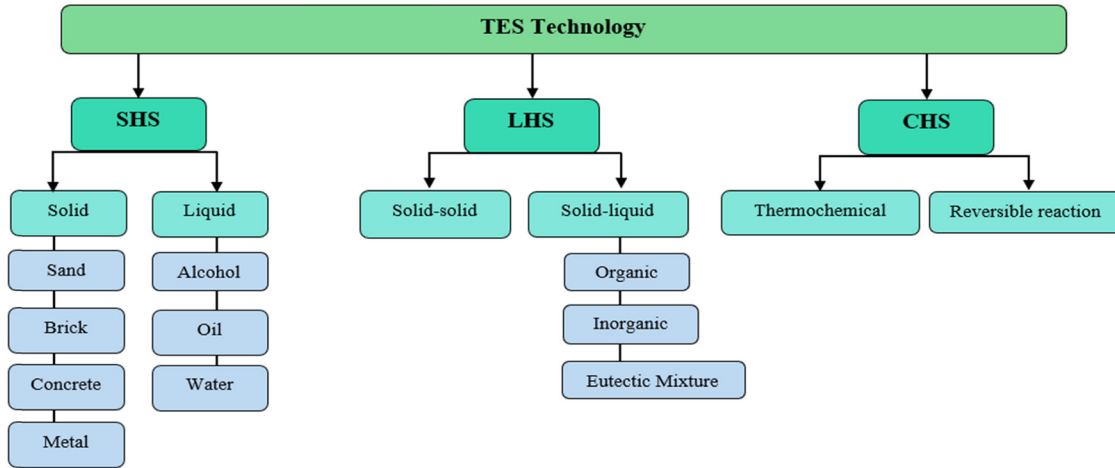
Figure 1: The different classes of TES technologies available.

as a result of being subjected to a temperature change without undergoing any physical phase change. Moreover, the supplied energy results in increasing temperature of the material which is attributed to the change caused to its internal energy which consequently results in energy storage within the material in form of sensible heat [21]. There are two types of SHS materials, namely (1) solid storage materials, and (2) liquid storage materials. Examples of solid SHS materials include metals and non-metals (*e.g.* concrete, rock, gravel, brick, marble, granite and sandstone rocks, stones, dry and wet earth/soil, iron, wood plasterboard and corkboard); and liquid SHS materials include water, oil, molten salt pure and derivatives of alcohols [20]. For operation that requires elevated temperatures above 100°C, molten salts, oils and liquid metals are commonly used for storing purposes, whereas for other purposes like heating the air, rock bed-type materials are preferable [22] because molten salts have desirable thermophysical properties; therefore, can be adopted in various elevated temperature TES applications, provided that special measures are taken to prevent corrosion, which could significantly increase the overall cost of the storage system. Energy systems that utilise liquids as heat storage and transfer material are preferred for wide range of applications from low-temperature to medium-temperature thermal storage. Water is the most common liquid used as storage material because it has high specific heat capacity and is abundantly

Table 1: Comparison of different TES technologies available

	SHS	LHS	Chemical heat storage (CHS)	Ref.
Storage medium	Solid: gravel, metal, soil, ceramic	Solid–liquid PCMs Solid–solid PCMs	Metal chlorides Metal hydrides	[12,20]
	Liquid: water, alcohol and their derivatives, oil	Solid–gas PCMs Liquid–gas PCMs	Metal oxides	
Type	Water-based system *e.g.* water tank and aquifer	Active storage	Thermochemical-/thermal-sorption *e.g.* ad- and absorption	[14]
	Rock or ground-based system	Passive storage	Reversible chemical reaction (high-temperature storage)	
Advantages	Environmentally friendly and cheap materials used	Higher energy density than SHS	Highest energy density than both SHS and LHS, thus system is compact	[12,14]
	Simple TES technology controlled easily Reliable	Thermal energy provided at constant temperature	Negligible heat loss	
Disadvantages	Low energy density, large volume required	Lack of thermal stability	Poor heat and mass transfer property under high density condition	[12,20]
	Self-discharge and heat loss issues	Crystallisation	Unsure cyclability	
	High cost in site construction	Corrosion High cost of storage material	High cost of storage material	

available at relatively low cost. Solid media including rock, metals, concrete, sand and brick are commonly used for both low and high temperature storage purposes because they have very high operating temperatures (*e.g.* over 100°C) along with excellent thermal conductivity [15]; however, their high cost tends to limit their potential use [13]. The TES performance of conventional building materials which are all SHS materials is presented in Table 2. SHS technology is reported as one of the oldest and well-developed concepts conventionally used for long-term and seasonal energy storage purposes to conserve primary energy consumption since it is comprised of numerous low-cost materials. Additionally, it is a simple and easy technology with high reliability; therefore, it has been implemented in numerous projects in the past [13,14]. Major drawbacks of using solid SHS materials is their inherently low specific heat capacity, which is on average around 1,200 kJ/(m^3 K), relatively low energy density, and loss of thermal energy at any temperature [23].

The partial factors that determine the quantity of energy stored by the SHS materials are the quantity of material used, temperature variation, and specific heat; and thus, may be represented by equation (1) [24,22,25] which indicates that the change in temperature has a linear relationship with thermal energy stored or released by the SHS material while the amount of thermal energy stored in SHS system depends mainly upon the specific heat capacity of the material/medium.

$$Q = \int_{T_i}^{T_f} mC_p dT = mC_p(T_f - T_i), \tag{1}$$

where Q is the quantity of SHS of a material (J), m is the mass of storage material (kg), C_p is the specific heat capacity of storage material at constant pressure (J/kg K), T_f is the final temperature (K), and T_i is the initial temperature (K).

2.2 PCBM working through LHS

LHS systems utilise PCMs, which are a class of "functional" materials capable of storing and releasing thermal energy by virtue of the phase transition phenomenon at their operating temperatures under isothermal conditions. PCMs are the most used energy storage material in LHS systems and play a vital role in efficient LHS applications, since their incorporation in TES systems enables adequate control over the operating parameters of the system through the utilisation of the exothermic and endothermic phase transitions, and they are classified based on their physical transformation of absorbing/storing or releasing thermal energy capabilities as a result of undergoing phase transformation from one state to another at their operating temperatures as either solid–solid, solid–liquid, solid–gas, or liquid–gas PCMs [8,28]. Hence, in latent heat thermal energy storage (LHTES) systems, thermal energy accumulated at molecular level within the material ensures that relevant phase transformation processes occur. In solid–solid PCMs, thermal energy is stored as the material gets transformed from one crystalline form to another, *e.g.* semi-crystalline or amorphous [29], and therefore, requires no encapsulation since no liquid gets generated during the phase transition process; however, they exhibit very small latent heat capacity which is attributed to the very small volume changes that occur during their phase transition process [30]. Solid–gas and liquid–gas PCMs present higher latent heat but they experience very high-volume changes during phase change, and therefore, require more stringent containers which makes them impractical and unsuitable for most applications [31]. Although solid–liquid PCMs exhibit smaller latent heat during phase change compared to that of solid–gas or liquid–gas, they are practical and thus, are conventionally utilised in most applications. Also, in the last 20 years, numerous studies

Table 2: Thermal performance of conventionally used SHS building materials [26,27]

Material name	Temperature range (°C)	Density (kg/m^3)	Thermal conductivity (W/m K)	Energy storage capacity (J/kg K)
Sand	20	1,555	0.15–0.25	800
Rock	20	2,560	2.00–7.00	879
Brick	20	1,600	1.04	840
Concrete	20	2,240	1.70	880
Granite	20	2,640	1.70–4.00	820
Aluminium	20	2,707	204	896
Cast iron	20	7,900	29.30	837
Sand-rock minerals	200–300	1,700	1.00	1,300
Reinforced concrete	200–400	2,200	1.50	850
Cast steel	200–700	7,800	40.0	600

have mainly focused on developing and testing solid–liquid PCMs [18].

PCM integration in building envelope components results in producing PCBMs, which are considered as the most promising strategy to improve the energy performance of buildings, which subsequently results in reducing its overall energy consumption and greenhouse gas emissions [32]. Currently, PCMs are utilised in different fields including building air conditioning, electronics cooling, waste heat recovery, textiles, preservation of food and milk, solar energy storage, fabrics, and many more [33,34]. Moreover, it has been a hot topic of research over the last few decades due to their high energy storage density characteristic [18,35].

The storage capacity of a LHTES system may be represented by Eqs. (2) and (3) [22,25].

$$Q = \int_{T_i}^{T_m} mC_p dT + ma_m \Delta h_m + \int_{T_m}^{T_f} mC_p dT, \qquad (2)$$

$$Q = m[C_{sp}(T_m - T_i) + a_m \Delta h_m + C_{lp}(T_f - T_m)], \qquad (3)$$

where Q is the quantity of LHS of a material (J), m is the mass of storage material (kg), C_p is the specific heat capacity (J/kg K), C_{sp} is the specific heat of solid phase (J/kg K), C_{lp} is the specific heat of liquid phase (J/kg K), a_m is the fraction of melted PCM (no unit), Δh_m is the latent heat of fusion (J/kg), T_m is the melting temperature (K), T_f is the final temperature (K), and T_i is the initial temperature (K).

3 PCBM through chemical TES

The principle of chemical energy storage is based on reversible chemical reaction of a compound, and it involves initiating a reversible chemical reaction using an energy source. Chemical energy storages allow wasted thermal energy of industries, power plants, and renewable energy to be stored [36], and are divided into two types, namely (1) chemical reaction storage and (2) thermochemical sorption storage [14]. Major desirable characteristic of CHS includes high energy storage density along with long-term storage duration at ambient temperature [5].

Thermochemical systems rely on the energy supplied to break existing molecular bonds, and the energy released when new bonds are formed during the endothermic and exothermic steps of a completely reversible chemical reaction. A reversible reaction can be defined as a reaction in which both forward and backward reactions occur simultaneously. The major operation of the thermochemical

energy storage system is charging, storing, and discharging (Figure 2), and the general reaction equation may be represented as shown in equation (4).

$$AB + \Delta H \leftrightarrow A + B, \qquad (4)$$
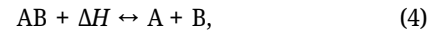
where ΔH is the amount of heat required to dissociate reactants A and B (*e.g.* energy required to break bonds).

In the charging process, energy is absorbed from the surrounding, and therefore, it is classified as an endothermic reaction [37], and the supplied thermal energy is used to decompose the chemical reactants into products (*e.g.* exothermic process). The sensible heat contained in the products of the reaction will be recovered in a heat exchanger. The products formed will be separated and stored in individual containers by sealing the connection during the storing period at ambient temperature until the requirement of the discharging process, which can be defined as the process by which the stored energy gets extracted from the system. The stored heat can only be kept for a long time if the products of reaction are stored separately. Provided the sensible heat effect is negligible compared to the heat of reaction, no heat loss is likely to occur. Before initiating the discharging process, the products are preheated to reach the reaction temperature, after this step, the products are combined *via* an exothermic reaction to retrieve the reactants. Energy will be released during the discharging process. The heat stored depends mainly upon the amount of storage material, the endothermic heat of reaction and the extent of conversion. This method is considered as the most viable and effective technology, especially for long-duration TES and transport [5,36].

The sorption storage process comprises of absorption and adsorption. In the adsorption process, gas molecules combine with the surface of a solid material *via* forming bonds, so no new material gets formed, while in the absorption process a new compound gets produced. There are in total four different thermochemical reactions, including (1) gas-gas reversible reactions, (2) liquid–gas reversible reactions, (3) liquid-liquid reversible reactions, and (4) solid–gas reversible reactions [38]. Thermochemical energy storage has the highest TES density of all TES; however, the reaction efficiency tends to reduce with time. Desirable characteristics of thermochemical energy storage materials include high reaction enthalpy, rapid reaction kinetics, high thermal conductivity, good cyclic stability, abundant availability, and non-toxic with no side reactions [39]. The main drawback that limits the application of this storage type is that the technology is still in an infant stage, and therefore, several questions in terms of its cyclic stability and ease of its integration with concentration solar power remain unanswered [40].
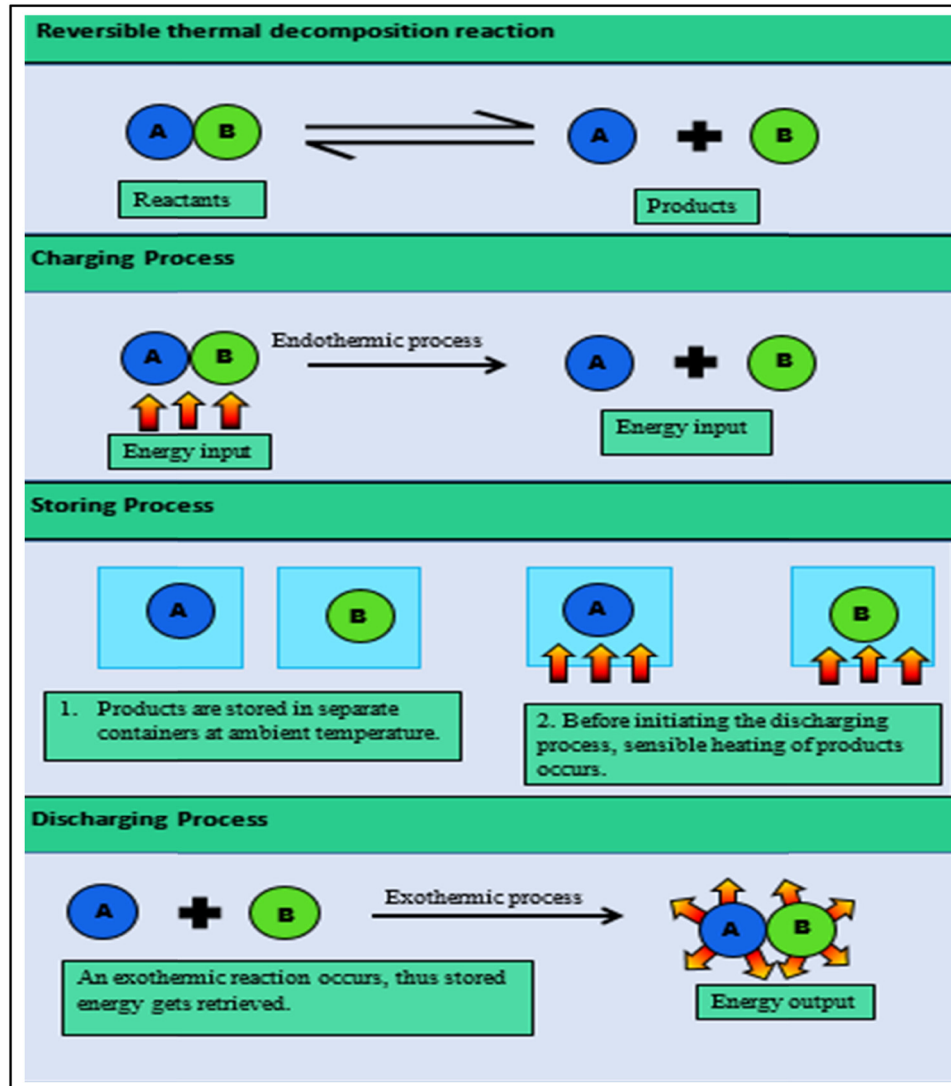
Figure 2: Schematic representation of a thermochemical energy storage system.

4 Materials for latent heat thermal storage PCBMs

4.1 Principal parameters of PCMs for PCBMs

The effectiveness of PCMs in enhancing the thermal performance of buildings depends entirely upon the type of PCM used; therefore, selecting the correct PCM is essential for the utilisation of its benefits in building applications [41]. One of the principal factors to consider when making the right selection of PCMs for building application is its operating temperature. For building envelopes, the defined human comfort level is between 23 and 27°C in summer, and therefore, the melting temperature of PCM should be between 19 and 24°C [42,43]. For sufficient heat transfer,

the temperature difference between air temperature and melting temperature of PCM should be within the range of 3–5°C [44]. However, the free cooling of buildings coupled with PCM storage unit can perform efficiently in climatic conditions even when the daytime temperature is in the range of 12–15°C. Hence, the melting point selection of PCM for the free cooling of buildings should be made according to the climatic conditions. The suitable working temperature ranges of building applications is 18–30°C [45,46]. Overall, selection of PCM to be used for any application in various fields such as construction, refrigerators, air-conditioning, textiles, food preparation, astronautics, and waste heat recovery is determined based on the operating temperature of the intended application [47]. Additionally, the PCM used for building application needs to meet a certain criterion in terms of physical, chemical, thermal,

Table 3: Summary of desirable characteristic PCMs

Property	Criteria
Physical	High density
	No supercooling/sub-cooling behaviours
	Low vapor pressure
	Low volume variations
	No segregation
Chemical	Good chemical stability
	Good compatibility with building materials
	Non-toxic
	Non-corrosive
	Non-explosive
Thermal	Suitable phase transition temperature
	High latent heat capacity
	High thermal conductivity
	High specific heat capacity
Kinetic	Exhibits sufficient crystallisation rate
	Exhibits no supercooling effects.
Economic and environmental	Available abundantly at relatively low cost
	Non-polluting
	Low environmental impact
	Recyclable
	Low embodied energy

kinetic, and economic properties as indicated in Table 3 [22,28,48] to make noticeable improvements in the indoor thermal comfort level of buildings, and thus to reduce indoor temperature fluctuations which results in reducing the energy consumption of buildings. However, it is impossible to find one PCM that possesses all the merits. Supercooling effect is a troublesome aspect of PCMs since it can impact its efficiency undesirably, and it can be defined as a phenomenon by which the PCM does not crystallise at its normal freezing point but at a much lower temperature which means the stored energy will not be discharged fully [49]. If the supercooling temperature is greater than

5–10°C, it will lead to improper energy extraction [50,51]. Overall, the selection procedure of PCM is considered as a highly complex and time-consuming process since an unlimited number of PCMs are available in market, and new PCMs are being developed over time. Since it is known that the thermophysical properties (*e.g.* thermal conductivity) of PCMs is necessary for the evaluation of its suitability, PCM with high thermal conductivity [52] are preferred if they exhibit suitable charging and discharging characteristics along with a suitable phase transition temperature that matches the heating and cooling temperature of the chosen operation. However, this information is not available in literature for most PCMs making the selection process even more challenging [53,54].

4.2 Solid–liquid PCMs

Solid–liquid PCMs, including organic, inorganic, and eutectic mixtures (Figure 3), are materials that undergo changes in their internal molecular arrangement from a highly ordered crystalline arrangement to a disordered amorphous arrangement (*i.e.* irregular arrangement of molecules) as result of being subjected to an elevated temperature, higher than its phase transition temperature. The vibrational energy increases with temperature which eventually causes breakage of the supramolecular bonds existing between the individual atoms, leading to a random arrangement of atoms in the liquid state. As temperature falls below the phase transition temperature, the nucleation process initiates (*e.g.* crystallisation process), whereby atoms rearrange to form a crystalline lattice. Phase changes in solid–liquid PCMs are accompanied by volume changes (*e.g.* volume increases) because PCM converts from solid to liquid [55]. Compared to solid–solid PCMs, they have higher LHS capacities. Vast number of solid–liquid PCMs have been prepared and characterised in the past for the development of highly effective storage systems at low costs; however, this has not been possible yet since solid–liquid PCMs
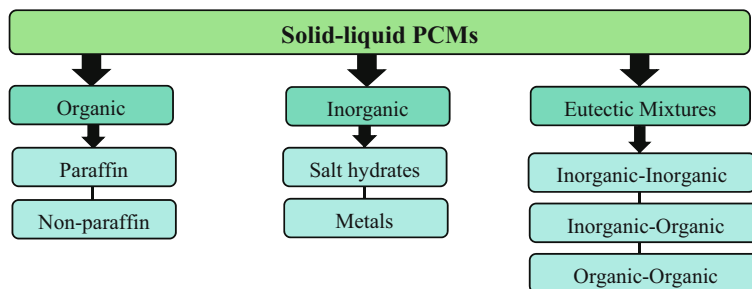

Figure 3: Types of solid–liquid PCMs available.

have poor shape-stability, which leads to leakage issues along with other operational problems including supercooling effect and corrosion [56]. Therefore, current research has mainly focused on overcoming these shortcomings of solid–liquid PCMs by employing either the encapsulation or shape stabilisation technology. The advantages and disadvantages of the different solid–liquid PCMs are outlined in Table 4.

4.2.1 Organic PCMs

There are two types of organic PCMs: (1) paraffins which are comprised of saturated linear and branched hydrocarbon chains, and (2) non-paraffins (*e.g.* fatty acids and fatty acid esters, unmodified/modified polymers, and polyalcohol).

4.2.1.1 Paraffin-based PCMs

Organic paraffins or paraffin waxes are derivatives of fossils and are usually found in natural gas, petroleum, or can be produced synthetically from coal. They are comprised of straight n-alkanes, CH_3–(CH_2)–CH_3 chain, and other hydrocarbon (CH) molecules. Their chemical composition can be determined using the general formula C_nH_{2n+1}, where n represents the number of carbon atoms in the compound, whereby alkane mixtures preferred for most applications exist as wax-like solids at room temperature which fall in the range of $20 \leq n \leq 40$. Most paraffins show a volume change by ~10–15% while having good thermal reliability which is attributed to their low specific gravity [59]. Paraffins are soft waxes, therefore will not generate large expansion forces. The latent heat of paraffins depends upon the crystallisation of the alkyl chain in the saturated hydrocarbon chain (*e.g.* the synthesis process of the methyl CH_3-chain) since this process is responsible for releasing energy in the form of latent heat. Hence, the crystallisation of CH_3 chain releases a significant amount of latent heat. The melting temperature of paraffins and paraffin waxes are a function of the number of carbon atoms in the chain according to Figure 4 [24,60]. Paraffins are hydrophobic, and therefore, will not dissolve in water or chemical solvents; thus, this makes them ideal candidates as PCMs in the encapsulation process [61,62]. Exposing them to elevated temperatures causes evaporation of short chain hydrocarbon molecules as result of paraffin bond breakage. Paraffins and waxes with melting temperature in the range of −12 to 71°C, corresponding to a latent heat of storage in the range of 128–198 kJ/kg [63], have been studied for commercialisation purposes in several studies. Paraffins show no phase segregation even after being subjected to numerous phase transition cycles; however, paraffin blends/waxes have commonly been used over pure paraffins due to their lower costs, and because their phase transition temperatures can be tailored easily for the intended application by mixing alkanes of different chain lengths [64]. Table 5 summarises the thermal properties of the selected paraffins and their waxes [65].

4.2.1.2 Non-paraffin based PCMs

Non-paraffin PCMs, namely fatty acids and fatty acid esters, are the abundantly available PCMs existing with highly varied properties, unlike the different paraffins and their waxes which exhibit very similar properties. They are usually characterised by the general formula $CH_3(CH_2)_{2n}COOH$, where n represents the number of carbon atoms in the compound [66]. Their melting temperature is in the same range as the paraffins and their waxes. Furthermore, non-paraffins can maintain a long-term thermal stability when exposed to elevated temperatures above their phase transition temperature. Compared to paraffins, they have lower vapor pressure; therefore, they are thermally more stable and less volatile. Moreover, they are environmentally friendly and non-flammable [67], and therefore, are more desirable in building applications.

Behzadi and Farid [67] investigated the potential changes that occurred in the thermal characteristics of organic PCMs such as RT21 and esters with time when exposed to elevated temperatures above their melting points. Results indicated that paraffin-based PCMs had experienced irreversible physical changes which caused changes in their intrinsic thermal characteristics. Hence, paraffin waxes have higher vapor pressure than esters, and therefore, they were observed to be more prone to weight loss and change in physical properties caused by the evaporation of their light compounds. Ester mixtures were observed to exhibit good stability since no changes in its mass occurred, and it remained thermally stable throughout the heating period. Fatty acids like stearic acid (SA), palmitic acid (PA), myristic acid (MA), and lauric acid (LA) are considered as the most promising PCMs for LHS applications since they have high latent heat capacity, along with other desirable characteristics such as they experience little or no supercooling effect [68] and they exhibit self-nucleating behaviour. Alkan and Sari [69] prepared fatty acids/poly (methyl methacrylate) (PMMA) blends using PMMA, a commercially available acrylic resin and different fatty acids, namely SA, PA, MA, and LA, through the simple solution casting approach, for LHTES applications. Results confirmed the presence of strong interaction between the fatty acid and the supporting material. PA is one of the most investigated fatty acids as PCM since it consists of a suitable phase change

Table 4: Summary of typical advantages and disadvantages of organic, inorganic, and eutectic mixtures PCMs

| PCM type	Advantages	Disadvantages	Ref.
Organic	High range of melting temperatures	Low thermal conductivity *i.e.* typically around 0.2 W /m K for paraffins	[22,48,57,58]
	No phase segregation during crystallisation process	Large volume change (especially paraffins)	
	High latent heat of energy storage	Expensive *i.e.* non-paraffins are around three times more expensive than paraffins	
	Good thermal performance even after subjection to prolonged thermal cycling *i.e.* good thermal behaviour	High flammability	
	Excellent freezing and melting properties		
	Good thermal stability		
	Smaller volume change		
	Adjustable transition zone		
	High compatibility with construction materials		
	Good nucleation rate		
	Can be incorporated directly		
	Recyclable		
	Can be impregnated into materials	Self-nucleation	
	Good chemical stability and inert, *i.e.* unreactive	Congruent melting	
	High TES		
Inorganic	High TES density	Prone to corrosion *i.e.* corrosive to most metals	[22,48,58]
	Small volume change		
	High thermal conductivity	Some degree of toxicity	
	Less expensive compared to organic PCMs	Requires container and support	
	High latent heat of fusion	Decomposition	
	Recyclable	Moderately compatible with construction materials *i.e.* not compatible with all building materials	
	Non-flammable	Supercooling	
		Incongruent melting and dehydration during thermal cycling	
	High phase change enthalpy and sharp phase change	Phase segregation	
		Poor nucleating properties – nucleating and thickening agents are required to their applications	
		Low thermal performance after subjection to prolonged thermal cycling, *i.e.* poor thermal behaviour	
		Low temperature range	
Eutectic mixtures	Sharp melting points	No phase segregation	[22,48,58]
		Some of them suffer from supercooling	
		Limited data are available in literature on their thermophysical properties	
	High volumetric storage density	No congruent phase change	
		Low total latent heat capacity	
		High cost	
		Strong odours	
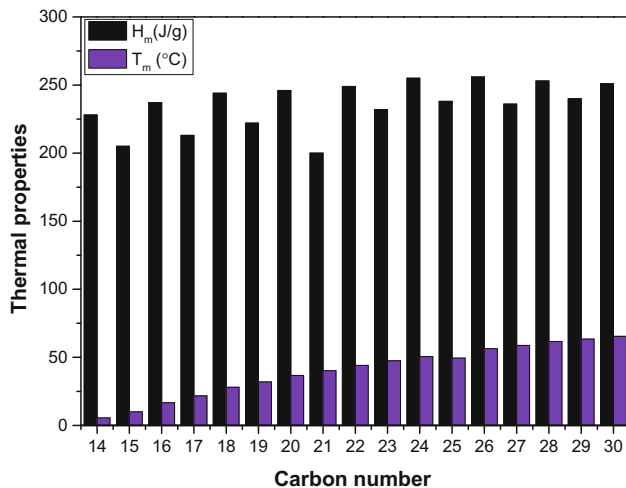
Figure 4: The relationship between the number of carbon atoms in the chain and thermal properties of paraffins.

Table 5: Phase transition temperature and the corresponding latent heat capacity of paraffin and their waxes

PCM name	Phase transition temperature (°C)	Latent heat (J/g)
Hexadecane	18–20	224
Cetane	18	231
Heptadecane	23	182
n-Eicosane	37	250
Paraffin ZDJN-28	26–28	231
Paraffin	44–46	259
Paraffin wax P56–58	42–72	250
Paraffin wax	18	237
Paraffin wax	44	190
Paraffin RT21	25	133

temperature range for solar passive application (*e.g.* 58–64°C), along with a high latent capacity usually in the range of 190–220 J/g [70]. Also, it experiences little or no supercooling effect and has no corrosion effect on metal construction materials, but its inherently low thermal conductivity tends to limit its potential application. Previous literature has solved this problem in several ways through the utilisation of heat-transfer promoters: (1) using finned configurations, (2) disperse particles of high thermal conductivity, and (3) dispersing metal matrix into the PCM. Although thermal conductivity of PCM gets enhanced, it has a negative impact on the overall weight and volume of the LHTES system. Moreover, both weight and volume of the LHTES system gets increased. Sari and Karaipekli [70] prepared PA/expanded graphite (EG) PCM composite containing 80 wt% of PA and 30 wt% of EG. Results indicated that PA and EG had good chemical compatibility, and that the resulting composites had enhanced thermal

conductivity of 0.60 W/m K, which was 2.5 times more than that of pure PA. Fang *et al.* [68] prepared PA/silicon dioxide (SiO$_2$) composites containing melamine which is a well-known non-corrosive flame retardant *via* the sol–gel method. Resulting composites were reported to have enhanced thermal stability and good fire-retardant property. Non-paraffin PCMs possess major drawbacks such as material availability for large-scale production and their high costs because they cost approximately 2–2.5 times more than conventional paraffin waxes [71] and 3 times more than paraffin PCMs [66]. Also, it is impossible to match their phase transition temperature completely with the temperature of the practical application field which limits their utilisation in building applications [72].

4.2.1.3 Poly(ethylene glycols) (PEGs) and their derivatives as PCMs

PEGs, also known as poly(oxyethylene), are a class of polymeric organic solid–liquid PCMs made up of linear dimethyl ether chains with hydroxyl (OH) ending groups. The general formula of PEGs is H–(O–CH$_2$–CH$_2$)$_n$–OH where *n* represents the number of carbon atoms in the chain. They are polar substances due to the presence of two terminal OH groups [73] in their chain and are comprised of a highly defined macromolecule [74] with good characteristics, such as non-toxicity, good biodegradability, and hydrophilicity. The width to height ratio (*e.g.* aspect ratio) of PEG particles are dictated by the molecular weight of PEG [75]. Moreover, this environmentally friendly polymer has proven to be suitable in several fields including cosmetics, food, pharmaceutical, and biomedical. Currently, they are reported as the most versatile environmentally friendly polymeric PCM due to its high phase change enthalpy, controllable and suitable phase change temperature *i.e.* phase change temperature is in the range of −55 to 100°C [76], and broad range of molecular weight, along with desirable characteristics including high latent heat capacity usually in the range of 150–180 J/g [77], congruent melting, non-toxicity, no super-cooling behaviour, low vapour pressure in melted state, high resistance to corrosion, chemically inert, small volume changes during phase change, high thermal and chemical stability even after long-term utility duration, and competitive pricing [78]. Also, they require no encapsulation but can be stabilised through both physical and chemical shape stabilisation approaches material [79]. Owing to their excellent desirable characteristics, they have been investigated in various TES applications, which range from building envelopes to fabrics, foams, and fibres. Melting temperatures of PEGs vary according to its molecular weight (Figure 5) [59], which
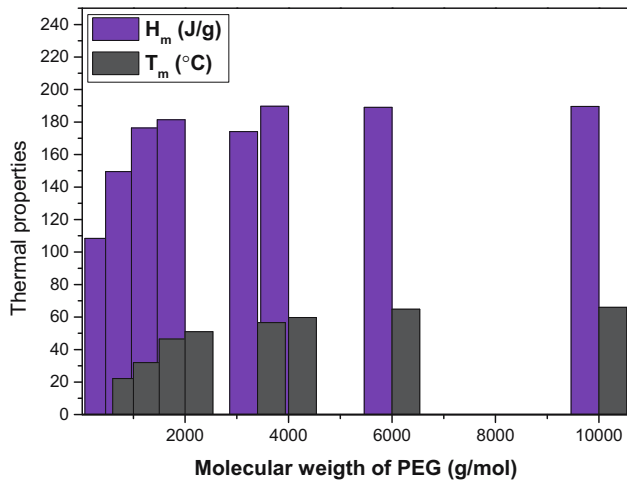
Figure 5: The relationship between the molecular weight of PEG and its thermal properties.

Figure 6: The latent heat and supercooling temperature of the selected salt hydrate PCMs.

enables their utilisation in various applications including industrial heat utilisation and electronic device management and protection. In addition, they can also be used in active and passive heating or cooling systems of buildings [80,81]. Adjusting the melting temperature and heat absorption capacity should be done by mixing PEGs with different molecular weights to enhance its feasibility.

4.2.2 Inorganic PCMs

Inorganic PCMs include salt hydrates, alloy of inorganic anhydrous salts with water, and metals and alloys, *e.g.* copper (Cu), zinc (Zn), aluminium (Al), magnesium (Mg), silicon (Si), and tin (Sn). They consist of several remarkable characteristics compared to organic PCMs, such as high latent heat capacity, high thermal conductivity, non-toxicity, non-flammability, and relatively low costs. Therefore, the is a high potential in several applications including building, concentrated solar plants (CSPs), and thermal management of lithium-ion battery.

4.2.2.1 Salt hydrate PCMs

Salt hydrates are ionic compounds usually composed of an alloy of inorganic anhydrous salts and few water molecules. They are characterised by the general formula $M \cdot n H_2O$, where n represents the number of water molecules present in the compound. Common salt hydrates investigated in literature include fluoride, chloride, and carbonate salts because they have good potential as high temperature PCMs. During the phase transition process, they experience phase transformations involving hydration and dehydration
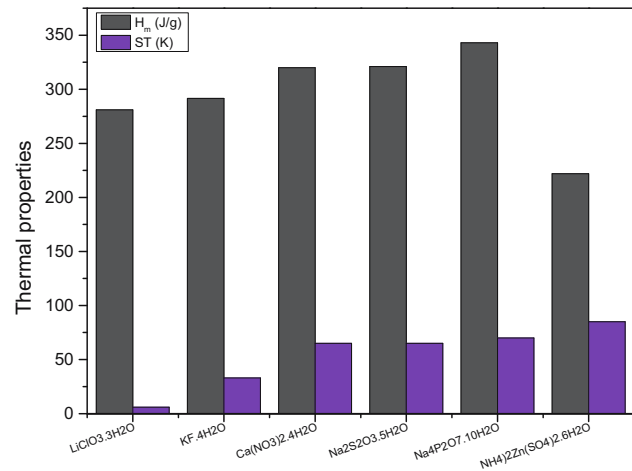
processes resembling the typical melting and crystallisation processes of other solid–liquid PCMs. Benefits of salt hydrates include high energy storage density (~350 MJ/m^3) and they are cheaper than paraffins, paraffin waxes [54,82], and metal PCMs; however, their major drawbacks such as incongruent melting and supercooling (Figure 6) tends to reduce its effectiveness as PCM. Thus, its disadvantages are reported to overshadow their advantages which makes them unsuitable for building applications [83]. Most of the salt hydrates available are observed to undergo changes in the stoichiometric composition during the heating and cooling processes [84]. Previous studies have reported that microencapsulating salt hydrate is difficult; however, Huang *et al.* (2013) [85] demonstrated the successful microencapsulation of disodium hydrogen phosphate heptahydrate ($Na_2HPO_4 \cdot 7H_2O$) by employing the suspension copolymerisation-solvent volatile method using modified PMMA as shell material. They concluded that microcapsules of smooth and compact surface with average diameter ranging from 650 to 740 μm was obtained. Table 6 [86] presents the thermal properties of salt hydrate PCMs with operating temperatures matching building applications.

Table 6: Thermal properties of salt hydrate PCMs suitable for building applications

Salt hydrate PCM	Melting temperature (°C)	Latent heat (J/g)
$KF \cdot 4H_2O$	19	231–330
$K_2HPO_4 \cdot 4H_2O$	19	231
$FeBr_3 \cdot 6H_2O$	21	105
$Mn(NO_3)_2 \cdot 6H_2O$	26	126–148
$CaCl_2 \cdot 6H_2O$	29	170–192
$Na_2CO_3 \cdot 10H_2O$	32–34	267
$LiBr \cdot 2H_2O$	30	296

4.2.2.2 Metal-based PCMs

Metals and alloys with low melting points have the potential to be used as LHS materials due to the several desirable characteristics they exhibit including high thermal conductivity, good electrical conductivity, low vapour pressure, and relatively low heat of fusion per unit weight attributed to their very large density. Compared to salt hydrates, which suffer from inherently low thermal conductivity that is usually resolved using sophisticated exchangers, both metal and alloy PCMs are conventionally investigated and utilised in high temperature applications [87]. Previous studies have used numerous metals, such as Cu, Zn, Al, Mg, Si, and Sn. One major drawback limiting the potential application of both metals and their alloys is the corrosion resulting from the reaction occurring between the molten metal ions and the container. However, this problem can be overcome by employing the encapsulation technology. Therefore, tremendous efforts have been made to prepare metal based PCMs *via* the encapsulation technology. Metals and alloys including Al–Si, Al–Si–Mg, and Al–Si–Cu have been investigated commonly in the past as high temperature PCMs. Maruoka *et al.* (2002) [88] prepared Cu-based PCM coated by a nickel film by the electroplating method for high temperature (*e.g. T* > 1,200 K) application. They reported that forming a film with a two-layer structure using either carbon or ruthenium was beneficial since it could prevent the formation of solution and such reaction between Cu and nickel. Encapsulated metal PCMs usually have poor durability as a result of getting exposed to high temperatures for a long term. Zhang *et al.* [89] prepared durable Cu-based PCMs by encapsulating Cu within a chromium-nickel bimetallic layer through an innovative approach called electroplating for high temperature TES application. Results demonstrated that the Cu capsules experienced no leakage even after being subjected to 1,000 charge–discharge cycles which was attributed to the presence of the chromium layer between nickel and copper. An investigation on copper–magnesium metallic alloys as intermediate/high temperature PCMs was carried out for LHS at CSPs [90]. It was found that the formation of a corrosive layer was governed by the diffusion of both magnesium and nickel from the base metal. They reported that this can be abided by selecting a construction material of proper composition. Blanco-Rodríguez *et al.* [91] also proved through lab scale experimental work the possibility of utilising metal alloy as latent heat energy storage materials. An approach involved using BN-based coating material to avoid corrosion of steel containers was attempted to prepare Al–Si PCMs [92]. Experimental results demonstrated the possibility of industrialising PCM-based high temperature TES. However, they reported that there is a need to study the mechanical behaviour of the coating in more detail. In summary, major drawbacks that limit the potential application of metal and alloys as PCMs include high cost and corrosion which arises due to its compatibility issues with the supporting materials. For building applications, metal-based PCMs are considered being unsuitable because their phase transition temperature does not match the operating temperature range of building applications [93].

4.2.3 Eutectic mixtures

Eutectic mixtures of PCMs are comprised of a combination of two or more chemical compounds of single chemical composition and solidify at a lower melting temperature than any other composition obtained from the same component. Therefore, they tend to melt and freeze congruently to produce a mixture of component crystals during the crystallisation process. A blend of crystals is formed during the freezing process. Eutectic mixtures may be composed of either inorganic with inorganic, organic with inorganic, and organic with organic. Table 7 shows the melting point and latent heat of different combinations of eutectic mixtures synthesised in the past with phase transition temperatures matching the operating temperature of building applications [63]. Due to the existence of large number of

Table 7: Combination of eutectic mixtures suitable for building applications [63]

Eutectic mixture PCM	Melting point (°C)	Latent heat (J/g)
Capric/LA	21.0	143.0
Capric/myristic	21.4	152.0
Capric/palmitate	22.1	153.0
Methyl stearate/cetyl stearate	22.2	180.0
Capric acid/MA	22.6	154.8
Methyl stearate/methyl palmitate	23.9	220.0
$C_{14}H_{28}O_2/C_{10}H_{20}O_2$	24.0	147.7
$C_{14}H_{28}O_2/C_{10}H_{20}O_2$	24.0	147.7
Tetradodecanol/LA	24.5	90.0
Capric acid/SA	24.7	178.6
$CaCl_2/MgCl_2 \cdot 6H_2O$	25.0	95.0
$CaCl_2 \cdot 6H_2O/nuclear/MgCl_2 \cdot 6H_2O$	25.0	127.0
Capric/stearate	26.8	160.0
CH_3CONH_2/NH_2CONH_2	27.0	163.0
Methyl stearate/cetyl palmitate	28.2	189.0
Triethylolethane/urea	29.8	218.0
$Ca(NO_3) \cdot 4H_2O/Mg(NO_3)_3 \cdot 6H_2O$	30.0	136.0
$CH_3COONa \cdot 3H_2O/NH_2CONH_2$	30.0	200.5
$CaCl_2/NaCl/KCl/H_2O$	26–28	188.0

individual salt species, and large number of mixtures, the combination space of eutectic mixtures is enormous. Main advantage is that their melting points can be easily adjusted by combining different weight percentages of components, which means for every temperature range several potential eutectic PCM mixtures can be obtained, which encourages optimal selection for the intended application. For instance, tetradecane with melting temperature in the range of 1.5–5.6°C can be obtained by combining octadecane, docosane, and hexadecane [94]. Moreover, eutectic mixtures have other desirable characteristics such as high thermal conductivity, density, and experiences no segregation and supercooling effect; however, their specific heat capacity is smaller than the ones of salt hydrates and paraffin, which limits their potential applications significantly.

5 PCM stabilisation for PCBM applications

Two main shortcomings that limit the potential application of solid–liquid PCMs are the leakage and inherently low thermal conductivity. However, previous studies have demonstrated the possibility of overcoming the issues by either employing the encapsulation or shape-stabilisation technology.

5.1 Type of encapsulation

The encapsulation was first introduced in the 1940s and 1950s by BK Green to overcome the leakage problem of solid–liquid PCMs [18,95]. Since then, this technology has evolved further and become the most researched and applied techniques in various fields, including chemistry, biology, and medicine which is attributed to their remarkable advantages [55,96]. Overall, value-added end products can be obtained *via* this encapsulation technology, and it can be defined as a process by which a PCM core comprised of one or more compounds in the form of a solid, liquid, or gas particle gets enclosed within an inert protective shell (*e.g.* supporting material) which results in the formation of a core-shell structure mainly to isolate and protect the PCM core from the surrounding [55,97]. The encapsulated PCM particles resulting from the different encapsulation techniques including nanoencapsulation, microencapsulation, and macroencapsulation are classified according to their size as shown in Figure 7, namely as nanocapsules, microcapsules, and macrocapsules [98–101].

Producing micro- and nanocapsules *via* the encapsulation technology is challenging since they involve producing smaller particles whereas the fabrication of macrocapsules tend to be much simpler since they are prepared by filling the chosen container such as pouches, shells, tubes, thin plates, or spheres with the chosen liquid PCM [99]. However, preparing capsules of reduced particle size is highly desirable for building applications (*e.g.* to produce PCBMs), because they have better structural stability and enhanced fracture resistance [102] since previous literature reports that incorporating encapsulated PCMs with poor fracture resistance reduces the compressive strength of concrete and cement mortar. Moreover, they get damaged during the mixing process [103,104]. The size and morphology of particles produced depend entirely upon the encapsulation approach and the design parameters like the type and amount of PCM, shell material, and chemicals used [105–108]. In the encapsulation technology, PCM and shell material selection is flexible and can be made according to
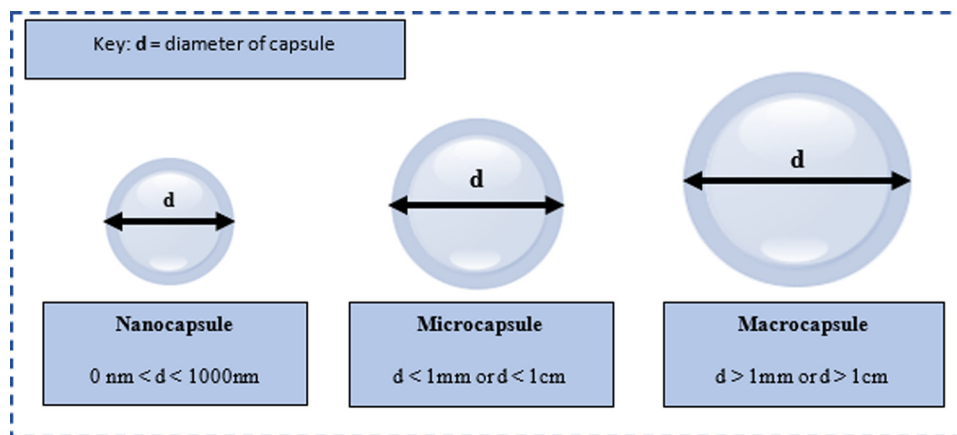
Figure 7: Classification of encapsulated PCM particle according to its size.

the practical requirement; however, it is important to select the correct design parameters like the core-to-shell ratio, PCM content, shell material, and encapsulation technique for the optimisation of encapsulated PCMs performance in building applications [109] but no standard selection procedure is available in the previous literature; and therefore, relevant information regarding the final properties and performance of microencapsulated PCMs (MPCMs) resulting from the different encapsulation approaches should be compiled which will subsequently identify the optimum design parameters for the fabrication of encapsulated PCMs for the preparation of PCBMs of enhanced thermal performance [22,48,58].

The geometry of MPCM produced depends entirely upon the type of encapsulation technique used. Due to the basic characteristic of encapsulation technology, it is possible to produce capsules in any shape such as rectangular, cylindrical, and spherical [99]. However, spherically shaped capsules are preferable in building applications. Capsules can be spherically shaped where its core is coated with a continuous polymeric material, or asymmetrical with inconsistently shaped particles, where a quantity of core material, in smaller droplet form, is embedded throughout the microcapsule. In general, it is possible to microencapsulate matter of all states such as solid, liquid, or gas, making handling of both liquid and gaseous phases easier, in addition to enabling safer handling of hazardous materials [107].

The morphology of MPCMs can be classified into three types: (1) mononucleus capsule in which core material is surrounded by the shell material, (2) polynucleus capsule consists of several cores bounded within the shell material, and (3) matrix encapsulation in which the core material is consistently distributed in the shell material evenly [107] as illustrated in Figure 8. However, in most studies, particles with the mononucleus morphology have been prepared and studied. Overall, the morphology of micro- or nano-encapsulated PCMs needs to be studied in detail to produce homogenous PCBMs since this will affect the structural integrity of the building material.

The key purpose of encapsulating solid–liquid PCMs is to overcome their major leakage problem. Therefore, it is crucial to know the factors that are likely to impact the microencapsulation efficiency of PCMs which can be defined as the ratio of mass of microcapsules with complete shell coating formed to the total number of microcapsules present in the sample, and it is commonly used to measure the yield of employed microencapsulation approach [110].

5.2 Encapsulation methodologies

The different encapsulation methods available and used to resolve the leakage problem of solid–liquid PCMs are presented in Figure 9.
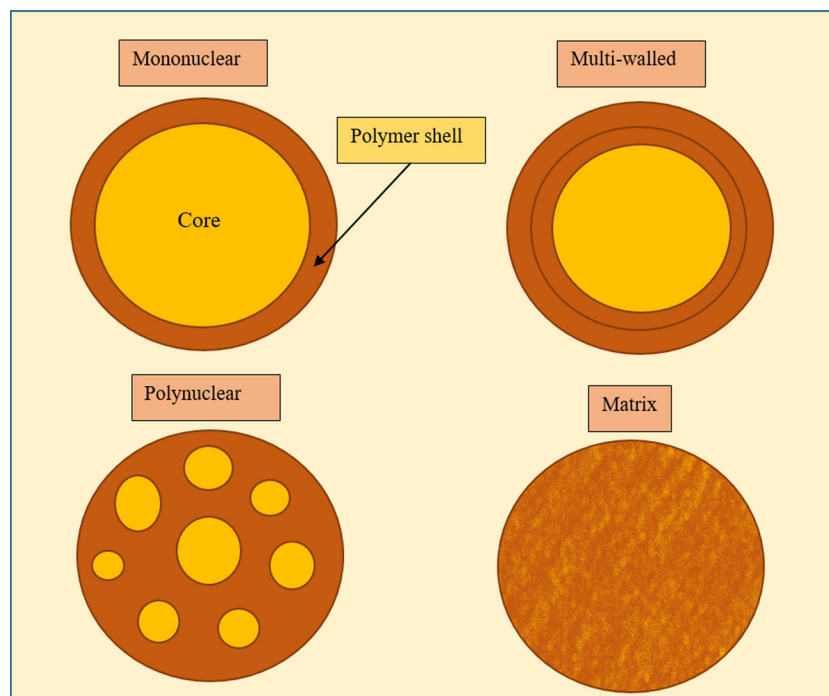

Figure 8: Shows the different morphologies of microcapsules reported in the literature.

5.2.1 Physical encapsulation methods

Here spray drying and solvent evaporation approaches will only be discussed since the remaining physical encapsulation approaches have not been used for the encapsulation of PCMs.

5.2.1.1 Spray drying

Spray-drying, pan-coating, air-suspension, and centrifugal are the physical encapsulation techniques available for the encapsulation of solid–liquid PCM cores. Spray drying was the first and one of the oldest physical methods developed in the 1930s, and since then it has attracted much attention [111], because the technology is simple, convenient, reproducible, and scalable [112–114]. Moreover, it is comparable with the "one stage drying operation" [112] and are comprised of simple steps of high feasibility. First, the chosen PCM gets dispersed in an aqueous coating solution to encourage the production of MPCM of desirable particle size under the spray drying process. Second, the atomisation of the liquid PCM results in producing droplets which are then passed through the drying chamber. Evaporation of water results in producing dried isolated droplets called MPCMs [112,113,115]. Figure 10 illustrates schematically the spray drying process [116].

Hawlader *et al.* [96] encapsulated paraffin wax within gelatine/acacia shell material and observed a reduction in microencapsulation efficiency with the increase in the core/shell ratio and concluded that enough shell material was required to successfully encapsulate the PCM within he chosen polymeric film. Incorporation of cross-linking agent in the range of 6–8 mL enhanced the microencapsulation efficiency significantly. Borreguero *et al.* [117] encapsulated paraffin with/without carbon nanofibres within a low-density polyethylene ethylvinylacetate shell material. Experimental results demonstrated that particles of better size and shape were obtained from the collection vessel; thus, microcapsules collected from the inside of the drying vessel were bound together, which is attributed to the melting of polymer. Fei *et al.* [118] encapsulated *n*-octadecane (C18) (*e.g.* paraffin) within a titania shell material *via* a rapid aerosol process and concluded that microcapsules of two structures, namely dense and hollow, with diameters in the range of 0.1–5.0 microns were produced successfully. Overall, the spray drying method is well-established approach in the food industry; however, the approach does not produce a good yield of encapsulated particles which is attributed to the agglomeration of the particles due to the use of very high temperatures during the process. Moreover, the spray drying equipment is bulky and expensive.

5.2.1.2 Solvent evaporation

In this approach, a coating polymer solution is formed initially by dissolving the chosen coating polymer material in the chosen volatile solvent with continuous stirring which eventually results in producing a coating polymer solution. This coating polymer solution is subjected to continuous agitation until the solvent gets partitioned into the aqueous phase, and as result of solvent evaporation MPCM particles will be produced. This approach is very simple, easy, and cheaper compared to the other physical approaches.

Table 8 summarises the properties of MPCM prepared though the commonly used physical encapsulation methods such as spray drying and solvent evaporation.
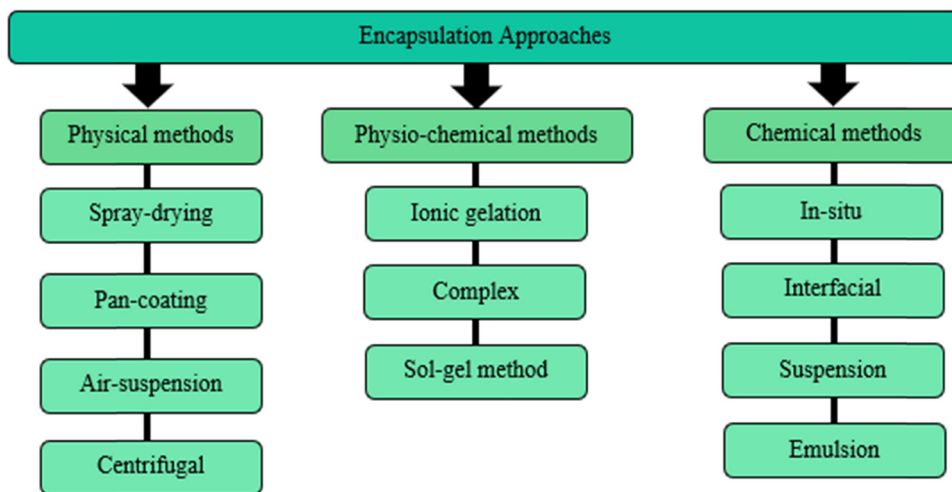

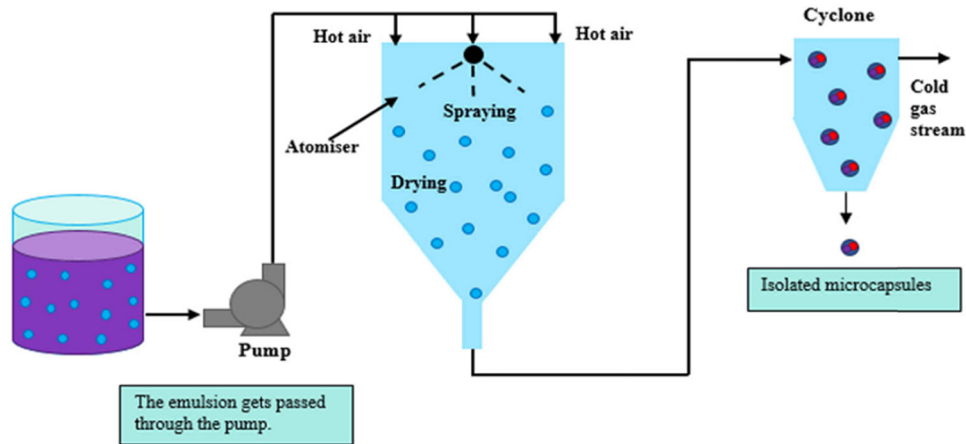**Figure 9:** Shows the different microencapsulation methods available.

Figure 10: Schematic illustration of the spray drying technique [116].

Table 8: Summary of properties of MPCMs prepared *via* the physical encapsulation approaches

Physical encapsulation method	PCM/shell material	Results	Ref.
Spray drying	Paraffin wax/gelatine-acacia	• The encapsulation efficiency was influenced greatly by the crosslinking agent and the core-to-shell material ratio • Using a crosslinking agent content between 6 and 8 mL resulted in optimising the encapsulation efficiency • At a core-to-shell material ratio of 2:1 the latent heat capacity was 216.44 J/g • MPCM had good potential as solar energy storage material	[96]
	Paraffin/polystyrene (PSt)	• The latent heat capacity of the spherically shaped encapsulated PCMs were 107.1 J/g. The thermal conductivity had reduced from 0.34 to 0.22 W/m K after encapsulation • Encapsulated PCMs had a particle size of 100 nm	[119]
	Paraffin RT27/carbon nanofibres	• MPCMs with an optimum PCM content of 48.61 wt% had a latent heat capacity of 96.7 J/g and a melting temperature of 28.46°C • The microencapsulation efficiency was 63% • Incorporating carbon nanofibres resulted in producing agglomerated particles	[117]
Solvent evaporation	Linseed oil/untreated and silane treated ethyl cellulose	• Optimum encapsulation efficiency of 97.6% was obtained with an oil content of 68.7% • At a core-to-shell ratio of 7:3, spherically shaped particles with an average size range of 5–35 µm and shell thickness in the range of 0.5–2.0 µm was produced	[120]
	PA/polylactic acid	• An optimum PCM content of 41.9 wt% resulted in producing particles with a size range of 90–100 µm; and latent heat capacity of 70.1 J/g and a melting temperature of 62.1°C	[83]
	MA/ethyl cellulose	• At an ideal core-to-shell ratio of 2:1, the particle had an optimum encapsulation efficiency of 62% and produced particles with an average size in the range of 3–5 µm • Optimum latent heat capacity of synthesised particles was 122.61 J/g and melting temperature was 53.32°C	[121]
	n-Eicosane/PMMA	• At an optimal core-to-shell ratio of 1:2, the encapsulation efficiency reached 58.2% and resulted in producing spherically shaped particles with size in the range of 5–10 µm • The encapsulated PCMs had a latent heat capacity of 150.8 J/g	[122]
	Capric acid and PA eutectic/ polyvinyl chloride	• An optimal core-to-shell ratio of 2:1 had an encapsulation efficiency of 57% and resulted in producing spherically shaped particles sized 159.3 µm • The latent heat capacity and melting temperature was 92.1 J/g and 17.1°C	[123]

5.2.2 Physio-chemical encapsulation methods

Pan-coating, air-suspension coating, and ionic gelation are all physio-chemical approaches used commonly in the pharmaceutical, food, and cosmetic industries for the encapsulation of the chosen core; and therefore, will not be discussed here since they have not been used for the encapsulation of PCMs. In the pan-coating method small, coated capsules are prepared by mixing the coating material with the solid particles followed by melting of coating material and then cooling to encourage solidification [105].

5.2.2.1 Coacervation

Coacervation technique used for the encapsulation of PCMs can be simple or complex. The formation mechanism of MPCMs is the same with the only exceptions being that both techniques use a different polymer system and approach

for phase separation. The simple coacervation process is comprised of simple steps as illustrated in Figure 11(a). First, the core substance gets dispersed in the shell polymer solution; and for the separation of coacervate from the solution, a desolvation agent gets added during this process. As a result, the core substance gets covered *via* the coacervate droplets and coalescence of coacervate results in the formation of a continuous shell around the core which leads to the formation of encapsulated capsules in the form of particles. The steps of the complex coacervation technique are illustrated in Figure 11(b). In the first step, an emulsion gets prepared by dispersing the core material into the aqueous polymer solution. Then, a second polymer solution gets added followed by the addition of relevant salt or dilution of medium to encourage the deposition of shell materials onto the core particles. Finally, crosslinking agents, desolvation, or thermal treatments are used for the stabilisation of microcapsules produced. Overall, this approach of encapsulation is cheap and
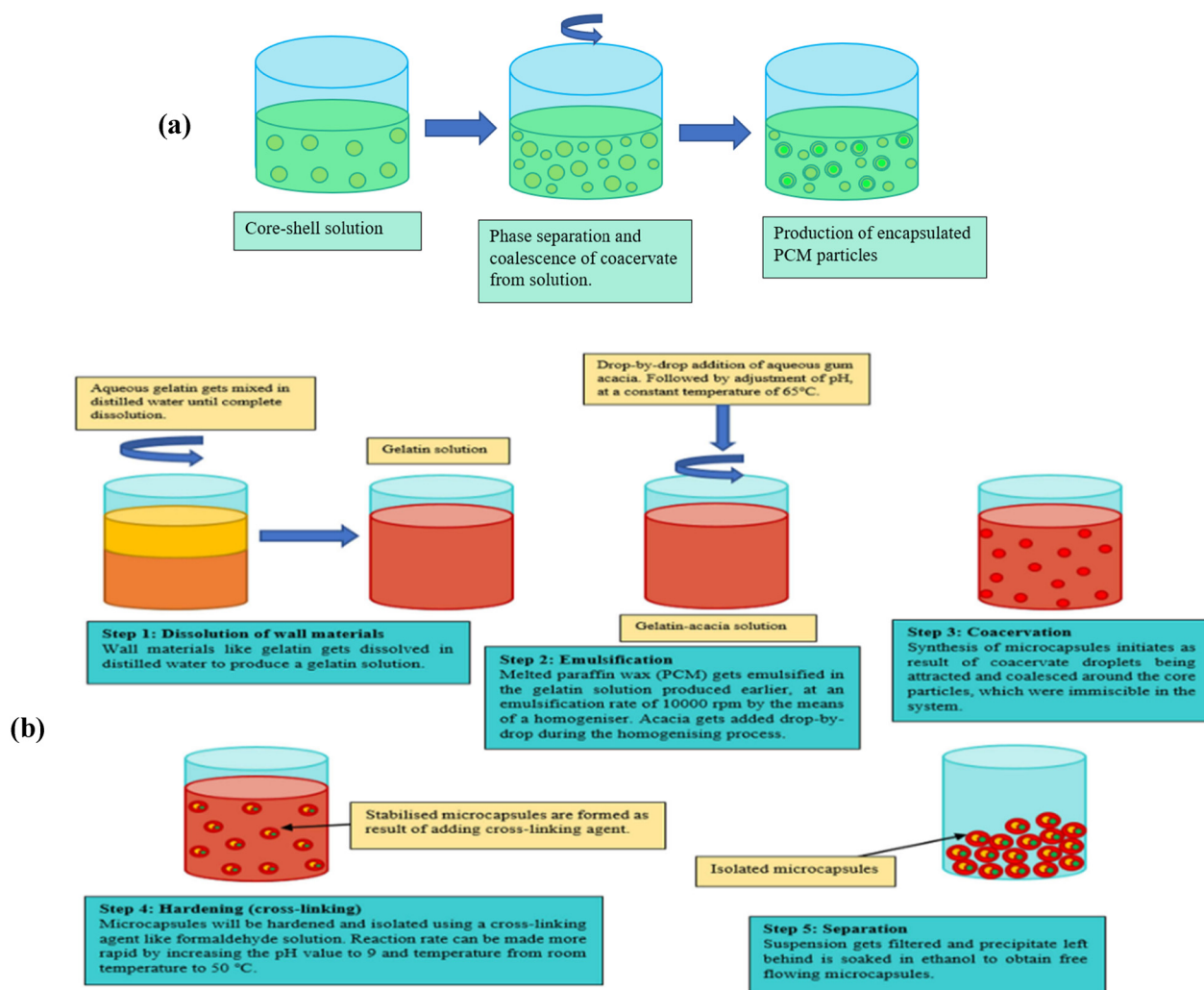

Figure 11: Schematic illustration of (a) simple and (b) complex coacervation techniques [116].

has a good control over the size of encapsulated particles produced, but the major drawbacks include the use of large amount of solvent during synthesis, agglomeration of particles, and difficulty in scaling-up the production [124].

5.2.2.2 Sol–gel method

In the term solution-gelation, sol refers to the stable dispersion of particles in solvent and gel refers to the three-dimensional network of covalent bonds and intermolecular forces comprised of aggregates of sol particles. The steps involved in this approach of encapsulation is illustrated schematically in Figure 12. In the first step, a solution (*e.g.* sol) is formed by mixing the chosen precursor (*e.g.* metal alkoxide) with the chosen solvent, catalyst, and complexing agent, which initiates the chemical hydrolysis and condensation reaction, and this results in producing a stable dispersion of polymers or colloidal particles in the solvent which are added to the PCM-in-water emulsion to form a gel consisting of discrete microcapsules with PCM droplets entrapped inside them. This approach allows the utilising of inorganic shell materials with high thermal conductivity, and they are suitable to produce nano sized PCM particles using silicon dioxide as shell [125].

5.2.3 Chemical encapsulation methods

The properties of the MPCMs prepared *via* different chemical approaches are presented in Table 9.
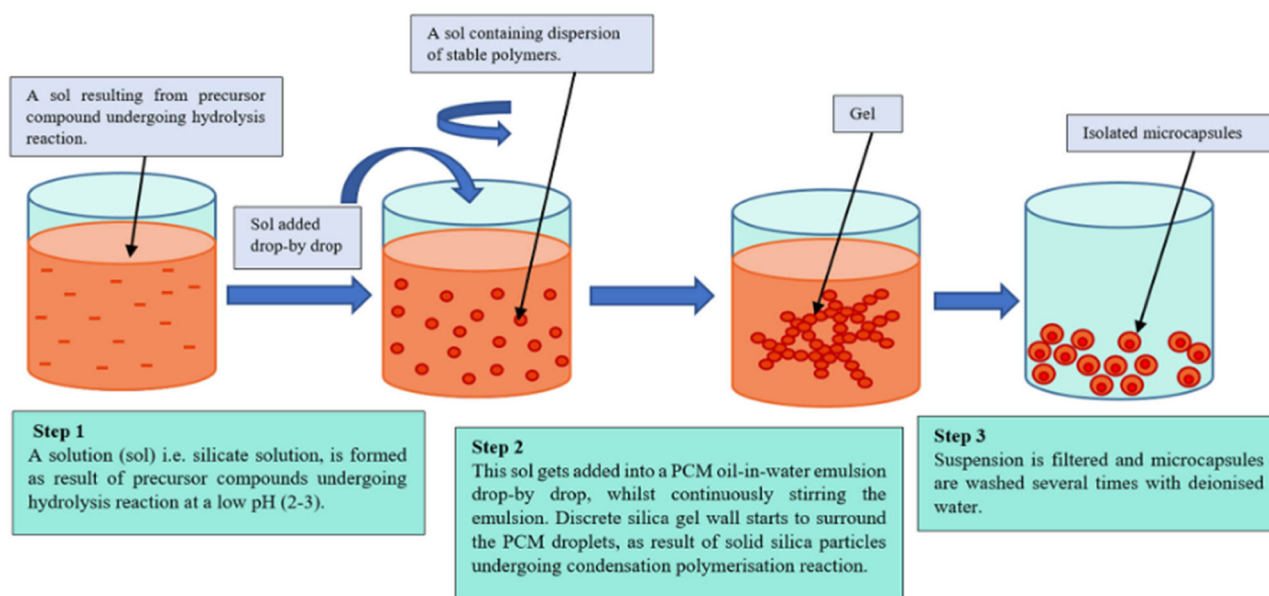
5.2.3.1 *In situ* polymerisation

In this approach, the core material is dispersed in the chosen aqueous phase containing a small amount of emulsifier. Then, the required amount of chosen monomer or pre-polymer gets added followed by the alteration of the pH level of the system to initiate the polycondensation reaction which leads to the formation of a crosslinked resins. As reaction proceeds, the molecular weight of resin increases and eventually gets optimised; and thus, remains insoluble in the aqueous phase which encourages the formation of a precipitate in form of a deposit at the oil–water interface of the droplet. Solidification/hardening of this resin results in the formation of microcapsules.

5.2.3.2 Interfacial/polycondensation polymerisation

In this process, the polymer wall (*e.g.* shell) of the microcapsule is formed at the interface existing between the two chosen phases in the presence of a suitable reaction monomer. Initially, the multifunctional monomer is dissolved in the chosen organic core material to produce a mixture containing emulsifier and protective colloid stabilisers in aqueous phase.

5.2.3.3 Suspension polymerisation

In this approach, the polymer gets dissolved in the organic core phase followed by the formation of the oil–water emulsion. Then, the monomer molecule gets segregated and precipitated from the core material which results in the formation of the solid shell. The encapsulation process

Figure 12: Sol–gel method of encapsulation [116].

Table 9: Properties of encapsulated PCMs prepared *via* the chemical encapsulation approaches

PCM/shell material	Encapsulation method	Properties of encapsulated PCMs	Reference
Styrene (St)/melamine-formaldehyde (MF) resin	*In situ* polymerisation	• Particle size was in the range of 20–71 μm • Core material content was ~60% • Decreasing the shell thickness from 270 to 150 nm resulted in increasing the encapsulated particle size from 39 to 71 μm • Increasing the stirring rate from 7,000 to 13,000 rpm resulted in producing particles with a lower core loading which was attributed to the reduced particle size	[80]
n-Octadecane/MF		• An optimum PCM content of 59 wt% resulted in producing particles with an average size of 2.2 μm with a narrow diameter distribution • The latent heat of PCM reduced from 244 to 144 J/g (*e.g.* 40.98% decrease) after encapsulation • The phase transition temperature of PCM increased insignificantly from 38.9 to 40.6°C • The thermal stability of the encapsulated PCMs decreased with the increase in the dropping rate	[126]
n-Octadecane MF		• PCM encapsulation was not possible when the stirring rate was below 3,000 rpm • Increasing the stirring rate resulted in reducing the size of encapsulated particles produced Hence, at stirring rate of 4,000 rpm, particle size was 9.2 μm, while increasing the stirring rate to 9,000 rpm resulted in producing particles with an average size of 0.9 μm • Optimum PCM content was 70 wt% which resulted in producing encapsulated particle with melting temperature and latent heat capacity of 30.5°C and 170 J/g	[127]
n-Octadecane/MF resin		• An optimum encapsulation efficiency of 92% was achieved at a core-to-shell ratio of 75:25 • The encapsulated PCM particles of average size 20 μm had a melting temperature and latent heat capacity of 26.91°C and 146.5 J/g • Varying the core-to-shell ratio resulted in producing encapsulated PCMs of different latent heat capacities and melting temperatures • The decrease in melting temperature and latent heat capacity of PCM was attributed to the phase change occurring within the encapsulated shell (*e.g.* a confined space)	[128]
n-Octadecane/urea-melamine-formaldehyde *n*-Nonadecane/urea-melamine-formaldehyde *n*-Eicosane/urea-MF		• At stirring rates of 6,000 and 10,000 rpm, encapsulated PCMs have the average particle size in the range of 0.30–6.40 μm and 0.40–1.10 μm • At PCM content of 72, 69, and 71 wt%, the latent heat capacity of encapsulated PCMs was 167, 161, and 172 J/g • Adding 10 wt% of 1-octadecanol (*e.g.* nucleating agent) resulted in decreasing the supercooling temperature from 26 to 12°C but this was also accompanied by a decrease in the latent heat capacity	[50]
PRS® Paraffin wax/PSt	Suspension polymerisation	• Particle diameter ~30 μm	[129]
Paraffin wax/St and methyl methacrylate (MMA)		• Energy storage capacity of 41.65 J/g	[130]

(Continued)

Table 9: *Continued*

PCM/shell material	Encapsulation method	Properties of encapsulated PCMs	Reference
PRS® Paraffin wax/St Tetradecane/St Rubitherm® R27/St Rubitherm® R20/St Nonadecane/St		• Latent heat per mass at MMA/St proportion of 4 was 84.04 J/g • Enhanced thermal conductivity and mechanical strength • Latent heat ~41.65 J/g (lower than pure paraffin) • Optimum melting heat (nonadecane) was 119.80 J/g • Mean diameter of Rubitherm® R20 was the smallest	[131]
Paraffin/MMA and triethoxyvinylsilane		• Enhanced thermal stability, thermal conductivity, and heat transfer rate, *e.g.* thermal conductivity was reported to reach an increment of 116% • Electrical resistance of PCM greater than 10^{10} Ω/sq	[109]
n-Octadecane/St-divinylbenzene		• Thermal decomposition temperature ~230°C • *N*-Octadecane content (at monomers/*n*-octadecane mass ratio 1:1) ~56.8 % • Optimum enthalpy of 57 J/g (at monomers/*n*-octadecane mass ratio of 5:2) • Average particle size ~71 µm (at stirring rate of 1,200 rpm)	[132]
Paraffin wax/PSt		• Average particle size was 4.53 µm • Average storage capacity (latent heat) was 104.7 J/g	[130]
Butyl stearate/polyurethane (PU)	Interfacial polymerisation	• Heat of fusion ~80 J/g • Melting point ~28.7°C • Particle diameter ~20–35 µm • Good property of thermal periodicity • Good thermal stability after subjection to 400 repetitive heating and cooling cycles	[133]
n-Octadecane/Si		• Particle size 17.0 µm • Good thermal stability • Enhanced thermal conductivity due to the presence of silica • Optimum thermal conductivity (at core/shell weight ratio of 50/50) ~0.6547 W m^{-1} K^{-1}	[61]
Octadecane/PU		• Particle size of 0.1–1 µm • Melting point of 28–30°C • Latent heat of fusion ~62.6–112 J/g • Heat of crystallisation was 20.9–22.7°C	[134]
Paraffin RT21/PU (IPDI and EDA as wall monomer)		• Mean particle diameter was 2.40 µm • Latent heat was 92.5 J/g • Good anti-osmosis property • Good anti-permeability and high stability	[135]
n-Octadecane/PU		• Mean particle size of 5–20 µm • Jeffamine-based microcapsules exhibited better phase change properties and anti-osmosis property but poorer thermal stabilities	[136]
Butyl stearate/cross-linked network polyurethane (PU) with pentaerythritol used as crosslinking agent		• Diameter of microcapsule was in the range of 10–35 µm • Enthalpy was in the range of 77–81 J/g. Thus, microcapsules have good LHS performance • Enhanced thermal stability due to the presence of network polyurethane shell	[137]
N-Octadecane/PMMA-TiO$_2$	Emulsion polymerisation	• At a core-to-shell ratio of 1:1, an optimum encapsulation efficiency of 67.2% was obtained, and	[138]

(Continued)

Table 9: *Continued*

PCM/shell material	Encapsulation method	Properties of encapsulated PCMs	Reference
		encapsulated PCM particles had a latent heat capacity of 179.9 J/g	
		• MPCMs produced had excellent nuclear shell structure and were covered uniformly with TiO$_2$	

is governed by several mechanism including coalescence and break-up of particles, secondary nucleation, and monomer diffusion towards the interface. Moreover, it is one of the most used methods by several researchers for the encapsulation of PCMs, because it is simple, cheap, robust, and environmentally friendly, comprising the dissolution of polymer monomer into chosen organic phase, formation of the oil/water emulsion, and separation and precipitation of monomer molecules from the core material [116].

5.2.3.4 Emulsion polymerisation

In this approach, the solvent containing the insoluble monomer gets dispersed uniformly by mechanical stirring in the reaction medium containing the chosen emulsifier and surfactant. Then, an initiator is added which results in the formation of a polymer membrane on the surface of the PCM core. This initiates the polymerisation reaction in the aqueous phase and as reaction progresses the polymer particles will grow.

5.3 Shell materials for encapsulation

There are in total three classes of shell materials, including organic, inorganic, and organic–inorganic hybrid shells. Based on information available in previous literature, it can be observed that shell material selection is made randomly, since the only aim of most researchers was to be able to successfully encapsulate the chosen PCM core within the designated polymeric film. Not all shell materials available in market have good encapsulation ability; therefore, it is important to compare the different shell materials used in previous literature and thereby, to determine the suitable shell materials which result in producing encapsulated PCMs with enhanced thermal performance. Moreover, selecting the correct shell material is considered crucial; however, this process is technically and scientifically challenging, since the chosen material should exhibit

acceptable chemical and physical properties and at the same time be able to encapsulate the designated PCM core fully. In previous literature, hard and dense polymers used as organic shell materials include gelatine/glutaraldehyde (GA) complex [139,140], epoxy resin [141–143], PMMA [144,145], melamine resin, MF resins, urea-formaldehyde (UF) resin [80,128,146,147], poly(urea-urethane) (PUU), PU [45,131,135,148–151], and PSt [45,131,150,151], and acrylic resins have been used mainly because they offer exceptional structural stability to the microcapsules. Also, the resulting microcapsules were found to have good durability even after being subjected to numerous repeated heating and cooling cycles. Major drawbacks of mentioned shell materials include poor chemical and thermal stabilities. Acrylic resins, which are methacrylate-based copolymers, are considered as the most promising organic supporting materials available compared to the others due to the numerous advantageous characteristics they exhibit: non-toxicity, easy handling, high mechanical strength, and good chemical resistance [152]. In the recent times, inorganic support materials like silica, titania, calcium carbonate, PSt, and zinc oxide have gained more attention due to their desirable intrinsic characteristics such as relatively high thermal conductivity and enhanced mechanical strength and durability, chemically inert, and non-toxic [110]. Thus, encapsulating organic PCMs like paraffins/paraffin waxes of high flammability within an inorganic shell material tends to reduce its flammability drastically [18]. Detachment of inorganic additives from the surface of the microcapsule is the major shortcoming of this approach; however, this can be overcome through the employment of the chemical hybridisation approach [152]. Organic–inorganic shell materials do result in producing microcapsules of improved intrinsic characteristics including superior thermal conductivity, good chemical stability, and mechanical robustness through the superficial attachment of inorganic additives including silver nanoparticles, iron nanoparticles, and silicon nitride. In general, natural polymers like gelatine and GA shell materials were rarely used in previous literature for the encapsulation of PCMs but are commonly used in the food industry for the

Table 10: Advantages and disadvantages of different shell materials used

Type	Shell material name	Advantages	Disadvantages	Ref.
Organic	• MF resin • UF resin • PU • PUU • Acrylic resin	• Good thermal reliability • Good structural stability • Good UV stability • Non-toxic • Good mechanical strength • Good chemical resistance	• Relatively low thermal and chemical stability • Inherently low thermal conductivity • Flammable	[80,96,158–160]
Inorganic	• Silica • Titania • Calcium carbonate • Zinc oxide • Alumina	• High thermal stability • High thermal conductivity • Susceptible to surface modification	• Poor long-term stability • Poor fracture resistance • Brittle	[61,79,111,161,162]
Organic–inorganic hybrid	• Silver nanoparticles in an organic shell • Silicon nitride in organic shell	• Very high thermal conductivity • Enhanced mechanical strength • Good chemical stability	• Inorganic additives can easily be detached from the surface	[116]

encapsulation of different essential oils like oregano oil to enhance their shelf lives [153]. However, Onder *et al.* [139] used gelatine and GA which are both natural polymers as shell materials to encapsulate paraffin waxes through the complex coacervation, to produce MPCM with an optimum PCM loading of 80% and 144 J/g latent heat capacity. In general, the strength of gelatine and GA shell is influenced greatly by the electrostatic force of attraction between the molecules of gelatine and GA; therefore, the durability of this shell material is affected undesirably in certain conditions such as when the pH level is too high or when the ionic strength is high which subsequently leads to the dissociation of gelatine/GA complex formed [154]. Pascu *et al.* [141] were the first to report the production of microcapsules using non-toxic epoxy resin as the shell material since epoxy results were believed to have good thermal, and mechanical properties

along with acceptable chemical resistance. However, in the recent times, they are commonly used for coating purpose to enhance the strength of the designated shell material because previous literature shows that most shell materials exhibited poor heat resistance when exposed to elevated temperatures in the range of 150–250°C [155]. Cheng *et al.* [156] prepared MPCMs *via* the polycondensation approach, and coated the resulting microcapsules with epoxy resin through a simple stirring to produce MPCM composite with latent heat of melting in the range of 32.41–50.75 J/g which were able to maintain good thermal stability below 300°C. The study carried by Wang *et al.* [157] demonstrated the possibility of overcoming the poor thermal stability of the prepared MPCMs through the employment of the secondary wrapping and pouring approach which involved wrapping the MPCMs with a layer of epoxy resin. Results indicated that the
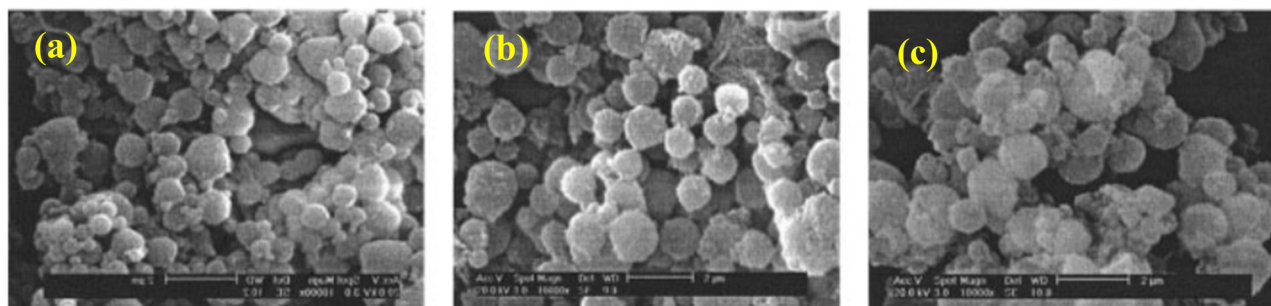
Figure 13: SEM images of MPCMs with (a) 0%, (b) 20%, and (c) 40% of cyclohexane [164].
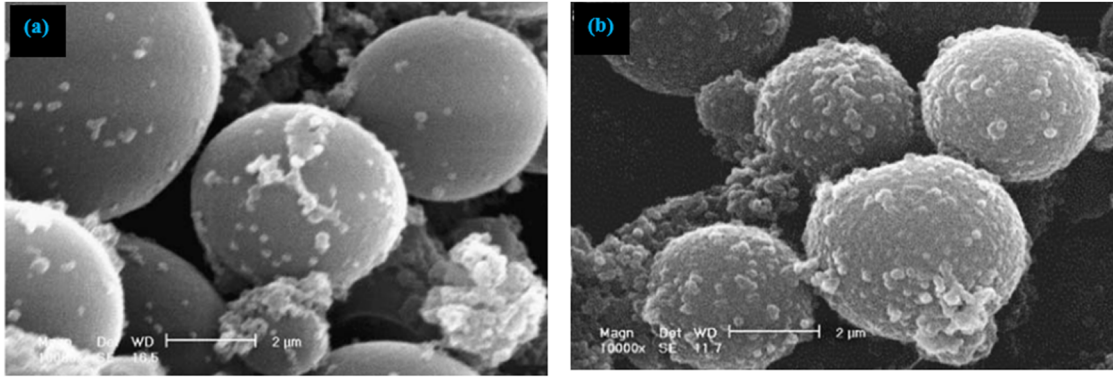
Figure 14: SEM images of MPCMs produced at immersion rate of (a) 0.5 mL/min and (b) 1 mL/min [165].

resulting products had an optimum latent heat capacity of 34.9 J/g along with good thermal stability provided that the mass ratio of MPCM to epoxy resin was 1:1; and therefore, they were reported as suitable fillers which could be incorporated in asphalt mixtures. Table 10 summarises the different classes of shell materials along with their advantages and disadvantages.

5.4 Morphological analysis of the encapsulated PCMs

Park *et al.* [163] found that particle size of microcapsules is influenced by the stirring rate and stirring time. The particle size reduced with the increase in the stirring rate and time. At higher stirring time, more microcapsules had formed. Zhang *et al.* [127] reported that microcapsules of good thermal stability was produced at urea-MF ratio of 0.2:0.8 with an average diameter in the range of 0.4–5.6 μm. Appearance of dimples on some of the microcapsules was caused by either the volume contraction of *n*-octadecane during crystallisation, or by the removal of cyclohexane. Further study by Zhang *et al.* [164] indicated that surface of microcapsules formed

without cyclohexane was much smoother and no dimples existed as shown in Figure 13.

Su *et al.* [165] produced microcapsules with MF shell material exhibiting a smooth and compact surface with an average diameter of 5 μm. Increasing the rate of immersion of shell from 0.5 to 1 mL/min resulted in affecting the surface morphology significantly; thus, particles were observed to have a rougher surface as shown in Figure 14 due to the inability of MF prepolymer to be capsulated on core slowly and tightly because dropping speed was too high.

Zhang and Wang [128] produced microcapsules with an average diameter of 20 μm, exhibiting better phase change properties compared to the other microcapsules. At a core-to-shell ratio of 75/25, an optimum encapsulation efficiency of 80 wt% was obtained; however, the SEM images indicated that the surface morphology of the resulting microcapsules were not smooth, and the particles were not spherical (Figure 15). Hence, at core-to-shell ratio of 65/35, microcapsules of desired shape and size were produced. Su *et al.* [166] produced PMMA-MAA microcapsules with average size in the range of 2–10 μm. Experimental results indicated that wrinkles had formed on the surface of the prepared microcapsules. The surface morphology was influenced greatly by the molar ratios of shell monomers and
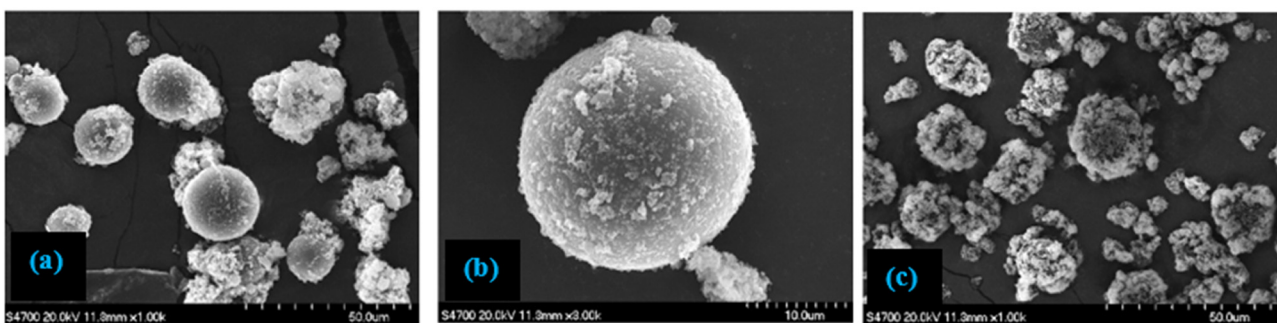

Figure 15: SEM images of microcapsules produced with core-to-shell ratio of (a) and (b) 65/35 and (c) 75/25 [128].
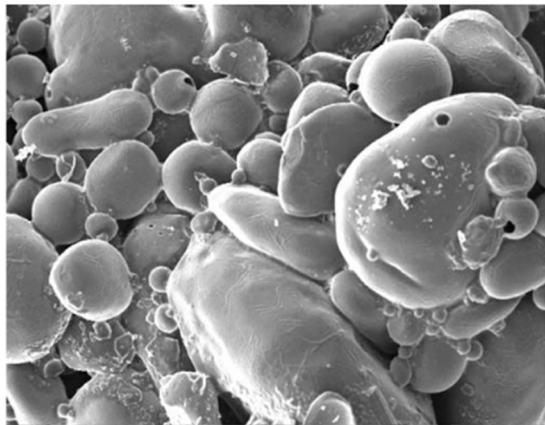
Figure 16: SEM image of MPCMs produced at a stirring rate of 900 rpm [129].

thermal initiator used. Optimum surface morphology was obtained at MMA:MAA weight ratio of 4:1 and 1 wt% of thermal initiator.

Fang *et al.* [167] concluded that the particle size is influenced by the stirring rate of the emulsion process. They reported that 1,500 rpm is the suitable stirring rate for the synthesis of nanocapsules with an average diameter of 100 nm. The stirring rate influences the size of the particles produced, therefore, its thermal storage capacity (Sánchez *et al.*, 2008). Using a low stirring rate results in affecting the surface morphology and increasing the stirring rate is reported to reduce the diameter of the MPCM particles. Sánchez *et al.* [129] stated that high stirring rate such as 900 rpm should be used for successful encapsulation of PCM but at this stirring rate desirable MPCMs were not prepared. Hence, particles had agglomerated, which resulted in the
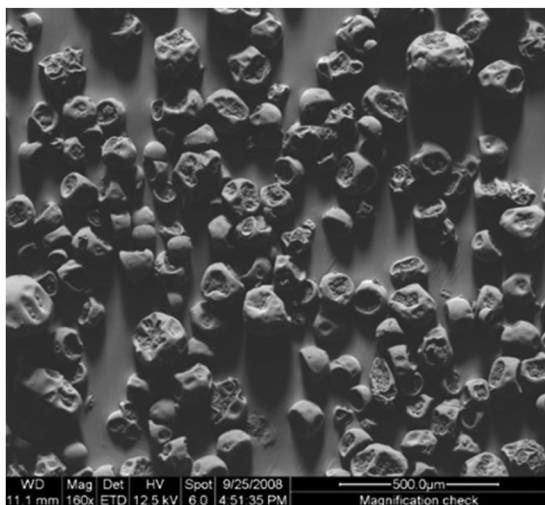
formation of large clusters as shown in Figure 16. You *et al.* [132] used a stirring rate of 1,200 rpm to obtain spherical microcapsules with an average diameter of 71 μm, and at this stirring rate, the particles did not agglomerate. Alkan *et al.* [145] produced microcapsules with an average diameter of 0.16 μm at an emulsion stirring rate of 2,000 rpm. However, Sarı *et al.* [168] obtained microcapsules with an average diameter of 0.26 μm at an emulsion stirring rate of 2,000 rpm, and later Sarı *et al.* [144] produced microcapsules with an average diameter of 0.25 μm at the same emulsion stirring rate. Alkan *et al.* [169] microencapsulated *n*-eicosane using the same method and material but obtained microcapsules with an average diameter of 0.7 μm. Results from these studies indicate that the type of PCM being encapsulated influences the size of the particles produced despite the fact that the same emulsion stirring rate was used. Particles of reduced diameters are considered to have the potential to be used for thermal storage applications since they exhibit large surface area per unit volume.

Further studies by Sánchez *et al.* [130] reported that provided the core/shell ratio did not exceed 1.0, microcapsules of comparable sizes to the ones reported earlier were obtained. The morphology of microcapsules was observed to improve significantly as the MMA/St mass ratio increased from 3.5 to 4.0. At MMA/St mass ratio of 3, microcapsules of non-spherical shape with a rough surface were produced. Most of these particles had either broken or consisted of an incomplete shell. The average diameter of microcapsules decreased with the increase in the amount of MMA. You *et al.* [132] observed the formation of concaves when the mass ratio of monomer/*n*-octadecane was lower than 5:3 (Figure 17), and the enthalpy resulting microcapsules had reduced when the mass ratio of monomer/*n*-octadecane was below 1:1.

Qiu *et al.* [170] encapsulated *n*-octadecane microcapsules with poly(lauryl methacrylate), and one or more dimples had formed on the surface of some microcapsules as
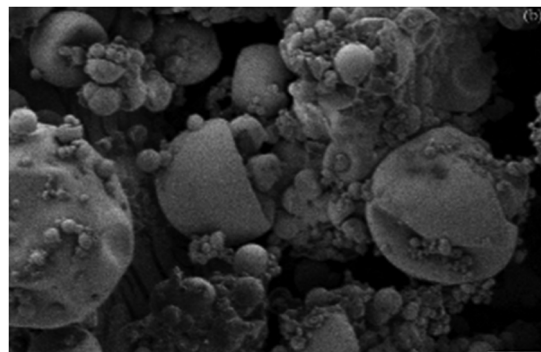

Figure 17: SEM image of MPCMs with concaves.

Figure 18: SEM image of MPCMs containing dimples.

shown in Figure 18. Depression on the surface resulted from the shrinkage of the polymeric shell. The average diameter of most microcapsules was around 9 µm, making them suitable for thermal regulation applications since such microcapsules exhibit increased surface area, and therefore, better heat transfer capacities.

Cho *et al.* [171] concluded that adding cellulose acetate (CA) will stabilise the particles to unimodal particles with an average diameter of 250 nm from bimodal particles with average diameter in the range of 100–500 nm. Nanocapsules with an average diameter of 80 nm was observed to exhibit a well-rounded spherical shape. Fortuniak *et al.* [172] obtained microcapsules with an average particle size in the range of 5–22 µm and concluded that the shape and size of particles were influenced by the conditions of their formation. Hence, if time taken for DVTMDS crosslinker to be added on the PHMS chain was too long, distorted microcapsules exhibiting good thermal properties had formed, whereas if the time was too short, microcapsules with deteriorated thermal properties had formed. Sarı *et al.* [42] obtained microcapsules exhibiting uniform spherical structures with a compact surface at PMMA/capric-SA eutectic mixture (c-SEM) ratio of 1:2. Deveci and Basal [173] microencapsulated *n*-eicosane with SF/CHI shell material to produce microcapsules in the range of 8–38 µm with an average diameter of 23 µm. Results showed that smaller particles exhibited better hand properties, uniform heat absorbing and releasing, and washing durability. Size of microcapsules produced are also influenced by the amount of crosslinking agent used. At SF/CHI ratio of 20, the inner layer of microcapsules was observed to be smooth whereas the outer layer appeared to be rougher, with a sponge-like texture. Konuklu *et al.* [174] produced microcapsules in the particle size range of 200 nm to 1.5 µm, and results indicated that emulsifiers had no effect on the geometry of the microcapsules produced.

5.5 Shape stabilisation technology

Due to the drawbacks of the encapsulation technology, including high processing cost, and difficulty in choosing and designing the correct materials according to the intended application, researchers have put more focus on the development of techniques that are more cost-effective and thus, shape-stabilisation technology was developed and in the recent times it has evolved very quickly [175]. Shape stabilisation process involves the confinement of PCMs such as fatty acids, polyalcohol, PEG, and others (*e.g.* soft segment) in the chosen polymer matrix (*e.g.* solid framework which acts as the hard segment) designed to retain the original solid state of PCM during phase transition process by capillarity. A wide range of polymers have been used, as matrix, porous and nanomaterials [176] as the supporting material in the past with limited number of references discussing about the benefits using biopolymers including cellulose, chitosan (C), and many more as supporting material to promote green chemistry [177]. The final product resulting from this shape-stabilisation technology is known as a composite PCM or a form-stable PCM, which is composed of a working substance (*e.g.* PCM) and a supporting material, where the working substance functions by storing or releasing latent heat during the phase transformation process, while the supporting material prevents leakage of PCM during this process but makes no contribution to LHS. In the recent times, this technology has become the key interest of many researchers because the produced form-stable PCMs tend to exhibit good thermal properties which make them suitable for different applications such as thermal management, *e.g.* in solar heating systems and thermal regulation in dwellings and commercial buildings [178]. This technology consists of both physical and chemical methods like the microencapsulation technology (Figure 19); however, approaches are much simpler, easier, and requires no expensive equipment.
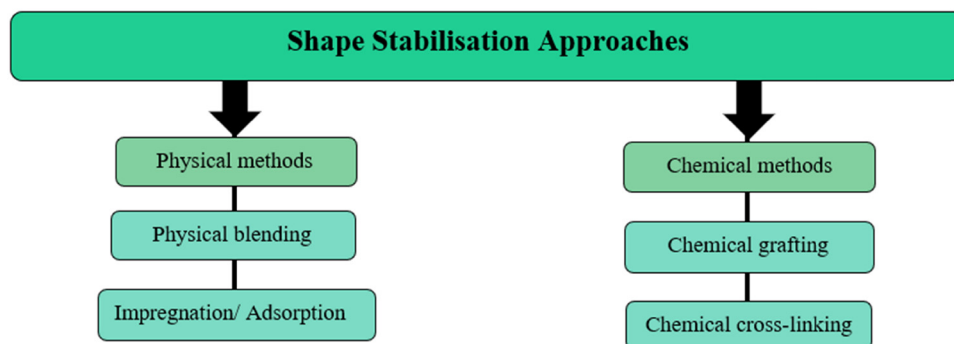

Figure 19: The different shape stabilisation techniques available.

Solid–solid PCMs function by absorbing, storing, and releasing like the other PCM states, with difference lying in terms of phase transitions they experience. Hence, during phase change process, particles are likely to change from highly crystalline phase to another phase such as amorphous or semi-crystalline. Researchers are currently focusing on the utilisation of polymeric solid–solid PCMs due to the numerous advantages; they require no encapsulation, can be processed into arbitrary shape (*i.e.* desired shape) [179], and can be incorporated with building materials directly, *e.g.* in concrete or gypsum without the need of encapsulation [180]. The well-known drawbacks of solid–solid PCMs are the smaller latent heat of phase transition and supercooling behaviour. Among the various solid–solid PCMs available, such as polyhydric alcohol (polyalcohol) and cross-linked polyethylene, polymers and hydrated inorganic salts are a few of many recently developed functional PCMs. Furthermore, using solid–solid PCMs will reduce preparation steps involved and thereby cut down the overall cost significantly. Common defects of solid–solid PCMs are high transition temperature, low transition enthalpy, and unstable thermal property, which tend to limit their applications greatly. Therefore, researchers have endeavoured to fabricate novel materials, polymeric solid–solid PCMs, to overcome these shortcomings, because they consist of excellent integrated performances [181]. Overall, shape stabilisation technology is not limited to the preparation of solid–solid PCMs, but it is used to enhance the shape stability of the chosen PCM so that it is able to retain its original solid state during the phase transition process. Developing materials from natural polymers for different applications is desirable, and thus has been a hot topic for several years, mainly to avoid the use of petroleum-based materials due to their increasing costs and environmental concerns [182].

Also, biopolymers are available in abundant quantities. Currently, petroleum based PCMs, *e.g.* paraffins, are commonly used in many sectors; however, it is more desirable to utilise environmentally friendly PCMs, such as PEGs in building construction applications to encourage sustainable development. PEG is used in many fields including cosmetics, food, biomedical applications, and pharmaceutical industry due to its inert nature and previous studies have proved its potential as PCMs in TES for the utilisation of renewable energy sources like solar energy. PEG is readily soluble in most solvents due to its hydrophilic nature which is the major drawback limiting its application as PCMs; therefore, encapsulation of PEG has not been established till date. One study reported that encapsulation of PEG is impossible based on experimental results obtained. Previous studies have all demonstrated the possibility of overcoming this shortcoming of PEG through the employment of the shape stabilisation technology. Either physical or chemical approaches can be applied to prepare PEG-based composites for the chosen application. Physical methods including blending, adsorption, and (vacuum) impregnation [183,184] involve the preparation of composite by dispersing PCMs in polymeric materials of higher melting point, which acts as the supporting material, and if the temperature is maintained below its melting point, the composite PCM can exist in its solid state. Moreover, they are known as passive modification, since it involves filling in the cavities of chosen supporting material, usually porous manmade materials like concrete, plaster, wallboards, and aerogels with chosen PCM such as PEG without any chemical reactions taking place. Resulting products are less durable since they are prone to phase segregation mainly because leakage of PCM is prevented by weak physical interactions including capillary and surface tension forces due to the presence of physical interactions between the functional groups of both PCM and supporting material [185–187], thus no chemical bonds have formed between the functional groups [188]. In contrast, chemical approaches including chemical grafting, blocking, and cross-linking copolymerisation are the most convenient methods for the synthesis of good solid–solid PCMs, in which the solid–liquid PCMs are commonly used as the working material component [181]. Chemical methods are preferable over the physical methods since final products have longer durability.

5.5.1 Supporting material for the shape stabilisation of solid–liquid PCM

The two major drawbacks of solid–liquid PCMs are their poor shape stability which causes leakage problems during phase change, and their inherently low thermal conductivity; however, they can be overcome by selecting a suitable supporting material. In cases where the leakage problem needs to be overcome, a porous material will be selected as the supporting material but if composite PCM is expected to have improved thermal conductivity, the porous material will be combined with the chosen nanomaterial since such materials have very high thermal conductivity. It is important to ensure that nanomaterial is not incorporated in excess since high contents of nanomaterial will reduce the latent heat of resulting composite PCM because the supporting material makes no contribution to latent heat. Vast number of papers have mainly utilised porous materials as supporting material due to the desirable characteristics they exhibit which includes increased surface area, high thermal conductivity, and enhanced chemical compatibility. The interaction existed between PCM and porous materials which arises due to Van der

Table 11: Characteristics of supporting materials used in shape stabilisation technology

Supporting material	Advantages	Disadvantages	Examples
Porous carbon	• Available abundantly • Non-toxic • Low density • Morphology susceptible to undergo modification. • Good capillarity	• Expensive • Highly complex steps are involved in its preparation protocol	• Tin tetrachloride reacted with sodium polyacrylate to produce porous carbon [190] • Eggplant porous carbon [191] • Mesoporous N-doped porous carbon [192]
Graphite	• High thermal conductivity • Highly porous • Good thermal stability • Low density • Flame retardant	• Expensive • Highly complex steps are involved in its preparation protocol	• EG
Polyurethane	• Good insulator • Lightweight • Exhibits tailor made properties Good corrosion resistance	• High flammability • Toxic since they are prepared using organic solvents	• Polyurethane foam resulting from crosslinking reaction
Silica	• Available abundantly at low costs • Highly porous • Good mechanical properties • Good chemical and thermal stability • Excellent insulation properties	• Expensive	• Mesoporous silica [193] • Silicon dioxide • Monolithic silica [194]
Clays	• Good thermal stability • Low cost • Good compatibility with building materials • Naturally porous	• Poor mechanical strength • Hygroscopic nature	• Diatomite • Expanded perlite • Expanded vermiculite • Bentonite • Kaolin • Sepiolite
Cellulosic material	• Available abundantly • Good mechanical properties • Can easily participate in reactions • Non-toxic		• Microcrystalline cellulose • Wood powder • Cellulose diacetate (CDA) • Cardboard • Plant fibres

Waals, hydrogen bonds, surface tension, and capillary force tend to prevent leakage of PCM, thus, enabling PCM to retain its solid-state during phase change. Moreover, the choice of supporting material used for the stabilisation has great impact on the final properties of the prepared composite PCM. The different types of supporting materials used in previous literature to stabilise the chosen PCM are presented in Table 11 with a summary of their characteristics [29,189].

5.5.2 PEG composite through physical blending

Physical blending also known as polymer blending is a contemporary method for the development of new polymeric materials and is an ideal technique for the synthesis of materials with desired properties. It consists of three simple steps as illustrated schematically in Figure 20 and they include the dissolution of the chosen PCM and supporting material in chosen solvent at 70°C followed by pouring solution onto a glass dish and then allowing solvent to evaporate at room temperature which results in the production of the desired composite PCM. Hence, using this method, it is possible to prepare final products of superior properties than the individual constituent polymers (Table 12). The final properties of synthesised polymers are influenced mainly by the miscibility of the composite blend [182]. Wang *et al.* [81] attempted PEG–EG composite PCM of mass ratio in the range of 50–90 wt%, and Sundararajan *et al.* [183] prepared PEG-cellulose acetate composites *via* a microwave-assisted
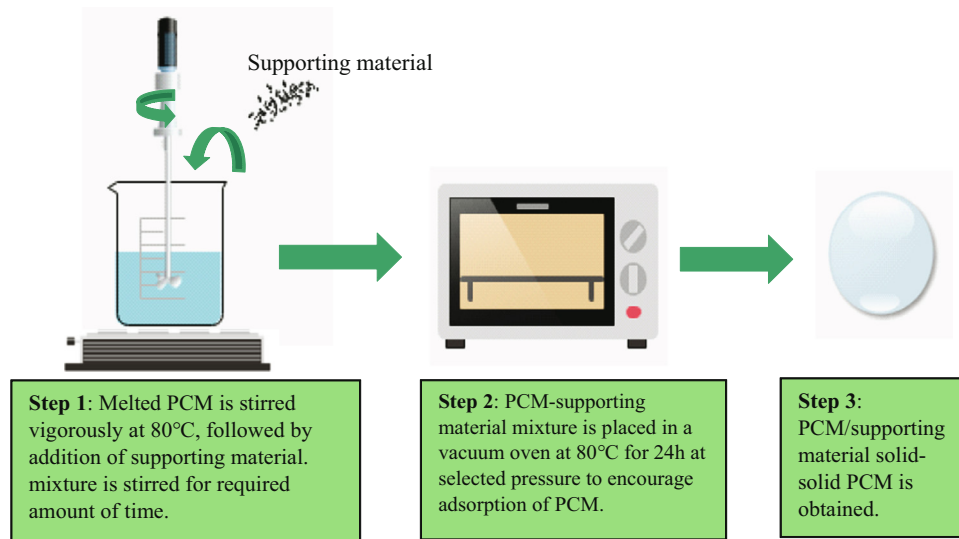
Figure 20: Schematic representation of physical vacuum impregnation approach for the synthesis of solid–solid PCMs.

blending approach and reported that optimum PEG content to form film composites was 60 wt%. Li *et al.* [195] developed a novel graphene oxide (GO)-PEG composite, as photo-thermal conversion material, with latent heat capacity higher than 180 J/g and a phase transition temperature of 50.5°C, *via* an ultrasonic assisted physical blending approach. Composites of high latent heat capacity was obtained since no changes occurred to the crystalline properties and chemical structure of PEG. A novel PEG/poly(L-lactic acid) (PLLA) composite PCMs were prepared and results indicated that the PLLA content caused no significant impact on the crystalline properties of PEG [175], which was attributed to the partial miscibility of PEG and PLLA but increasing PLLA content above 30 wt% reduced the crystallinity of PEG in the composite PCM from 80 to 70%, and this was observed to decrease the latent heat capacity insignificantly. Moreover, it was concluded that PEG/PPLA blends with PLLA content less than 35 wt% were suitable for TES purposes since they had latent heat capacity greater than 100 J/g and good thermal reliability even after being subjected to 100 thermal cycles.

5.5.3 Thermal properties of composite PCMs prepared *via* physical shape stabilisation approaches

Vacuum impregnation is the most used physical approach for the stabilisation of PCMs because it is simple, yet highly effective [200–203]. Vacuum conditions are usually used to enhance the impregnation efficiency by forcing the liquid PCM into the pore system of the supporting material, and the conventional set-up used in previous literature is shown in Figure 20.

Since physical shape stabilisation processes is very simple, easy and a highly feasible approach along with a flexible design which means any PCM and supporting material can be selected and used. Therefore, previous studies have prepared numerous composite PCMs using variety of PCMs and supporting material; thus, unlimited PCM/supporting material combinations have been prepared and investigated in literature as shown in Table 13. However, there is a lack of understanding regarding the changes caused to the thermal properties of PCM, namely its phase transition temperature and latent heat after the physical shape stabilisation process, which are discussed in the following paragraphs by comparing the design parameters of different studies; thereby, determining major factors influencing the thermal properties of PCMs.

In general, after the shape stabilisation through either physical, chemical, or a combination of both, the thermal properties determined using differential scanning calorimetry (DSC) shows that the phase transition temperatures (*e.g.* melting and crystallisation temperatures) and the corresponding latent heat of PCM gets reduced but the main reasons for this is yet to be established since results produced in literature varies a lot. This section focuses on identifying design parameters that alternates the phase transition temperature and latent heat since thermal performance of final composite PCM prepared depends entirely upon this. Also, knowing the key parameters that decline the intrinsic thermal properties of PCMs means more attention can be paid during synthesis process, and it would be easier to propose formulation procedures that produce composite PCMs with optimum thermal performance. Moreover, it reveals the ways of tailoring phase transition temperature

Table 12: Properties of shape stabilised composite PCM from physical approaches

PCM Composite	Method	Melting (PEG)		Crystallisation (PEG)		Melting (PEG composite)		Crystallisation (PEG composite)		Reference
		T_{onset} (°C)	ΔH_{fusion} (J/g)	T_{onset} (°C)	ΔH_{fusion} (J/g)	T_{onset} (°C)	ΔH_{fusion} (J/g)	T_{onset} (°C)	ΔH_{fusion} (J/g)	
PEG6000-bone char (BC) composites	Impregnation	59.87	162.07	45.56	161.32	BC1: 58.51 BC2: 59.36	62.67 71.17	43.02 42.36	59.93 68.43	[196]
PEG8000-cellulose acetate blend (with microwave)	Blend	63	189.5	—	—	46–61	23–155	—	—	[183]
Cellulose-graft-PEG1100	Synthesis in ionic liquid	46.2	140.3	—	—	42.8	94.7	—	—	[197]
Cellulose-graft-PEG2000	Synthesis in ionic liquid	53.2	183.3	—	—	51.0	129.9	—	—	[197]
Cellulose-graft-PEG5000	Synthesis in ionic liquid	60.1	204.7	—	—	58.9	153.1	—	—	[197]
PEG-MCS	Blending + impregnation	58.95	183.10	41.74	171.60	57.03	122.10	44.10	106.80	[198]
PEG10000-PGMA	Ring open crosslink	63.40	166.70	39.20	161.80	55.9	73.20	31.10	69.80	[179]
PEG-CDA	Blending	—	186.7	—	—	—	104.5	—	—	[199]
PEG-CDA	Chemical crosslink	—	186.7	—	—	—	73.6	—	—	[199]

to match the operating temperature of building application (*e.g.* 18–30°C) because PCMs with high phase transition temperatures are reported to have higher latent heat capacities. Nomura *et al.* [203] prepared erythritol/expanded perlite (EP) composite PCM with latent heat of 332.2 J/g which was lower than pure erythritol which had a latent heat of 354.7 J/g, and this phenomenon was predicted to occur due to the existence of an unusual interaction between the PCM and the nano-sized pores of EP. While Lee *et al.* [204] prepared erythritol/EG composite PCMs *via* a simple melting method with latent heats of 317.5, 322.1, 327.7, 334.3, 38.5, and 351.2 J/g, respectively. The difference in latent heat of the composite PCMs was because the interlayer distance of EG varied and the change in latent heat of pure erythritol (380.5 J/g) was reported to be attributed to the presence of EG in the composite but according to literature other factors (*e.g.* temperature) may have affected the latent heat but this was not addressed in this study. Jeong *et al.* [205] prepared *n*-hexadecane/diatomite composite PCMs with melting temperature and latent heat of 23.68°C and 120.1 J/g using pure hexadecane with melting temperature and latent heat of 20.84 and 254.7 J/g, respectively. The cause for the change in melting temperature and latent heat of melting and freezing was not reported. The reduction in the crystallisation temperature from 16.78 to 13.17°C (*e.g.* 21.51% decrease) was attributed to the poor intermolecular forces existing between *n*-hexadecane molecule and pore walls of diatomite. Li *et al.* [206] prepared paraffin/diatomite composite PCMs *via* a simple mixing/surface absorption approach and observed that the phase transition temperature of paraffin reduced insignificantly from 26.1 to 25.2°C (*e.g.* 3.45% decrease) which was due to the interaction generated between paraffin and diatomite, and due to the confinement of paraffin within the pores of diatomite but reason for the drastic reduction in the latent heat capacity of pure paraffin from 133.7 to 45.96 J/g in the composite PCM was not evaluated and reported in the study. This may be attributed to the PCM content present in the composite PCM. Hence, composite PCM with 47.9 and 34.4% of PCM had latent heats of 63.98 and 45.96 J/g which suggests that higher PCM loading results in producing composite PCMs of better thermal performance.

Karaman *et al.* [207] prepared PEG/diatomite composite PCMs *via* the vacuum impregnation and observed changes in the melting temperature of pure PEG from 33.32 to 27.7°C (*e.g.* 16.87% decrease) and reported that the insignificant changes in the phase transition temperature may be attributed to the physical interaction existing between PEG and diatomite. DSC results showed changes in the latent heat of PEG in composite PCM containing optimum content of PEG (*e.g.* 50 wt%) from 143.16 to 87.09 J/g in the composite; however, this was not addressed in the study

Table 13: Summary of the design parameters and thermal properties of composite PCMs synthesised *via* the physical shape stabilisation approaches

Composite PCM (PCM/support material)	Design parameters	Thermal properties				Ref.
		Phase transition temperatures		Latent heat (J/g)		
		Melting point (°C)	Freezing point (°C)	Melting	Crystallisation	
n-Hexadecane/diatomite *via* vacuum impregnation	• 80 g PCM and 50 g diatomite • Oven drying at 80°C for 24 h. • Removal of excess PCM through filtration	23.68	13.17	120.1	118.0	[205]
n-Octadecane/diatomite *via* vacuum impregnation	• 80 g PCM and 50 g diatomite • Oven drying at 80°C for 24 h • Removal of excess PCM through filtration	31.29	23.65	116.8	112.9	[205]
Paraffin wax/diatomite *via* vacuum impregnation	• 80 g PCM and 50 g diatomite • Oven drying at 80°C for 24 h • Removal of excess PCM through filtration	54.24	50.23	61.96	59.74	[205]
Erythritol/expanded perlite (EP) *via* vacuum impregnation	• Melting solid erythritol at 150°C using furnace	—	—	332.2	—	[203]
Erythritol/EG *via* the melting method	• Melting process took place at 120°C • 10 g of erythritol was melted followed by the addition of 0.25 g EG • The reaction mixture was stirred under heating for 5 min	— — — — — — —	— — — — — — —	317.5 322.1 327.7 334.3 338.5 348.5 351.2	— — — — — — —	[204]
Paraffin/diatomite *via* simple mixing and surface absorption	• Heating diatomite at 105°C for 24 h to remove moisture • Melting paraffin at 60°C before mixing • Unknown amounts of PCM and support material was added and mixed in a mixing vessel	22.3 23.6 23.3	— — —	63.93 47.93 45.96	— — —	[206]
PEG/diatomite *via* vacuum impregnation	• Vacuum impregnation was carried out at an unknown temperature and vacuum pressure of 65 kPa for 90 min	27.7	32.19	87.09	82.22	[207]
Paraffin (*n*-docosane)/EG *via* the melting method	• 3–4 g of vacuum oven dried EG at 60°C for 16 h was heat treated at 800°C • Unknown amount of paraffin was melted at 65°C followed by the addition of EG with stirring	48.93	—	161.45	—	[62]
Paraffin/EG *via* the vacuum impregnation	• Unknown amount of paraffin was melted, and impregnated in EG with mass fraction 2, 4, 7, and 10% in a duration of 60 min to reach optimum saturation • Temperature used to melt paraffin was not reported	41.10 41.00 40.70 40.20	— — — —	192.6 188.0 181.9 178.3	— — — —	[208]
Paraffin/graphene oxide (GO) *via* vacuum impregnation	• Paraffin and GO was placed in a vacuum furnace at 100 kPa for 2 h to remove any entrapped air in GO • Temperature was increased to 90°C to melt down paraffin followed by immersing GO sheets in liquid paraffin for 3 h	54.60 51.48 52.33 53.57	44.78 45.76 44.63 44.59	63.11 62.53 59.12 63.76	64.45 63.34 60.73 64.89	[209]

(Continued)

Table 13: *Continued*

Composite PCM (PCM/support material)	Design parameters	Thermal properties				Ref.
		Phase transition temperatures		Latent heat (J/g)		
		Melting point (°C)	Freezing point (°C)	Melting	Crystallisation	
Paraffin/Si *via* vacuum impregnation	• To remove excess paraffin, which was not impregnated in the pores of GO, furnace temperature was increased to 120°C • Si spheres immersed into the liquid paraffin mixture and allowed to impregnate. Hence, no vacuum was used • Temperature used to melt paraffin and duration of impregnation is unknown	26 26.5 25.5	20 23 22	68 80 95	50 71 70	[211]
PEG600/gypsum through impregnation	• Unknown amount of PEG600 was melted and poured into the flask containing gypsum • The flask was heated at 25°C and shaken at 150 rpm to produce a homogeneous mixture	10.55	10.85	24.18	21.64	[210]
PEG600/natural clay through impregnation	• Unknown amount of PEG600 was melted and poured into the flask containing natural clay • The flask was heated at 25°C and shaken at 150 rpm to produce a homogeneous mixture	15.79	16.28	28.79	26.02	[210]
n-Octadecane/light weight sand *via* vacuum impregnation	• Oven dried light weight sand was poured into container containing melted PCM • The composite PCM was then vacuum oven dried at 80°C for 24 h to remove excess PCM present on the surface	19.67–25.36	24.10–31.54	19.011–19.114	—	[212]
Paraffin/porous TiO$_2$ foam *via* vacuum impregnation	• After removing air from the enclosed container containing unknown amount of solid paraffin and foam, the container was heated at 80°C under vacuum to facilitate the impregnation of liquid paraffin into the pores of the foam • For the removal of excess paraffin, the synthesised composite PCMs were heated in an oven at 80°C for an unknown duration of time	49.27	50.65	97.27	99.05	[188]
PEG10000/(CNT)/poly(vinyl alcohol) (PVC)/C *via* blending/impregnation	• Unknown amount of PEG10000 was melted and dissolved in absolute alcohol for 0.5 h at 80°C • Prepared CNT/PVC/C (CPC) supporting material was evenly distributed in the PEG solution formed, and the mixture was dissolved at 80°C for 2 h to produce the monolithic composite PCM	36.80	68.40	150.90	152.00	[214]
PCM/carbon foam *via* vacuum impregnation	• Beaker containing 50 g of solid PCM and 0.5 g of carbon foam was heated at 60°C for 2 h • The prepared composite PCM was heated for another 4 h at 60°C to remove excess PCM	26.10 24.90 26.20 26.60	24.20 23.10 24.00 24.10	85.60 80.50 95.00 105.20	91.00 84.90 91.80 105.40	[215]

but could have been explained by studying and evaluating changes in the crystalline properties of PEG because PEG is a polymeric PCM. The leakage problem of PEG was resolved, and this was attributed to the prevention caused by physical interactions such as capillary and surface tension forces, resulting from physical interactions existing between the functional groups of both PEG and diatomite. Results from thermal cycling test indicated that the composite PCM exhibited good thermal reliability and chemical stability, even after being exposed to 1,000 repeated heating and cooling cycles. Zhang and Fang [62] prepared paraffin/EG composite PCMs *via* the melting approach with melting temperature and latent heat of 48.93°C and 161.45 J/g. The melting temperature and latent heat of pure paraffin was 57.99°C and 188.69 J/g, respectively. Results showed that the physical stabilisation of paraffin had affected its thermal properties, but the authors concluded that significant changes did not occur because no chemical reaction took place between paraffin and EG.

Sari and Karaipekli [208] prepared paraffin/EG composite PCMs and investigated the influence of EG content on thermal properties of paraffin. Mass fraction of 2, 4, 7, and 10% of EG led to the production of composite PCMs with melting temperatures of 41.10, 41.00, 40.70, and 40.20°C and corresponding latent heats of 192.6, 188.0, 181.9, and 178.3 J/g, respectively. Results demonstrated that increasing the amount of supporting material tends to impact the latent heat of chosen PCM negatively; thus, the thermal performance of composite PCM becomes poor when EG content is high. The melting temperature and latent heat of composite PCM was lower than pure paraffin which had a melting temperature and latent heat of 41.6°C and 194.6 J/g, respectively, but the cause for the change in melting temperature and latent heat of paraffin in the composite PCM was not discussed anywhere in the study. Mehrali *et al.* [209] prepared paraffin/graphene oxide (GO) composite PCMs *via* vacuum impregnation using paraffin with melting temperature and latent heat of 53.46°C and 130.92 J/g, respectively. The composite PCM containing the highest mass percentage of paraffin (*e.g.* 48.3%) had melting and crystallisation temperatures of 53.57 and 42.25°C, respectively; thus, no significant changes had occurred in the melting temperature, but the crystallisation temperature increased; however, the reason for the change was not reported. The latent heat of composite PCM seemed to have a positive correlation with the paraffin content (in wt%) because composite PCMs with 44.3, 47.39, 47.80, and 48.30 wt% had latent heats of 59.12, 62.53, 63.11, and 63.77 J/g, but the enhancement in latent heat was not significant. Pure paraffin had a latent heat of melting of 131.92 J/g so the percentage difference between latent heat of pure and composite PCM containing optimum paraffin content was 51.7% which is very high,

therefore, indicating that thermal properties of paraffin was affected greatly by elevated temperature exposure during the vacuum impregnation process. Sari [210] prepared PEG600/gypsum and PEG600/natural clay composite PCMs with maximum absorption ratio of 18 and 22 wt% *via* the vacuum impregnation approach and observed changes in the phase transition and latent heat of pure PEG600 after impregnation, which was due to the confinement of PEG600 into the pores of gypsum or natural clay by capillary and surface tension forces which resulted in restricting the mobility of PEG chain during phase change. The cubicles of PEG600/gypsum and PEG600/natural clay composites, constructed at small scale, exhibited good thermal properties such as thermal reliability and chemical stability, even after being subjected to a lengthy thermal cycling test. Li *et al.* [189] prepared paraffin/TiO$_2$ foam composite PCMs of three-dimensional interpenetrating structures [189]. The composite PCMs had enhanced melting and freezing temperatures with a difference of no more than 3°C which was reported to be attributed to the surface tension forces and the capillary effect present between paraffin and the TiO$_2$ foam. Reduction in latent heat of melting and freezing from 184.3 and 182.67 J/g to 97.27 and 99.05 J/g suggested that the thermal properties of paraffin had changed after vacuum impregnation although no chemical reactions occurred between paraffin and foam. Hence, calculated percentage difference of 47 and 46% suggests that major changes in phase change properties had occurred after shape stabilisation which was due to the presence of solid content in the composite; thus, the porosity and pore size of the supporting material was reported as the two influential factors likely to impact the thermal properties of paraffin compared to the surface tension forces and capillary forces. The composite PCMs were observed to undergo thermal degradation when exposed to an elevated temperature of 150°C and thus, its onset degradation temperature was higher than that of paraffin which suggests that the composite PCMs had enhanced thermal stability below 200°C. Zhang *et al.* [211] prepared paraffin/silica composite PCMs containing 30, 50, 55, and 60 wt% of paraffin *via* the blending/impregnation approach. The melting temperature and latent heat of composite PCM with optimum paraffin content was 25°C and 95 J/g, respectively. The latent heat of paraffin was observed to have reduced from 168 to 95 J/g which was attributed to the accommodation of paraffin in the pores of silica. Kim *et al.* [212] prepared paraffin/light weight sand composite PCMs through a simple blending/impregnation approach with melting temperature in the range of 19.67–25.36°C and latent heat in the range of 19.01–19.11 J/g, respectively. Incorporating 50 and 100% of the prepared composites in cement mortar resulted in enhancing its latent heat by 6 J/g.

Sarı et al. [76] impregnated PEG within a binary composite consisting of raw diatomite (RD)/carbon nanotubes (CNTs) to prepare composite PCMs of enhanced thermal conductivity, and with latent heat capacity and melting temperature in the range of 51.4–62.9 J/g and 7–8°C. Leakage test results showed that the skeleton of RD/CNTs pre-composite prepared could absorb an optimum PEG content of ~51.0 wt% without sacrificing its structural stability which indicates the feasibility of incorporating them successfully in conventional building elements without fearing PCM leakage. They also showed good thermal reliability and chemical stability even after the long-term cycling operation, making them suitable for low-temperature passive solar cooling applications in buildings. Presence of CNTs enhanced the thermal durability of the composites significantly. Yang et al. [213] prepared the PEG/EG composite, by filling the pores of EG with liquid PEG under vacuum by air pressure and pore syphoning. Cheng et al. [214] prepared PEG10000/CNTs/PVC/C (CPC) composite PCMs via a blending/impregnation approach and reported that 8% increase in latent heat of melting of the composites was attributed to the hydrogen bonds present between the PCM and the supporting material.

Liu et al. [215] prepared novel PCM/carbon composite PCMs using carbon foam derived from insulation materials polyisocyanurate foam. Pure PCM was reported to have a degree of supercooling of around 4.10°C while the composite PCMs only experienced a degree of supercooling in the range of 1.90–2.50°C which was attributed to the enhancement of thermal conductivity of PCM in the composite due to the presence of carbon foam. With the increase in the PCM content, the melting temperature shifted, and the degree of supercooling was observed to increase which was suggested to be caused by the physical interaction existing between PCM molecules, and the three-dimensional foam structure. Also, the latent heat of melting and freezing was observed to be impacted by the PCM content; thus, increasing PCM loading from 76 to 90.8 wt% resulted in increasing the latent heat of melting from 80.5 to 105.2 J/g which indicated that the thermal properties of the prepared composite PCMs were influenced greatly by the total pore volume of the carbon foam.

5.5.4 Thermal properties of composite PCMs prepared via chemical shape stabilisation approaches

Chemical processes of enhancing the shape stability of solid–liquid PCMs involve combining the chosen PCM with the supporting material with the help of a suitable crosslinking agent. It is important that both the PCM and the supporting material consists of suitable functional groups which enables

the formation of chemical bonds called covalent bonds between them. Preparing chemically bonded composite PCMs via chemical approaches like chemical crosslinking is preferred over non-covalently bonded composite PCMs prepared via physical approaches since the latter exhibit drawbacks including poor mechanical performance and solvent resistance [216]. Also, if supporting material gets damaged by external forces or solvent, the PCM will suffer from leakage in addition to phase segregation due to poor compatibility between the PCM and the supporting material. Whereas covalently bonded composite PCMs acquire better mechanical performance and solvent resistance along with enhanced anti-leakage properties. In general, covalently bonded composite PCMs are prepared by reacting the chosen polymeric PCM like PEG with the chosen supporting material since PEG are susceptible to chemical modification due to the presence of plentiful of OH groups, while paraffins are saturated hydrocarbons which means they hardly react due to their inert nature [217,218]. Li et al. [181] prepared PEG10000/4,4′-diphenylmethane diisocyanate (MDI)/pentaerythritol (PE) composite PCM via chemical crosslinking. The latent heat of pure PEG10000 was reported to reduce from 189.45 to 152.97 J/g after chemical crosslinking which suggests possible weakening of the intrinsic endothermic and exothermic capacity of PEG due to the reduction in total number of crystallisable segments available attributed to the presence of the rigid benzene ring in the crosslinked structure. In addition, the crystalline regions had become smaller which was reflected by a decrease in phase transition temperature from 59.43 to 58.68°C. Chen et al. [219] prepared PEG10000/CA composite PCMs via electrospinning/crosslinking reaction with melting temperature and latent heat of 52.14°C and 36.72 J/g. The latent heat of PEG10000 was observed to have dropped by more than 50% in the composite which was attributed to the restriction of PEG phase due to the presence of interchain crosslinks within the molecules which caused confinement of PEG on the surface of the CA fibres during the phase transition process. Subjecting the crosslinked composite PCMs to 100 repeated heating and cooling cycles resulted in changing the melting temperature and latent heat from 52.14 to 52.12°C and 36.79 to 36.72 J/g, respectively. Thus, insignificant changes were caused to its thermal properties after thermal cycling exposure since the percentage difference was 0.038 and 0.19% which indicates that crosslinked composite PCMs have enhanced thermal stability which was accompanied by a reduction in the latent heat compared to the non-covalently bonded composite PCMs. Jiang et al. [199] prepared a series of PEG/cellulose acetate composite PCMs via crosslinking and discussed in their study the phenomenon

behind the reduction in latent heat of pure PEG after cross-linking. First, the crosslinked composite PCM consisted of cellulose acetate impurity which resulted in destructing the perfection of the crystallisation course. Second, end OH groups of PEG were attached onto the backbone of cellulose acetate which meant PEG was no more able to form crystals freely due to the confinement of its crystalline segments. Also, it was evaluated that if the composite contains low PEG content, the latent heat of resulting composite PCM will be almost zero since at extremely low concentrations PEG is unable to aggregate which is necessary for it to form crystals. Xi *et al.* [220] prepared novel polymeric solid–solid PCMs and reported that the latent heat of prepared composites was lower than the pure PCM due to the incorporation of support materials which makes no contribution to latent heat. Chen *et al.* [219] prepared PEG/cellulose acetate composite PCMs with latent heat capacity of 36.79 J/g *via* the chemical cross-linking approach for TES applications [219]. A novel PEG/MDI/(PE) tertiary cross-linking copolymer achieved a solid–solid phase change with phase transition temperature of 58.68°C and enthalpy of 152.97 kJ/kg *via* a two-step condensation reaction at 90°C for 24 h [181]. It is apparent that the solid–solid composite PCMs had enhanced thermal resistance; therefore, it was able to retain its solid state even when exposed to elevated temperature conditions. Chen *et al.* [179] prepared PEG10000/poly(glycidyl methacrylate) (PGMA) *via* chemical crosslinking. The latent heat of melting and freezing of pure PEG reduced after chemical crosslinking from 166.7 and 161.8 J/g to 69.8 and 73.2 J/g, and its melting temperature and freezing temperature reduced from 63.4 and 39.20°C to 55.9 and 31.1°C. This was attributed to the confinement of PEG molecular chain by PGMA skeleton which resulted in suppressing and partially restricting the orientation of the PEG molecules due to the steric effect which caused reduction in the crystallinity. Overall, the number of crystallisable segments and crystalline regions had reduced after crosslinking. This had impacted the intrinsic thermal performance of PEG negatively. Chen *et al.* [64] prepared paraffin/polyurethane (PU) composite PCMs containing PEG as soft segment *via* the bulk polymerisation approach. The phase transition temperature of the composite PCMs were observed to increase with the increase in the PEG content which was attributed to the attainment of a more ordered polymer which led to the enhancement of the crystalline properties of the resulting composite PCM. Three different paraffins, namely *n*-octadecane, *n*-eicosane, and paraffin were used to prepare the composite since this was predicted to enhance the latent heat and broaden the phase transition temperature of the resulting composite. As a result, two dips were observed in the heating cycle at 36.93 and 53.96 which indicates that no chemical bonds had formed in the composite PCM, instead weak intermolecular forces existed between the PCM and the supporting material. In the composite, insignificant changes were caused to the melting temperature of pure paraffin in the composite. However, increasing paraffin content reduced the latent heat and the melting temperature of the composite PCM because the lubrication of paraffin enhanced the mobility of the soft PEG chain. The synthesised composite PCMs were susceptible to thermal degradation when exposed to an elevated temperature of 300°C because this caused severe thermal destruction to the PEG chain present in the composite. Polarised optical microscopy (POM) analysis confirmed changes in crystallinity of PEG in the composite PCM. Hence, the spherulite size were observed to reduce with increasing 2,4-toluene diisocyanate (TDI) and 1,4-butanediol BDO (*e.g.* hard segment); therefore, the characteristic spherulite shape was not evident because the hard segment had reduced the degree of crystallisation significantly which is the main reason why the latent heat of the composite PCMs had changed after synthesis. Yanshan *et al.* [147] prepared a series of PEG/melamine/formaldehyde composite PCMs using PEG with different molecular weights (*e.g.* 1,000, 2,000, 4,000, 6,000, and 10,000) *via* condensation/crosslinking reaction. The latent heat of pure PEG was observed to have reduced in the composite PCMs mainly due to two reasons: (1) in the covalently crosslinked network structure, fewer crystallisable segments were available due to the fixation of nitrogen atoms in the end groups of PEG caused by the steric hindrance effect which resulted in reducing the crystallinity of PEG chains; and (2) reduced mobility of PEG chain and its fixed end groups meant that its crystal lattice was unable to arrange regularly to form perfect crystals. The melting temperature of pure PEG10000 and its composite was 61.46 and 54.84°C, respectively. Reduction in melting temperature was associated with the formation of covalent linkages near the end groups of PEG, *e.g.* bonds between PEG and nitrogen atoms from amino in melamine, which resulted in reducing the number of crystallisable segments of PEG available near the end groups of PEG.

PEGs are semicrystalline polymers which means they are comprised of both crystalline and amorphous phases. The degree of crystallinity also known as the crystallinity index (CI) can be calculated using the XRD data obtained from XRD analysis using equation (5), and it is conventionally used in previous literature to evaluate changes caused to the crystalline phases of PEG since this is known to affect its thermal properties like the latent heat capacity and the phase transition temperature. In addition, changes in the XRD patterns will indicate changes caused to the crystal morphology of PEG which impacts the thermal properties of PEG. Therefore, the current section will focus on studying the changes caused to the crystalline properties of PEG in

the different composite PCMs prepared in the previous literature since this is influenced by various factors including reaction condition, temperature, time, chemical composition of the reaction mixture, type of crosslinking agent, solvent, *etc.*

$$CI\ (\%) = \frac{\text{Area of crystalline peaks}}{\text{Area of crystalline and amorphous peaks}} \times 100\%. \quad (5)$$

Li and Ding [181] reported that the formation of the crosslinked network did not affect the crystal type since the XRD pattern of PEG remained almost unchanged after the chemical reaction; however, changes in the intensity of the crystalline peaks indicated that the size of the crystals of PEG had reduced which was attributed to the restricted mobility of PEG during the crystallisation process in the crosslinked network formed. Thus, the CI value of pristine PEG10000 was observed to have decreased insignificantly from 85.05 to 81.76% (*e.g.* 3.87% decrease) which suggested that the crystalline regions of PEG10000 was preserved and remained intact after chemical reaction. This is in good agreement with the DSC results which showed that the latent heat of melting of pristine PEG10000 had decreased from 189.45 to 152.97 kJ/kg (*e.g.* 19.26% decrease) due to the insignificant decrease in the number of crystalline phases. The POM images were in good agreement with the XRD results since it showed that the shape of PEG crystal did not change but the size of the crystals had reduced. Overall, PEG10000-based composite PCMs were observed to have good latent heat capacity because the chemical reaction was observed to cause no major changes to its crystallinity; however, the prepared composite PCMs were reported to have a melting temperature of 58.68°C which is outside the operating temperature range of building applications.

Li *et al.* [197] prepared a series of PEG-microcrystalline cellulose based composite PCMs using PEG of three different molecular weights, namely 1,100, 2,000, and 5,000 g/mol *via* the chemical stabilisation approach using MDI as crosslinking agent. The latent heat of melting of the prepared composite PCMs were reported to lie in the range of 46–153.6 J/g and was observed to depend mainly upon the molecular weight of PEG and the PEG content in wt% because composite PCM prepared using PEG5000 containing an optimum PEG content of 90.1 wt% was reported to have an optimum latent heat of melting of 153.6 J/g and a melting temperature of 58.9°C. Based on the experimental result, conclusion was made that increasing the PEG content (*e.g.* the working material) resulted in enhancing the latent heat capacity but this is not always true since PEG is a semicrystalline polymer; therefore, increasing PEG content does not only increase the crystalline phases but will

be accompanied by an increase in the number of amorphous phases. For PEG-cellulose composites containing 57.6, 70.5, and 77.4 wt% of PEG1100, the latent heat of melting was determined to be 46.0, 60.5, and 73.3 J/g which was much lower than the one of pristine PEG1100 which had an enthalpy of 140.3 J/g. Hence, crosslinking reaction had caused enthalpy of PEG1100 to decrease significantly which was attributed to the restricted mobility of the PEG chain due to the formation of the highly crosslinked structure. In addition, the incorporation of the amorphous cellulose resulted in destructing the perfection of the crystal lattice of PEG which resulted in decreasing the latent heat enthalpy of PEG drastically. The phase transition temperatures of pristine PEG experienced negligible changes since after chemical crosslinking, it was observed to reduce from 27.0 to 25.7, 25.1, and 26.0°C which was attributed to the reduced lamellae thickness of the crystals that led to the formation of low melting point crystals. Overall, the study demonstrated the possibility of preparing PEG–cellulose composite PCMs with latent heat in the range of 79.9–94.7 J/g and the phase transition temperature in the range of 26.0–27.0°C which is within the operating temperature of building applications. However, the main drawback of current study was the use of MDI crosslinking agent since it is toxic even though it enhances the thermal resistance of the resulting composite PCMs due to the introduction of the phenyl groups in the crosslinked structure [185].

Yanshan *et al.* [147] reported that the degree of crystallinity of PEG6000-based composites was lower than pristine PEG6000 which indicated that the crystallite size became larger after reaction. In addition, small amount of supporting material in the composite was reported to cause no significant changes in the crystallinity of PEG. Changes in crystallinity was confirmed with the POM images obtained. The characteristic cross petal shaped spherulites of PEG at room temperature was less apparent in the composite which confirms the reduction in PEG crystallinity in the composite PCMs. Sundararajan *et al.* [184] prepared PEG8000/hyperbranched composite PCMs *via* crosslinking and reported that reduction in latent heat was attributed to the interference of hard polyurethane segment with PEG during the crystallisation process. Also, formation of a highly branched structure was another cause for making PEG less crystallisable. However, increasing PEG content seemed to have a positive effect on its thermal properties; thus, with the increase in the PEG content, less hard segment and increased number of crystallisable segments were present in the composite which resulted in enhancing the crystallinity of PEG. POM images confirm that the crystallite size of PEG had reduced after chemical crosslinking reaction which indicates that

crystalline properties of PEG get changed after chemical reaction which may be due to elevated temperature exposure during reaction. Sari *et al.* [221] synthesised novel polystyrene-*co*-maleic anhydride (SMA)-graft-PEG copolymers as solid–solid PCMs (S-SPCMs) for solar passive TES applications. The phase transition temperature was in the range of 39–45°C, with latent heat capacity in the range of 107–155 J/g. Hence, the phase transition enthalpies and temperature were influenced greatly by the amount of PEG side chains bonded to the backbone. The resulting copolymers were reported to exhibit good thermal reliability and chemical stability even after 5,000 heating–cooling cycles because negligible changes in their LHTES properties was observed and no changes in their chemical structures occurred. Zhou *et al.* [222] prepared a novel PEG/cellulose nanocrystal (CNC) PCM *via* a UV-induced thiol-ene click chemistry and solvent exchange. Results showed that the loading capacity of PEG could be as high as 97% with latent heat capacity of 150 J/g. The phase transition of pristine PEG was observed to reduce from 40.1 to 33.5°C which was attributed to high specific area of CNC network, and the presence of strong intermolecular hydrogen bonds between PEG and CNC. Zhou *et al.* [223] prepared PCM/PVA composite PCMs and reported that changes in latent heat of PCM was attributed to the incorporation of supporting material and crosslinking agents since both make no contribution to latent heat. Also, increasing GA content (*e.g.* crosslinker content) was reported to cause no changes to the phase transition and latent heat of the composite PCMs, and subjecting the crosslinked composites to 100 repeated heating and cooling cycles only reduced the latent heat by 2 and 1 J/g. Yin *et al.* [224] prepared PEG6000/Poly (glycerol-itaconic acid) (PGI) composite PCMs with optimum PCM content of 72.67% and corresponding latent heat of 86.93 J/g. The crystallinity of the prepared composites was observed to be lower than the one of pure PEG6000 which was attributed to the incorporation of PGI which acts as an impurity to impact the crystallinity of PEG. Also, hydrogen bonds between PEG and PGI were also reported to influence the crystallinity of PEG. Increasing PCM content in the composites from 62.76% to 68.70% to 72.67% resulted in increasing the crystallinity from 50.15% to 60.78% to 60.95% which indicates that the mobility of the PEG chain appears to improve with the increase in the PCM content; thus, composite PCM containing optimum PCM content of 72.67% had the highest latent heat of melting of 86.93 J/g which suggests that composite PCMs with high crystallinity have higher number of crystallisable segments.

Kuru and Aksoy [225] prepared PEG-cellulose composite PCMs using PEG1000 and PEG2000 as PCMs, cotton waste as supporting material and GA as the crosslinking agent. The latent heat capacity and melting temperature of the prepared composite PCMs were in the range of 8.1–33.8 J/g and 17.3–51.2°C. The results demonstrated that using PEG with low molecular weights resulted in producing composite PCMs of poor thermal properties. Also, it had an operating temperature outside one of building applications. Qin *et al.* [226] prepared PEG based composite PCMs *via* the chemical process called free radical polymerisation and reported that the crystalline properties of pristine PEG experienced negligible changes after the chemical reaction because the two characteristic peak of pristine PEG4000 appearing at 2θ = 19.4 and 23.5° attributed to the lattice planes of (1 2 0) and (1 3 2) of the triclinic crystal remained intact. The XRD pattern of both PEG and the prepared composite PCMs were observed to be similar but in the XRD pattern of the prepared composite PCMs, a wide broad hump was observed at 2θ = 21.0° which confirmed the existence of amorphous structures in the crosslinked composite PCMs. The calculated CI values indicated that the formation of a crosslinked structure resulted in decreasing the crystallinity of PEG which was attributed to the increased number of amorphous phases in the PEG based composite PCMs. Overall, XRD results suggested that the crystal structure of PEG became less perfect after the chemical reaction which resulted in impacting its latent heat of melting and crystallisation negatively. Table 14 shows the relationship between design parameters and the thermal properties of prepared composite PCMs and outlines the characteristic properties and performance of PEG/cellulosic material based composite PCMs prepared in previous literature.

5.6 PCBMs

The investigation of PCM application in buildings predates 1980 owing to their intrinsic TES potential [227], which is reported to enhance the energy efficiency and thermal performance of buildings. In general, building applications of PCMs are divided into two parts: (1) combining PCM with the cooling/heating system for energy storage and (2) implementing PCBMs to construct the building envelope since the building envelope is responsible for regulating heat exchange between the outdoor and indoor environments; therefore, they influence greatly the quality and the control of the indoor conditions, irrespective of the outdoor conditions. Table 15 shows the thermal properties of PCMs used for the preparation of PCBMs and Table 16 summarises the properties of PCBMs prepared and investigated.

Table 14: Thermal properties of PEG-cellulose composite PCMs

Composite PCM (PCM/support material)	Design parameters	Thermal properties				Ref.
		Phase transition temperatures		Latent heat (J/g)		
		Melting point (°C)	Freezing point (°C)	Melting	Crystallisation	
PEG/cellulose diacetate (CDA) *via* crosslinking with PEG with molecular weight in the range 2,000 to 20,000 g/mol	1/3 and 1/10 weight of dried PEG and CDA was dissolved in acetone separately In PEG solution containing di-*n*-butyl tin dilaurate catalyst, TDI crosslinking agent was added dropwise and the resulting mixture was heated at 313 K for 4 h which resulted in producing a gel-like substance Complete desiccation of gel resulted in the formation of hard/solid product	—	—	—	—	[199]
PEG10000/PGMA	Unknown amount of PEG was dissolved in dichloromethane followed by the addition of succinic anhydride and pyridine solution under heating at 90°C under reflux for 24 h Final product was precipitated using ether and filtered off, washed with ether and dried in vacuum	55.90	31.10	73.20	69.80	[179]
Paraffin/ polyurethane (PU) *via* crosslinking	25 g of PEG6000 and 1 g of PDMS-b-PPO were placed in an oven at 100°C to prepare the melt	37.99; 58.91	—	46.25; 77.66	—	[64]
	3.78 g of 4,4'-diphenylmethane diisocyanate (L-MDI), 0.64 g of BDO, and required amount of n-octadecane was added and reaction mixture was stirred for 1 min at 1,000 rpm	27.81; 58.52	—	18.60; 104.2	—	
	The mixture was poured into a mould and placed in an oven at 100°C for 4 to 6 h	28.57; 57.81	—	34.56; 95.36	—	
		28.12; 57.18	—	40.52; 89.11	—	
		28.60; 58.14	—	30.83; 92.42	—	
PEG/melamine/ formaldehyde *via* crosslinking with PEG1000, PEG2000, PEG4000, PEG6000 and PEG10000 *via* condensation/ crosslinking	36 wt% of melamine and formaldehyde and unknown amount of PEG were added into a three necked round bottomed flask containing water with an overhead stirrer Reaction temperature was in the range of 30 to 70°C To obtain solid composite PCM, the reaction mixture was oven dried at 110°C until all water had evaporated	46.56	25.96	89.70	92.70	[147]
		49.13	28.30	91.10	85.30	
		55.50	35.31	103.10	97.90	
		57.75	36.88	109.40	103.90	
		54.84	32.30	95.60	96.20	
Solid–solid polymeric PCM *via* crosslinking	Polyethylene glycol monomethyl ether (MPEG) phase change unit was first reacted with TDI and *N*-hydroxymethylacrylamide at 40 °C for 6 hours to form a copolymer (PD) by modifying the hydrogen group present in MPEG	57.70	18.30	108.5	81.60	[220]
		55.80	11.70	90.30	63.40	

(Continued)

Table 14: *Continued*

Composite PCM (PCM/support material)	Design parameters	Thermal properties				Ref.
		Phase transition temperatures		Latent heat (J/g)		
		Melting point (°C)	Freezing point (°C)	Melting	Crystallisation	
	The copolymerisation of PD and phenyl ethylene then took place at 70 °C for 24 h to produce polymeric based solid–solid PCM (PD)	55.40 54.00 53.20	8.40 4.30 1.50	75.90 53.40 47.20	49.60 44.0 33.90	
PEG10000/cellulose acetate *via* electrospinning/crosslinking	15 wt% of cellulose acetate was added into acetone/dimethyl acetamide solution. 15 wt% of PEG10000 was added into this solution PEG/CA composites of thickness around 0.1 mm was immersed in10 wt% of TDI/ toluene solution at 40°C followed dropwise addition of dibutyltin dilaurate (*e.g.* catalyst) The resulting composites were oven dried at 30°C for 24 h	52.14	40.99	36.72	25.92	[219]
Dodecanol dodecanoate/polyvinyl alcohol (PVA) *via* electrospinning/crosslinking	To prepare PVA solution, 20 g of PVA was dissolved in mL of deionised water at 90°C for 3 h. In 60 mL of deionised water, 0.88 g of SDS and 0.22 g of span-80 (*e.g.*, emulsifiers) were added and stirred, followed by the addition of 10 g of PCM. The final reaction mixture was stirred at 10,000 rpm for 35 min	28.53 28.60	24.04 24.36	63.78 65.32	64.89 64.89	[223]
PEG6000/PGI *via* solvent free crosslinking	Unknown amounts of glycerol, Itaconic acid and PEG6000 was mixed under heating at 180°C for 6 h. This resulted in producing a light-yellow viscous oil	28.38 29.24	24.10 24.02	64.68 65.40 86.93	64.52 65.39 83.65	[224]
PEG10000/(MDI)/(PE) *via* crosslinking	Required amount of MDI was dissolved in dimethyl formamide (DMF) and added into a four-necked flask equipped with an agitator, and immersed in an oil bath at 65°C. Temperature of oil bath was increased to 90°C followed by the dropwise addition of PA-DMF within 2 h and continuing reaction for another 4 h afterwards. PEG10000-DMF solution within two hours, and reaction was allowed to continue for another 4 h and then 24 h. Reaction mixture was washed with deionised water and dried in an oven at 70°C for 30 min to obtain the composite PCMs	58.68	—	152.97	—	[181]
PEG8000/hyperbranched *via* crosslinking	0.001 mol of dried PEG8000 was melted and combined with slightly excess IPDI (crosslinking agent) in the presence of a catalyst, and reaction was carried out for 3 h at 70°C. Trimethylolpropane was added into the reaction mixture to promote the formation of the hyperbranched polymer. Product was vacuum oven dried					[184]

5.6.1 Shape stabilised composite PCMs in buildings

Major advantage of PCMs is that they can be incorporated virtually into all constituent building elements such as wall, floor, ceiling, and roof due to its easy installation process for the enhancement of the thermal performance and energy efficiency of buildings [63]. Different approaches have been used to combine PCM with the building envelope: direct incorporation, immersing incorporation, shape-stabilisation method, and encapsulation. In general, lightweight buildings are known to suffer from indoor temperature fluctuations which is attributed to their low thermal mass. Hence, literature reports that the indoor temperature of lightweight buildings (LWB) are usually 10°C higher than the outdoor temperature which results in decreasing the indoor thermal comfort level while increasing the energy consumption of air-conditioning [244]. Kuznik and Virgone [245] installed shape stabilised in LWB and the results showed that PCM was capable of effectively controlling indoor temperature fluctuations and increase during summer; thus, the optimum indoor temperature was decreased by 8.5°C. Kim et al. [246] demonstrated the possibility of stabilising the indoor room temperature and reducing the heating load in winter by installing a paraffin-polypropylene/elastomer composite PCM sheets of melting temperature in the range of 19.0–26.0°C and latent heat of 62.24 J/g on the floors, walls, and ceilings of a building. The power consumption of a hut without and with composite PCM sheets were 15.30 and 12.48 MJ. Thus, installation of PCM had resulted in reducing the power consumption by 18.40% and increasing the PCM installation area was observed to reduce the power consumption

further. Findings suggested that the effectiveness of PCMs in buildings depended mainly upon the PCM installation area, PCM content, and position of PCM. Yao et al. synthesised a novel composite PCM wallboard (PCMW) by a horizontal vacuum absorption rotate roller technique, in which paraffin and EP was used as the PCM and supporting material. They embedded the composite PCMs in the walls, and roofs of the test room of dimensions 1.7 m × 1.7 m × 2.2 m. PCMW can be used in building envelopes since they had sufficient latent heat capacities: latent heat of melting and freezing was 67.13 and 69.06 J/g, respectively. The latent heat values of PCMW were greater than the criterion (50 J/g), therefore fabricated composite PCMs are feasible to be utilised in buildings. The incremental cost of PCMW can be fully recovered in 5.84 years. The potential composites can be used to enhance the thermal comfort as well as the energy efficiency of buildings. Dodecanol is one of the commonly used fatty acid as PCM for the preparation of composite PCMs using different building materials. In 2013, Memon et al. [247] prepared Dodecanol/cement composite PCMs with a very low latent heat capacity of 18.39 J/g with a melting temperature of 21.06°C. Therefore, majority of current studies have worked on optimising the latent heat capacity of the resulting PCBMs. Concrete and cement are the most used building material; therefore, incorporating PCM in concrete and cement can reduce energy consumption of buildings greatly. One of the commonly employed methods of increasing the energy performance of the building envelope includes employing innovative super-insulating or functional mortars which are prepared by combing PCMs in cement mortars. Li et al. [248] incorporated cement mortar with EG and PCM with melting temperature and

Table 15: PCMs used for the preparation of PCBMs

Name	Latent heat of melting (kJ/kg)	Phase transition temperature (°C)	Ref.
Rubitherm 28 (RT28)	135.80	28.00	[228]
Rubitherm 27 (RT27)	98.14	27.00	[161,229,230]
n-octadecane	128.84	22.70	[231]
n-octadecane	186.50	29.90	[138]
n-Eicosane	185.89	29.87	[232]
n-octadecane/CaCl$_2$	84.37	29.19	[233]
n-paraffin	170.00	25.00	[234]
Paraffin n-octadecane	180.00	28.00	[235]
Capric acid-myristic eutectic PCM (75:25)	153.19	22.17	[236]
Graphite modified MPCM	124.80	27.70	[237]
Micronal PCM	110.00	26.00	[238]
Micronal DS 5001 X	110.00	23.00	[103]
Micronal DS 5038 X	110.00	26.00	[239]
Micronal DS5001	146.00	26.00	[240]
Micronal DS-5008X	102.60	23.50	[241]
Dodecanol	111.50	25.80	[242]
BioPCM Q25	250.00	25.00	[243]

Table 16: Summary of properties of different PCBMs

PCBM name	T_m (°C)	H_m (J/g)	T_c (°C)	H_c (J/g)	Highlights	Ref.
PCM/cement	—	—			• Optimum PCM content was 20% to produce mortar of acceptable compressive strength • Compressive strength reduced after incorporation of MPCM which was attributed to the increased porosity of the cement mortar	[259]
Capric acid-myristic PCM/cement	21.13	47.78	17.90	39.56	• CA-MA (eutectic PCM) had good compatibility with cement • The prepared composite PCMs had good thermal reliability since 1,000 repeated heating and cooling cycles resulted in reducing its latent heat by 5.0–5.9%	[236]
20%MPCM/cement	26.76	14.57	18.87	12.71	• MPCM was well distributed in the matrix, and good interfacial bonding existed between MPCM and cement in the composite	[228]
25%MPCM/cement	27.87	22.35	19.44	23.25	• Integration of boards containing 20% of MPCM/cement resulted in decreasing the maximum indoor temperature of the test room	
30%MPCM/cement	28.52	34.02	18.76	33.85	• An optimum MPCM content of 30% resulted in decreasing the compressive strength of cement mortar by 58.4%	
Dodecanol/cement	21.06	18.39	—	—	• Cement was able to retain 5% of PCM without seepage • TGA results confirmed that the prepared composite PCMs had good thermal and chemical stability	[247]
CenoPCM/cement mortar	23.8	119.83	22.7	128.84	• Incorporating cenoPCM in cement mortars resulted in causing lower reduction in the compressive strength which was attributed to the higher mechanical strength of the cenoPCM • 3% of PCM incorporation resulted in reducing the compressive strength by 10–15%	[231]
MPCM-SiO$_2$/gypsum	—	111.2	—	—	• Incorporating 15 wt% of MPCM in the gypsum composites presented the lowest agglomeration, and thus, MPCMs were observed to be distributed into the pores of gypsum • Addition of MPCM resulted in reducing the density of gypsum equal to or greater than 600 kg/m^3	[161]

latent heat capacity of 28.8°C and 209.3 kJ/kg and reported that the resulting composite PCMs had a melting temperature and latent heat capacity of 28.55°C and 183 kJ/kg. PCM incorporation had reduced the compressive strength of the cement mortar greatly; thus, results indicated that the optimum PCM content was less than 20% to produce functional cement mortars of adequate compressive strength of 5 MPa.

5.6.2 MPCMs in buildings

Main obstacle for long-term use of PCM in building application is that they are susceptible to leakage. Also, direct incorporation of PCM with building materials will influence their intrinsic properties by interacting with its building structure. Integrating MPCMs into conventional building materials can overcome this problem [249]. MPCMs since its introduction has commonly been applied in building materials for the preparation of PCBMs. The following paragraph describes the thermal performance of different PCBMs prepared in the past since the impacts caused by PCM to different building materials is known to vary; however, literature is yet to compile relevant information regarding this. Thereby, better understanding the compatibility between PCMs and the different building materials can be determined.

In general, incorporation of encapsulated PCMs in building material is considered crucial to avoid affecting the function and the intrinsic properties of the building material [231]. Gypsum plaster and boards are one of the most popular and conventionally used material in building construction of internal and external walls and ceilings because they are available at relatively low costs, have good fire-resistance and aesthetics, and are non-toxic. Therefore, gypsum board and/or plaster containing MPCMs have been used increasingly in surrounding wall construction of buildings for the optimisation of building energy performance. Schossig et al. [250] conducted both simulation and experiments for a duration of 5 years to investigate the feasibility of applying MPCMs in building materials. Cabeza et al. [251] conducted experiments to compare the performance of two small house sized cubicles: one with integrated MPCMs; and the other without MPCMs, for a duration of 6 months. They used PCM with a melting point of 26°C and a phase change enthalpy of 110 kJ/kg. Incorporating 5% of PCM in concrete resulted in producing composite PCM with compressive strength and tensile strength of 25 and 6 MPa. They reported that the results demonstrated a real opportunity in energy savings for buildings because energy storage in concrete walls integrated with MPCMs had enhanced its thermal inertia and caused reduction in the inner temperatures. Lee et al. [252] prepared microcapsules with

latent heat capacities of 210 J/g (23°C) and 200 J/g (24°C) and integrated these microcapsules into gypsum wallboards and olefin film for building materials. The thermal conductivity of gypsum board without PCM (0.144 W/m K) increased significantly. Gypsum board with PCM had a thermal conductivity in the range of 0.128–0.163 W/m K. Also, with the increase in the thickness of the olefin film, the thermal storage capacity inside the chamber increased. For practical applications, the thickness of PCM plate must not exceed 20 mm to cause significant reduction in the indoor fluctuation temperature [253]. The amount of PCM incorporated in the gypsum board dictates its thermal performance. Oliver [254] found that increasing the PCM content from 37.5 to 44.5% resulted in improving the thermal performance of the gypsum-based composite by 20% and concluded that 45 wt% of PCM incorporation was capable of absorbing five times the energy that traditional plasterboards could absorb. Barzin et al. [255] investigated the thermal performance of PCM impregnated gypsum board and reported that an energy saving of 93% was achieved which corresponded to a cost saving of 92% provided that PCM charging was facilitated by a combination of night ventilation and free cooling method since improper control strategy of PCM led to an increase in the amount of air-conditioning energy required. Borreguero et al. [256] studied the thermal performance of three gypsum boards one without PCM and two containing 4.7 and 7.5 wt% of Rubitherm® (RT27) MPCMs at an optimal core/coating mass ratio of 1.50. Results indicated that gypsum board incorporated with 7.5 wt% of MPCM could enhance the thermal comfort of the indoor conditions by either increasing or decreasing the room temperature by 1.3°C. Borreguero et al. [257] discovered that incorporating 15% of MPCM in the gypsum board could save 4.5 kW h of energy per operating cycle in a standard room covered with 1 m^3 of gypsum board; however, presence of MPCM in the pores of gypsum resulted in reducing its compressive strength which was attributed to the decreased bulk density of gypsum due to the modification of its porosity. Impregnating fresh concrete/or cement mortars with PCM is a traditional approach used to effectively enhance its energy efficiency. Moreover, it is reported to have an adverse effect on the mechanical strength of concrete. MPCMs are added into concrete and cement mortars to avoid PCM bleeding during the melting process. Cabeza et al. [251] reported that MPCM had real opportunity in energy savings for buildings since incorporation of MPCM in concrete wall caused significant enhancement of thermal inertia which subsequently resulted in decreasing the indoor temperature because for the enhancement of the thermal performance of buildings, the thermal conductivity of concrete needs to reduce and the TES capacity of concrete needs

to increase. Hunger *et al.* [104] reported that an inclusion of 4–5% of PCM with a phase transition temperature in the range 24–36°C optimised the thermal mass of concrete to 6,800 J/K which corresponded to an energy saving of up to 12% which was accompanied by a significant compressive strength loss; and 3% incorporation of PCM resulted in producing PCM-concrete with a compressive strength of 35 N/mm^2 which was reported as being acceptable for constructional purposes. Entrop *et al.* [258] investigated the effects of applying MPCM with a melting point of 23°C and latent heat capacity of 110 J/g. Results showed that concrete floors containing 5% of PCM was able to reduce the additional need of heating in houses. Also, concrete floors with a thickness of 50 mm were observed to have a large latent heat capacity but its charging period was too long. Overall, the main problem of incorporating PCMs encapsulated within an organic polymeric film *via* the microencapsulation approach is that it reduces the compressive strength of concrete drastically. Increasing the PCM content in cement mortar results in decreasing the thermal conductivity and the compressive strength which is attributed to the increased porosity of cement mortar after MPCM incorporation [259].

However, this problem was demonstrated to be overcome through the incorporation of macro-encapsulated PCMs since these techniques causes no intrinsic changes to the concrete because the PCM is stored in containers of desired shape. Metals like steel is conventionally used as the container for this purpose since they can overcome both the leakage problem and the inherently low thermal conductivity of PCMs. Dong *et al.* [260] encapsulated an optimum PCMs mass of 80.3% within hollow steel ball (HSB) containers with an outer diameter of 22 mm. To investigate the influence of PCM-HSB on the thermal performance and compressive strength of concrete, 25, 50, 75, and 100% of coarse aggregates in concrete was replaced with PCM-HSB, and results indicated that the compressive strength of concrete decreased with the increase in the PCM-HSB content. Cui *et al.* [261] reported that exceeding a replacement level of aggregates by 75% of PCM-HSB will cause severe reduction in the compressive strength of concrete (*e.g.* 55% reduction). Shi *et al.* [262] investigated the effects of using straight and hooked steel fibres on the compressive strength of concrete because steel fibres are reported to enhance the mechanical and thermal properties of concrete which is attributed to its high bending resistance, tensile strength, and thermal conductivity. Thus, incorporating steel fibres in concrete containing PCM-HSB as aggregate is known to improve the compressive strength concrete. Therefore, Cui *et al.* [263] used steel fibre reinforced PCM-HSB concrete for the enhancement of energy piles performance. Results showed that incorporating 0.70% of steel fibre in PCM-

HSB concrete resulted in enhancing the compressive strength by 63% and the heat capacity of concrete was also observed to have improved. Kuznik and Virgone [245] investigated experimentally, under controlled thermal and radiative effects, the thermal performance of a PCM composite wall containing 60% of microencapsulated paraffin within the copolymer in a full-scale test room. The tests were carried out in three different external climates: summer, winter, and mid-season, to evaluate the potential of PCM wallboards. Tested PCM could maintain the room air temperature within the comfort zone by reducing the maximum air temperature of the room to 4.2°C. Enhancement of thermal comfort is very critical in cases where the wall surface temperature is lower for PCMWs compared to the regular ones. Also, no thermal stratification was observed in the room containing PCM wallboard which indicated that natural convection existed with PCMWs.

6 Conclusion and insights for future work

A comprehensive investigation regarding the stabilisation of different solid–liquid PCMs using the encapsulation and shape stabilisation technology was investigated and analysed. Additionally, investigation on a selected number of PCBMs was performed to evaluate the thermal performance of PCBMs. Although PCMs and PCBMs have the potential to enhance the thermal efficiency of buildings when used for the construction of the building envelope, there is still scope for further research as summarised below:

1) There is a necessity to study the compatibility between PCM and different building materials in more detail for the optimisation of the interfacial bonding existing between them both which subsequently enhances the structural integrity of the resulting PCBM.

2) Comprehensive cost analysis for the stabilisation of PCM *via* encapsulation and shape stabilisation and for the fabrication of PCBMs was never reported. For the acceptance of this technology world-wide, it is essential to carry out an extensive cost analysis.

3) Encapsulation and shape stabilisation technologies rely mainly on using petroleum-based synthetic supporting materials. To promote green industry, biopolymers like cellulose, nanocellulose, or chitosan should be utilised instead, since they are available abundantly at lower costs.

4) A standard procedure for the development of composite PCMs and PCBMs is yet to be prepared. It would be necessary to propose and establish a standard mixing

code for the preparation of encapsulated PCMs and PCBMs meeting the requirements of various climatic conditions and of adequate thermal performance for the commercialisation of PCM technology on a large scale.

5) Majority of previous studies have investigated PCBMs, but the thermal properties are rarely reported. Fully understanding thermal behaviour is vital to widen the potential use of PCMs for the preparation of PCBMs of optimised thermal performance.

6) The energy saving potential of PCBMs depends mainly upon the intrinsic thermal properties of the chosen PCM. Most studies have selected a PCM with a phase transition temperature within the operating temperature range of building applications; however, studies could try incorporating PCMs with higher transition temperatures since they have higher latent heat capacities and because the results from previous literature showed that the phase transition temperature of PCM changed after being integrated with the chosen building component.

7) Numerous studies have evaluated the thermal properties of PCBMs using DSC analysis. However, the test sample is in milligrams, and therefore, is not a representative of the actual heat storage properties of the chosen PCBM. This could be replaced by the T-history approach since it is reported to produce more reliable test results.

8) Numerous papers have managed to convert PEG into a solid–solid PCM for TES applications only. However, understanding factors influencing the intrinsic phase change properties of PCM is crucial to promote the development of form stable PCMs of exceptional performance. Moreover, to widen the potential application of PCM-composites in building construction, it is essential to determine a synthesis route which enables the development of PCM-composites operating within the room temperature range.

9) Numerous design parameters including PCM, supporting material, and processing temperature tend to influence the thermal properties including the melting and freezing temperatures and the corresponding latent heats of the PCMs; however, extensive research on how each parameter impacts the phase change properties must be carried out to get a better understanding on its degree of influence. Also, the impact of processing temperature on the intrinsic properties of PCM needs to be investigated, studied, and evaluated since PCMs are sensitive to temperature.

Author contributions: All authors have accepted responsibility for the entire content of this manuscript and approved its submission.

Conflict of interest: The authors state no conflict of interest.

References

[1] Nazir H, Batool M, Bolivar Osorio FJ, Isaza-Ruiz M, Xu X, Vignarooban K, et al. Recent developments in phase change materials for energy storage applications: A review. Int J Heat Mass Transf. 2019;129:491–523. doi: 10.1016/j.ijheatmasstransfer.2018.09.126.

[2] Subin MC, Chowdhury S, Karthikeyan R. A review of upgradation of energy-efficient sustainable commercial greenhouses in Middle East climatic conditions. Open Agric. 2021;6:308–28. doi: 10.1515/opag-2021-0017.

[3] Cao X, Dai X, Liu J. Building energy-consumption status worldwide and the state-of-the-art technologies for zero-energy buildings during the past decade. Energy Build. 2016;128:198–213. doi: 10.1016/j.enbuild.2016.06.089.

[4] Al-Yasiri Q, Szabó M. Experimental study of PCM-enhanced building envelope towards energy-saving and decarbonisation in a severe hot climate. Energy Build. 2023;279:112680. doi: 10.1016/j.enbuild.2022.112680.

[5] Yan T, Wang RZ, Li TX, Wang LW, Fred IT. A review of promising candidate reactions for chemical heat storage. Renewable Sustainable Energy Rev. 2015;43:13–31. doi: 10.1016/j.rser.2014.11.015.

[6] Shin Y, Yoo D, il, Son K. Development of thermoregulating textile materials with microencapsulated Phase Change Materials (PCM). II. Preparation and application of PCM microcapsules. J Appl Polym Sci. 2005;97(3):910–5. doi: 10.10.1002/app.21438.

[7] Jamekhorshid A, Sadrameli SM, Farid M. A review of microencapsulation methods of phase change materials (PCMs) as a thermal energy storage (TES) medium. Renew Sus Energy Rev. 2014;31:531–42. doi: 10.1016/j.rser.2013.12.033.

[8] Hua W, Zhang L, Zhang X. Research on passive cooling of electronic chips based on PCM: A review. J Mol Liq. 2021;340:117183. doi: 10.1016/j.molliq.2021.117183.

[9] Mousavi S, Rismanchi B, Brey S, Aye L. PCM embedded radiant chilled ceiling: A state-of-the-art review. Renewable Sustainable Energy Rev. 2021;151:111601. doi: 10.1016/j.rser.2021.111601.

[10] Bielek B, Szabó D, Klem J, Kaniková K. Application of physical theory of cavity in the construction of double skin facades. Curved and Layered Struct. 2022;9:40–53. doi: 10.1515/cls-2022-0004.

[11] Gholamibozanjani G, Farid M. Application of an active PCM storage system into a building for heating/cooling load reduction. Energy. 2020;210:118572–81. doi: 10. 10.1016/j.energy.2020.118572.

[12] Jouhara H, Zabnienska-Gore A, Khordehgah N, Ahmad D, Lipinski T. Latent Thermal Energy Storage Technologies and Applications : A Review. Int J Thermofluid. 2020;6:100039. doi: 10.1016/j.ijft.2020.100039.

[13] Tatsidjodoung P, le Pierrès N, Luo L. A review of potential materials for thermal energy storage in building applications. Renewable Sustainable Energy Rev. 2013;18:327–49. doi: 10.1016/j.rser.2012.10.025.

[14] Xu J, Wang RZ, Li Y. A review of available technologies for seasonal thermal energy storage. Sol Energy. 2014;103:610–38. doi: 10.1016/j.solener.2013.06.006.

[15] Singh Rathore PK, Shukla SK, Gupta NK. Potential of microencapsulated PCM for energy savings in buildings: A critical review. Sustain Cities Soc. 2020;53:101884. doi: 10.1016/j.scs.2019.101884

[16] Yu X, Chang J, Huang R, Huang Y, Lu Y, Li Z, et al. Sensitivity analysis of thermophysical properties on PCM selection under steady and fluctuating heat sources: A comparative study. Appl Therm Eng. 2021;186:116527. doi: 10.1016/j.applthermaleng.2020.116527.

[17] Milián YE, Gutiérrez A, Grágeda M, Ushak S. A review on encapsulation techniques for inorganic phase change materials and the influence on their thermophysical properties. Renew Sus Energy Rev. 2017;73:983–99. doi: 10.1016/j.rser.2017.01.159.

[18] Salunkhe PB, Shembekar PS. A review on effect of phase change material encapsulation on the thermal performance of a system. Renew Sus Energy Rev. 2012;16:5603–16. doi: 10.1016/j.rser.2012.05.037.

[19] Koukou MK, Vrachopoulos MG, Tachos NS, Dogkas G, Lymperis K, Stathopoulos V. Experimental and computational investigation of a latent heat energy storage system with a staggered heat exchanger for various phase change materials. Thermal Sci and Eng Prog. 2018;7:87–98. doi: 10.1016/j.tsep.2018.05.004.

[20] Elias CN, Stathopoulos VN. A comprehensive review of recent advances in materials aspects of phase change materials in thermal energy storage. Energy Procedia. 2019;161:385–94. doi: 10.1016/j.egypro.2019.02.101.

[21] Yang X, Cai Z. An analysis of a packed bed thermal energy storage system using sensible heat and phase change materials. Int J Heat Mass Transf. 2019;144:118651. doi: 10.1016/j.ijheatmasstransfer.2019.118651.

[22] Wahid MA, Hosseini SE, Hussen HM, Akeiber HJ, Saud SN, Mohammad AT. An overview of phase change materials for construction architecture thermal management in hot and dry climate region. Appl Therm Eng. 2017;112:1240–59. doi: 10.1016/j.applthermaleng.2016.07.032.

[23] Kalaiselvam S, Parameshwaran R. Thermal energy storage technologies for sustainability. Academic Press; 2014.

[24] Sharma A, Tyagi Vv, Chen CR, Buddhi D. Review on thermal energy storage with phase change materials and applications. Renewable Sustainable Energy Rev. 2009;13:318–45. doi: 10.1016/j.rser.2007.10.005.

[25] Cárdenas B, León N. High temperature latent heat thermal energy storage: Phase change materials, design considerations and performance enhancement techniques. Renewable Sustainable Energy Rev. 2013;27:724–37. doi: 10.1016/j.rser.2013.07.028.

[26] Ayyappan S, Mayilsamy K, Sreenarayanan VV. Performance improvement studies in a solar greenhouse drier using sensible heat storage materials. Heat and Mass Transfer/Waerme- Und Stoffuebertragung. 2016;52:459–67. doi: 10.1007/s00231-015-1568-5.

[27] Tian Y, Zhao CY. A review of solar collectors and thermal energy storage in solar thermal applications. Appl Energy. 2013;104:538–53. doi: 10.1016/j.apenergy.2012.11.051.

[28] Rathore PKS, Shukla SK. Enhanced thermophysical properties of organic PCM through shape stabilization for thermal energy storage in buildings: A state of the art review. Energy Build. 2021;236:110799. doi: 10.1016/j.enbuild.2021.110799.

[29] Khomein P, Nallapaneni A, Lau J, Lilley D, Zhu C, Kaur S, et al. Random copolymer of poly(polyethylene glycol methyl ether) methacrylate as tunable transition temperature solid–solid phase change material for thermal energy storage. Solar Energy Materials and Solar Cells. 2021;225. doi: 10.1016/j.solmat.2021.111030.

[30] Gotoh R, Totani T, Wakita M, Nagata H. Controlling heat release of crystallization from supercooling state of a solid–solid PCM, 2-amino-2-methyl-1,3-propanediol. Int J Heat Mass Transf. 2019;137:1132–40. doi: 10.1016/j.ijheatmasstransfer.2019.03.151.

[31] Rao VV, Parameshwaran R, Ram VV. PCM-mortar based construction materials for energy efficient buildings: A review on research trends. Energy Build. 2018;158:95–122. doi: 10.1016/j.enbuild.2017.09.098.

[32] Piselli C, Prabhakar M, de Gracia A, Saffari M, Pisello AL, Cabeza LF. Optimal control of natural ventilation as passive cooling strategy for improving the energy performance of building envelope with PCM integration. Renew Energy. 2020;162:171–81. doi: 10.1016/j.renene.2020.07.043.

[33] Alehosseini E, Jafari SM. Nanoencapsulation of phase change materials (PCMs) and their applications in various fields for energy storage and management. Adv Colloid Interface Sci. 2020;283:102226. doi: 10.1016/j.cis.2020.102226.

[34] Skurkytė-Papievienė V, Abraitienė A, Sankauskaitė A, Rubezienė V, Dubinskaitė K. Enhancement of thermal properties of bio-based microcapsules intended for textile applications. Open Chem. 2020;18:669–80. doi: 10.1515/chem-2020-0064.

[35] Yun H, Zhang X. Fabrication and characterization of hexadecyl acrylate cross-linked phase change microspheres. E-Polymers. 2020;20:69–75. doi: 10.1515/epoly-2020-0008.

[36] Mehrpooya M, Pakzad P. Introducing a hybrid mechanical – Chemical energy storage system: Process development and energy/exergy analysis. Energy Convers Manag. 2020;211:112784. doi: 10.1016/j.enconman.2020.112784.

[37] Sunku Prasad J, Muthukumar P, Desai F, Basu DN, Rahman MM. A critical review of high-temperature reversible thermochemical energy storage systems. Appl Energy. 2019;254:113733. doi: 10.1016/j.apenergy.2019.113733.

[38] Clark RJ, Mehrabadi A, Farid M. State of the art on salt hydrate thermochemical energy storage systems for use in building applications. J Energy Storage. 2020;27:101145. doi: 10.1016/j.est.2019.101145.

[39] Li W, Klemeš JJ, Wang Q, Zeng M. Salt hydrate–based gas-solid thermochemical energy storage: Current progress, challenges, and perspectives. Renew Sus Energy Rev. 2022;154:111846. doi: 10.1016/j.rser.2021.111846.

[40] Prieto C, Cooper P, Fernández AI, Cabeza LF. Review of technology: Thermochemical energy storage for concentrated solar power plants. Renew Sus Energy Rev. 2016;60:909–29. doi: 10.1016/j.rser.2015.12.364.

[41] Vadhera J, Sura A, Nandan G, Dwivedi G. Study of Phase Change materials and its domestic application. Mater Today Proc. 2018;5:3411–7. doi: 10.1016/j.matpr.2017.11.586.

[42] Sari A, Alkan C, Özcan AN. Synthesis and characterization of micro/nano capsules of PMMA/capric-stearic acid eutectic

mixture for low temperature-thermal energy storage in buildings. Energy Build. 2015;90:106–13. doi: 10.1016/j.enbuild.2015.01.013.

[43] Sari A, Alkan C, Döğüşcü DK, Kizil C. Micro/nano encapsulated n-tetracosane and n-octadecane eutectic mixture with polystyrene shell for low-temperature latent heat thermal energy storage applications. Sol Energy. 2015;115:195–203. doi: 10.1016/j.solener.2015.02.035.

[44] Butala V, Stritih U. Experimental investigation of PCM cold storage. Energy Build. 2009;41:354–9. doi: 10.1016/j.enbuild.2008.10.008.

[45] Kahraman D, Biçer A, Sar A, Alkan C. Microencapsulated n-alkane eutectics in polystyrene for solar thermal applications. Sol Energy. 2018;160:32–42. doi: 10.1016/j.solener.2017.11.072.

[46] ben Romdhane S, Amamou A, ben Khalifa R, Saïd NM, Younsi Z, Jemni A. A review on thermal energy storage using phase change materials in passive building applications. J Build Eng. 2020;32:101563. doi: 10.1016/j.jobe.2020.101563.

[47] Mishra A, Shukla A, Sharma A. Latent heat storage through phase change materials. Resonance. 2015;20:532–41. doi: 10.1007/s12045-015-0212-5

[48] Amaral C, Vicente R, Marques PAAP, Barros-Timmons A. Phase change materials and carbon nanostructures for thermal energy storage: A literature review. Renewable Sustainable Energy Rev. 2017;79:1212–28. doi: 10.1016/j.rser.2017.05.093.

[49] Shamseddine I, Pennec F, Biwole P, Fardoun F. Supercooling of phase change materials: A review. Renewable Sustainable Energy Rev. 2022;158:112172. doi: 10.1016/j.rser.2022.112172.

[50] Zhang XX, Fan YF, Tao XM, Yick KL. Crystallization and prevention of supercooling of microencapsulated n-alkanes. J Colloid Interface Sci. 2005;281:299–306. doi: 10.1016/j.jcis.2004.08.046.

[51] Zahir MH, Mohamed SA, Saidur R, Al-Sulaiman FA. Supercooling of phase-change materials and the techniques used to mitigate the phenomenon. Appl Energy. 2019;240:793–817. doi: 10.1016/j.apenergy.2019.02.045.

[52] Xiao M, Feng B, Gong K. Preparation and performance of shape stabilized phase change thermal storage materials with high thermal conductivity. Energy Convers Manag. 2002;43:103–8. doi: 10.1016/S0196-8904(01)00010-3.

[53] Cui Y, Xie J, Liu J, Wang J, Chen S. A review on phase change material application in building. Advances in Mechanical Engineering. 2017;9:1–15. doi: 10.1177/1687814017700828.

[54] Farid MM, Khudhair AM, Razack SAK, Al-Hallaj S. A review on phase change energy storage: Materials and applications. Energy Convers Manag. 2004;45:1597–615. doi: 10.1016/j.enconman.2003.09.015.

[55] Huo X, Li W, Wang Y, Han N, Wang J, Wang N, et al. Chitosan composite microencapsulated comb-like polymeric phase change material via coacervation microencapsulation. Carbohydr Polym. 2018;200:602. doi: 10. 10.1016/j.carbpol.2018.08.003.

[56] Bayon A, Liu M, Sergeev D, Grigore M, Bruno F, Müller M. Novel solid–solid phase-change cascade systems for high-temperature thermal energy storage. Sol Energy. 2019;177:274–83. doi: 10.1016/j.solener.2018.10.085.

[57] Huang X, Guo J, He J, Gong Y, Wang D, Song Z. Novel phase change materials based on fatty acid eutectics and triallyl isocyanurate composites for thermal energy storage. J Appl Polym Sci. 2017;134:1–8. doi: 10.1002/app.44866.

[58] Silva T, Vicente R, Rodrigues F. Literature review on the use of phase change materials in glazing and shading solutions.

Renewable Sustainable Energy Rev. 2016;53:515–35. doi: 10.1016/j.rser.2015.07.201.

[59] Sarier N, Onder E. Organic phase change materials and their textile applications: An overview. Thermochim Acta. 2012;540:7–60. doi: 10.1016/j.tca.2012.04.013.

[60] Kahwaji S, Johnson MB, Kheirabadi AC, Groulx D, White MA. A comprehensive study of properties of paraffin phase change materials for solar thermal energy storage and thermal management applications. Energy. 2018;162:1169–82. doi: 10.1016/j.energy.2018.08.068.

[61] Zhang H, Sun S, Wang X, Wu D. Fabrication of microencapsulated phase change materials based on n-octadecane core and silica shell through interfacial polycondensation. Colloids Surf A Physicochem Eng Asp. 2011;389:104–17. doi: 10.1016/j.colsurfa.2011.08.043.

[62] Zhang Z, Fang X. Study on paraffin/expanded graphite composite phase change thermal energy storage material. Energy Convers Manag. 2006;47:303. doi: 10. 10.1016/j.enconman.2005.03.004.

[63] Akeiber H, Nejat P, Majid MZA, Wahid MA, Jomehzadeh F, Zeynali Famileh I, et al. A review on phase change material (PCM) for sustainable passive cooling in building envelopes. Renew SusEnergy Rev. 2016;60:1470–97. doi: 10.1016/j.rser.2016.03.036.

[64] Chen K, Yu X, Tian C, Wang J. Preparation and characterization of form-stable paraffin/polyurethane composites as phase change materials for thermal energy storage. Energy Convers Manag. 2014;77:13–21. doi: 10.1016/j.enconman.2013.09.015.

[65] Wang X, Li W, Luo Z, Wang K, Shah SP. A critical review on phase change materials (PCM) for sustainable and energy efficient building: Design, characteristic, performance and application. Energy Build. 2022;260:111923. doi: 10.1016/j.enbuild.2022.111923.

[66] Shafigh P, Asadi I, Mahyuddin NB. Concrete as a thermal mass material for building applications - A review. J Build Eng. 2018;19:14–25. doi: 10.1016/j.jobe.2018.04.021.

[67] Behzadi S, Farid MM. Long term thermal stability of organic PCMs. Appl Energy. 2014;122:11–6. doi: 10.1016/j.apenergy.2014.01.032.

[68] Fang G, Li H, Chen Z, Liu X. Preparation and properties of palmitic acid/SiO2 composites with flame retardant as thermal energy storage materials. Solar Energy Mater Solar Cells. 2011;95:1875–81. doi: 10.1016/j.solmat.2011.02.010.

[69] Alkan C, Sari A. Fatty acid/poly(methyl methacrylate) (PMMA) blends as form-stable phase change materials for latent heat thermal energy storage. Sol Energy. 2008;82:118–24. doi: 10.1016/j.solener.2007.07.001.

[70] Sari A, Karaipekli A. Preparation, thermal properties and thermal reliability of palmitic acid/expanded graphite composite as form-stable PCM for thermal energy storage. Solar Energy Mater Solar Cells. 2009;93:571–6. doi: 10.1016/j.solmat.2008.11.057.

[71] Abhat A. Low temperature latent heat thermal energy storage: Heat storage materials. Sol Energy. 1983;30:313–32. doi: 10.1016/0038-092X(83)90186-X.

[72] Ma G, Sun J, Zhang Y, Jing Y, Jia Y. Preparation and thermal properties of stearic acid-benzamide eutectic mixture/expanded graphite composites as phase change materials for thermal energy storage. Powder Technol. 2019;342:131–40. doi: 10.1016/j.powtec.2018.09.074.

[73] Wilhelm E, Richter C, Rapp BE. Phase change materials in microactuators: Basics, applications and perspectives. Sens Actuators A Phys. 2018;271:303–47. doi: 10.1016/j.sna.2018.01.043.

[74] Krieghoff J, Gronbach M, Schulz-Siegmund M, Hacker MC. Biodegradable macromers for implant bulk and surface engineering. Biol Chem. 2021;402:1357–74. doi: 10.1515/hsz-2021-0161.

[75] Lucht N, Hinrichs S, Gro ßmann L, Pelz C, Felgenhauer E, Clasen E, et al. Synthesis of magnetic ferrogels: A tool-box approach for finely tuned magnetic- and temperature-dependent properties. Phys Sci Rev. 2021;14:0120. doi: 10.1515/psr-2019-0120.

[76] Sarı A, Bicer A, Al-Sulaiman FA, Karaipekli A, Tyagi VV. Diatomite/CNTs/PEG composite PCMs with shape-stabilized and improved thermal conductivity: Preparation and thermal energy storage properties. Energy Build. 2018;164:166–75. doi: 10.1016/j.enbuild.2018.01.009.

[77] Deng Y, Yang L. Preparation and characterization of polyethylene glycol (PEG) hydrogel as shape-stabilized phase change material. Appl Therm Eng. 2017;114:1014–7. doi: 10.1016/j.applthermaleng.2016.11.207.

[78] Yang J, Qi GQ, Liu Y, Bao RY, Liu ZY, Yang W, et al. Hybrid graphene aerogels/phase change material composites: Thermal conductivity, shape-stabilization and light-to-thermal energy storage. Carbon N Y. 2016;100:693–702. doi: 10.1016/j.carbon.2016.01.063.

[79] Zhang L, Zhang P, Wang F, Kang M, Li R, Mou Y, et al. Phase change materials based on polyethylene glycol supported by graphene-based mesoporous silica sheets. Appl Therm Eng. 2016;101:217–23. doi: 10.1016/j.applthermaleng.2016.02.120.

[80] Wang H, Yuan Y, Rong M, Zhang M. Microencapsulation of styrene with melamine-formaldehyde resin. Colloid Polym Sci. 2009;287:1089–97. doi: 10.1007/s00396-009-2072-6.

[81] Wang W, Yang X, Fang Y, Ding J, Yan J. Preparation and thermal properties of polyethylene glycol/expanded graphite blends for energy storage. Appl Energy. 2009;86:1479–83. doi: 10.1016/j.apenergy.2008.12.004.

[82] Mondal S. Phase change materials for smart textiles - An overview. Appl Therm Eng. 2008;28:1536–50. doi: 10.1016/j.applthermaleng.2007.08.009.

[83] Fashandi M, Leung SN. Preparation and characterization of 100% bio-based polylactic acid/palmitic acid microcapsules for thermal energy storage. Mater Renew Sustain Energy. 2017;6:1–10. doi: 10.1007/s40243-017-0098-0.

[84] Kenisarin M, Mahkamov K. Salt hydrates as latent heat storage materials:Thermophysical properties and costs. Solar Energy Materials and Solar Cells. 2016;145:255–86. doi: 10.1016/j.solmat.2015.10.029.

[85] Huang J, Wang T, Zhu P, Xiao J. Preparation, characterization, and thermal properties of the microencapsulation of a hydrated salt as phase change energy storage materials. Thermochim Acta. 2013;557:1–6. doi: 10.1016/j.tca.2013.01.019.

[86] Li Y, Li C, Lin N, Xie B, Zhang D, Chen J. Review on tailored phase change behavior of hydrated salt as phase change materials for energy storage. Mater Today. Energy. 2021;22:100866. doi: 10.1016/j.mtener.2021.100866.

[87] Wang G, Xu C, Wei G, Du X. Numerical study of a novel dual-PCM thermal energy storage structure filled with inorganic salts and metal alloy as the PCMs. Energy Procedia. 2019;158:4423–8. doi: 10.1016/j.egypro.2019.01.774.

[88] Maruoka N, Sato K, Yagi JI, Akiyama T. Development of PCM for recovering high temperature waste heat and utilization for producing hydrogen by reforming reaction of methane. ISIJ Int. 2002;42:215–9. doi: 10.2355/isijinternational.42.215.

[89] Wang Y, Zhang Y, Xia T, Zhao W, Yang W. Effects of fabricated technology on particle size distribution and thermal properties of stearic-eicosanoic acid/polymethylmethacrylate nanocapsules. Solar Energy Mater Solar Cells. 2014;120:481–90. doi: 10.1016/j.solmat.2013.09.028.

[90] el Karim Y, Grosu Y, Faik A, Lbibb R. Investigation of magnesium-copper eutectic alloys with high thermal conductivity as a new PCM for latent heat thermal energy storage at intermediate-high temperature. J Energy Storage. 2019;26:100974. doi: 10.1016/j.est.2019.100974.

[91] Blanco-Rodríguez P, Rodríguez-Aseguinolaza J, Gil A, Risueño E, D'Aguanno B, Loroño I, et al. Experiments on a lab scale TES unit using eutectic metal alloy as PCM. Energy Procedia. 2015;69:769–78. doi: 10.1016/j.egypro.2015.03.087.

[92] Dindi A, Lopez Ferber N, Gloss D, Rilby E, Calvet N. Compatibility of an Aluminium-Silicon metal alloy-based phase change material with coated stainless-steel containers. J Energy Storage. 2020;32:101961. doi: 10.1016/j.est.2020.101961.

[93] Kalnæs SE, Jelle BP. Phase change materials and products for building applications: A state-of-the-art review and future research opportunities. Energy Build. 2015;94:150–76. doi: 10.1016/j.enbuild.2015.02.023.

[94] Su W, Darkwa J, Kokogiannakis G. Review of solid–liquid phase change materials and their encapsulation technologies. Renew Sus Energy Rev. 2015;48:373–91. doi: 10.1016/j.rser.2015.04.044.

[95] Madene A, Jacquot M. Review flavour encapsulation and controlled release – a review. Int J Food Sci Technol. 2006;41:1–21. doi: 10.1111/j.1365-2621.2005.00980.x.

[96] Hawlader MNA, Uddin MS, Khin MM. Microencapsulated PCM thermal-energy storage system. Appl Energy. 2003;74:195–202. doi: 10.1016/S0306-2619(02)00146-0.

[97] Comunian TA, Favaro-Trindade CS. Microencapsulation using biopolymers as an alternative to produce food enhanced with phytosterols and omega-3 fatty acids: A review. Food Hydrocoll. 2016;61:442–57. doi: 10.1016/j.foodhyd.2016.06.003.

[98] Chen W, Lv G, Hu W, Li D, Chen S, Dai Z. Synthesis and applications of graphene quantum dots: A review. Nanotechnol Rev. 2018;7:157–85. doi: 10.1515/ntrev-2017-0199.

[99] Liu Z, Yu ZJ, Yang T, Qin D, Li S, Zhang G, et al. A review on macro-encapsulated phase change material for building envelope applications. Build Environ. 2018;144:281–94. doi: 10.1016/j.buildenv.2018.08.030.

[100] Magdalena A, Pop A, Cimpeanu C, Turcus V. Nanoencapsulation techniques for compounds and products with antioxidant and antimicrobial activity - A critical view. Eur J Med Chem. 2018;157:1326–45. doi: 10.1016/j.ejmech.2018.08.076.

[101] Zangabad PS, Mirkiani S, Shahsavari S, Masoudi B, Masroor M, Hamed H, et al. Stimulus-responsive liposomes as smart nano-platforms for drug delivery applications. Nanotechnol Rev. 2018;7:95–122. doi: 10.1515/ntrev-2017-0154.

[102] Li J, Yao M, Shao Y, Yao D. The application of bio-nanotechnology in tumor diagnosis and treatment: A view. Nanotechnol Rev. 2018;7:257–66. doi: 10.1515/ntrev-2018-0011.

[103] Eddhahak-Ouni A, Drissi S, Colin J, Neji J, Care S. Experimental and multi-scale analysis of the thermal properties of Portland cement concretes embedded with microencapsulated Phase Change Materials (PCMs). Appl Therm Eng. 2014;64:32–9. doi: 10.1016/j.applthermaleng.2013.11.050.

[104] Hunger M, Entrop AG, Mandilaras I, Brouwers HJH, Founti M. The behavior of self-compacting concrete containing micro-

encapsulated phase change materials. Cem Concr Compos. 2009;31:731–43. doi: 10.1016/j.cemconcomp.2009.08.002.

[105] Jamekhorshid A, Sadrameli SM, Farid M. A review of microencapsulation methods of phase change materials (PCMs) as a thermal energy storage (TES) medium. Renewable Sustainable Energy Rev. 2014;31:531–42. doi: 10.1016/j.rser.2013.12.033.

[106] Martins IM, Barreiro MF, Coelho M, Rodrigues AE. Microencapsulation of essential oils with biodegradable polymeric carriers for cosmetic applications. Chem Eng J. 2014;245:191–200. doi: 10.1016/j.cej.2014.02.024.

[107] Tyagi Vv, Kaushik SC, Tyagi SK, Akiyama T. Development of phase change materials based microencapsulated technology for buildings: A review. Renewable Sustainable Energy Rev. 2011;15:1373–91. doi: 10.1016/j.rser.2010.10.006.

[108] Chanda S, Bajwa DS. A review of current physical techniques for dispersion of cellulose nanomaterials in polymer matrices. Rev Adv Mater Sci. 2021;60:325–41. doi: 10.1515/rams-2021-0023.

[109] Ng DQ, Tseng YL, Shih YF, Lian HY, Yu YH. Synthesis of novel phase change material microcapsule and its application. Polymer (Guildf). 2017;133:250–62. doi: 10.1016/j.polymer.2017.11.046.

[110] Alva G, Lin Y, Liu L, Fang G. Synthesis, characterization and applications of microencapsulated phase change materials in thermal energy storage: A review. Energy Build. 2017;144:276–94. doi: 10.1016/j.enbuild.2017.03.063.

[111] Methaapanon R, Kornbongkotmas S, Ataboonwongse C, Soottitantawat A. Microencapsulation of n-octadecane and methyl palmitate phase change materials in silica by spray drying process. Powder Technol. 2020;361:910–6. doi: 10.1016/j.powtec.2019.10.114.

[112] Arpagaus C, Collenberg A, Rütti D, Assadpour E, Jafari SM. Nano spray drying for encapsulation of pharmaceuticals. Int J Pharm. 2018;546:194–214. doi: 10.1016/j.ijpharm.2018.05.037.

[113] Samantha SC, Bruna ASM, Adriana RM, Fabio B, Sandro AR, Aline RCA. Drying by spray drying in the food industry: Microencapsulation, process parameters and main carriers used. African. J Food Sci. 2015;9:462–70. doi: 10.5897/ajfs2015.1279.

[114] Bhat A, Budholiya S, Raj SA, Sultan MTH, Hui D, Shah AUM, et al. Review on nanocomposites based on aerospace applications. Nanotechnol Rev. 2021;10:237–53. doi: 10.1515/ntrev-2021-0018.

[115] Rajabi H, Ghorbani M, Mahdi S, Sadeghi A, Rajabzadeh G. Food Hydrocolloids Retention of saffron bioactive components by spray drying encapsulation using maltodextrin, gum Arabic and gelatin as wall materials. Food Hydrocoll. 2015;51:327–37. doi: 10.1016/j.foodhyd.2015.05.033.

[116] Sivanathan A, Dou Q, Wang Y, Li Y, Corker J, Zhou Y, et al. Phase change materials for building construction: An overview of nano-/micro-encapsulation. Nanotechnol Rev. 2020;9:896–921. doi: 10.1515/ntrev-2020-0067.

[117] Borreguero AM, Valverde JL, Rodríguez JF, Barber AH, Cubillo JJ, Carmona M. Synthesis and characterization of microcapsules containing Rubitherm®RT27 obtained by spray drying. Chem Eng J. 2011;166:384–90. doi: 10.1016/j.cej.2010.10.055.

[118] Fei B, Lu H, Qi K, Shi H, Liu T, Li X, et al. Multi-functional microcapsules produced by aerosol reaction. J Aerosol Sci. 2008;39:1089–98. doi: 10.1016/j.jaerosci.2008.07.007.

[119] Wu W, Bostanci H, Chow LC, Ding SJ, Hong Y, Su M, et al. Jet impingement and spray cooling using slurry of nanoencapsulated phase change materials. Int J Heat Mass Transf. 2011;54:2715–23. doi: 10.1016/j.ijheatmasstransfer.2011.03.022.

[120] Es-haghi H, Mirabedini SM, Imani M, Farnood RR. Preparation and characterization of pre-silane modified ethyl cellulose-based microcapsules containing linseed oil. Colloids Surf A Physicochem Eng Asp. 2014;447:71–80. doi: 10.1016/j.colsurfa.2014.01.021.

[121] Lin Y, Zhu C, Alva G, Fang G. Microencapsulation and thermal properties of myristic acid with ethyl cellulose shell for thermal energy storage. Appl Energy. 2018;231:494–501. doi: 10.1016/j.apenergy.2018.09.154.

[122] Wang F, Zhang Y, Li X, Wang B, Feng X, Xu H, et al. Cellulose nanocrystals-composited poly (methyl methacrylate) encapsulated n-eicosane via a Pickering emulsion-templating approach for energy storage. Carbohydr Polym. 2020;234:115934. doi: 10.1016/j.carbpol.2020.115934.

[123] Xing J, Zhou Y, Yang K, Chang J, Yu Y, Cai L, et al. Microencapsulation of fatty acid eutectic with polyvinyl chloride shell used for thermal energy storage. J Energy Storage. 2021;34:101998. doi: 10.1016/j.est.2020.101998.

[124] Giro-Paloma J, Martínez M, Cabeza LF, Fernández AI. Types, methods, techniques, and applications for microencapsulated phase change materials (MPCM): A review. Renew Sus Energy Rev. 2016;53:1059–75. doi: 10.1016/j.rser.2015.09.040.

[125] Liu C, Rao Z, Zhao J, Huo Y, Li Y. Review on nanoencapsulated phase change materials: Preparation, characterization and heat transfer enhancement. Nano Energy. 2015;13:814–26. doi: 10.1016/j.nanoen.2015.02.016.

[126] Li W, Zhang XX, Wang XC, Niu JJ. Preparation and characterization of microencapsulated phase change material with low remnant formaldehyde content. Mater Chem Phys. 2007;106:437–42. doi: 10.1016/j.matchemphys.2007.06.030.

[127] Zhang XX, Fan YF, Tao XM, Yick KL. Fabrication and properties of microcapsules and nanocapsules containing n-octadecane. Mater Chem Phys. 2004;88:300–7. doi: 10.1016/j.matchemphys.2004.06.043.

[128] Zhang H, Wang X. Fabrication and performances of microencapsulated phase change materials based on n-octadecane core and resorcinol-modified melamine-formaldehyde shell. Colloids Surf A Physicochem Eng Asp. 2009;332:129–38. doi: 10.1016/j.colsurfa.2008.09.013

[129] Sánchez L, Sánchez P, Carmona M, de Lucas A, Rodríguez JF. Influence of operation conditions on the microencapsulation of PCMs by means of suspension-like polymerization. Colloid Polym Sci. 2008;286:1019–27. doi: 10.1007/s00396-008-1864-4.

[130] Sánchez P, Sánchez-Fernandez MV, Romero A, Rodríguez JF, Sánchez-Silva L. Development of thermo-regulating textiles using paraffin wax microcapsules. Thermochim Acta. 2010;498:16–21. doi: 10.1016/j.tca.2009.09.005.

[131] Sánchez L, Sánchez P, de Lucas A, Carmona M, Rodríguez JF. Microencapsulation of PCMs with a polystyrene shell. Colloid Polym Sci. 2007;285:1377–85. doi: 10.1007/s00396-007-1696-7.

[132] You M, Wang X, Zhang X, Zhang L, Wang J. Microencapsulated n-Octadecane with styrene-divinybenzene co-polymer shells. J Polym Res. 2011;18:49–58. doi: 10.1007/s10965-010-9390-8.

[133] Liang C, Lingling X, Hongbo S, Zhibin Z. Microencapsulation of butyl stearate as a phase change material by interfacial polycondensation in a polyurea system. Energy Convers Manag. 2009;50:723–9. doi: 10.1016/j.enconman.2008.09.044.

[134] Cho JS, Kwon A, Cho CG. Microencapsulation of octadecane as a phase-change material by interfacial polymerization in an emulsion system. Colloid Polym Sci. 2002;280:260–6. doi: 10.1007/s00396-001-0603-x.

[135] Zhan S, Chen S, Chen L, Hou W. Preparation and characterization of polyurea microencapsulated phase change material by interfacial polycondensation method. Powder Technol. 2016;292:217–22. doi: 10.1016/j.powtec.2016.02.007.

[136] Zhang H, Wang X. Synthesis and properties of microencapsulated n-octadecane with polyurea shells containing different soft segments for heat energy storage and thermal regulation. Solar Energy Materials and Solar Cells. 2009;93:1366–76. doi: 10.1016/j.solmat.2009.02.021.

[137] Lu S, Shen T, Xing J, Song Q, Shao J, Zhang J, et al. Preparation and characterization of cross-linked polyurethane shell microencapsulated phase change materials by interfacial polymerization. Mater Lett. 2018;211:36–9. doi: 10.1016/j.matlet.2017.09.074.

[138] Li C, Yu H, Song Y, Liang H, Yan X. Preparation and characterization of PMMA/TiO2 hybrid shell microencapsulated PCMs for thermal energy storage. Energy. 2019;167:1031–9. doi: 10.1016/j.energy.2018.11.038.

[139] Onder E, Sarier N, Cimen E. Encapsulation of phase change materials by complex coacervation to improve thermal performances of woven fabrics. Thermochim Acta. 2007;467:63–72. doi: 10.1016/j.tca.2007.11.007.

[140] Shaddel R, Hesari J, Azadmard-Damirchi S, Hamishehkar H, Fathi-Achachlouei B, Huang Q. Use of gelatin and gum Arabic for encapsulation of black raspberry anthocyanins by complex coacervation. Int J Biol Macromol. 2018;107:1800–10. doi: 10.1016/j.ijbiomac.2017.10.044.

[141] Pascu O, Garcia-Valls R, Giamberini M. Interfacial polymerization of an epoxy resin and carboxylic acids for the synthesis of microcapsules. Polym Int. 2008;57:995–1006. doi: 10.1002/pi.2438.

[142] Hia IL, Lam WH, Chai SP, Chan ES, Pasbakhsh P. Surface modified alginate multicore microcapsules and their application in self-healing epoxy coatings for metallic protection. Mater Chem Phys. 2018;215:69–80. doi: 10.1016/j.matchemphys.2018.05.021.

[143] Shah AH, Zhang Y, Xu X, Dayo AQ, Li X, Wang S, et al. Reinforcement of stearic acid treated egg shell particles in epoxy thermosets: Structural, thermal, and mechanical characterization. Materials. 2018;11:1872. doi: 10.3390/ma11101872.

[144] Sari A, Alkan C, Karaipekli A, Uzun O. Microencapsulated n-octacosane as phase change material for thermal energy storage. Sol Energy. 2009;83:1757–63. doi: 10.1016/j.solener.2009.05.008.

[145] Alkan C, Sari A, Karaipekli A, Uzun O. Preparation, characterization, and thermal properties of microencapsulated phase change material for thermal energy storage. Solar Energy Materials and Solar Cells. 2009;93:143–7. doi: 10.1016/j.solmat.2008.09.009.

[146] Lee HY, Lee SJ, Cheong IW, Kim JH. Microencapsulation of fragrant oil via in situ polymerization: Effects of pH and melamine-formaldehyde molar ratio. J Microencapsul. 2002;19:559–69. doi: 10.1080/02652040210140472.

[147] Yanshan L, Shujun W, Hongyan L, Fanbin M, Huanqing M, Wangang Z. Preparation and characterization of melamine/formaldehyde/polyethylene glycol crosslinking copolymers as solid–solid phase change materials. Solar Energy Materials and Solar Cells. 2014;127:92–7. doi: 10.1016/j.solmat.2014.04.013.

[148] Iqbal N, Tripathi M, Parthasarathy S, Kumar D, Roy PK. Polyurea spray coatings: Tailoring material properties through chemical crosslinking. Prog Org Coat. 2018;123:201–8. doi: 10.1016/j.porgcoat.2018.07.005.

[149] Giraud S, Bourbigot S, Rochery M, Vroman I, Tighzert L, Delobel R, et al. Flame retarded polyurea with microencapsulated ammonium phosphate for textile coating. Polym Degrad Stab. 2005;88:106–13. doi: 10.1016/j.polymdegradstab.2004.01.028.

[150] Konuklu Y, Paksoy H. Polystyrene-based caprylic acid microencapsulation for thermal energy storage. Solar Energy Materials and Solar Cells. 2017;159:235–42. doi: 10.1016/j.solmat.2016.09.016.

[151] Sari A, Alkan C, Altintaş A. Preparation, characterization and latent heat thermal energy storage properties of micro-nanoencapsulated fatty acids by polystyrene shell. Appl Therm Eng. 2014;73:1160–8. doi: 10.1016/j.applthermaleng.2014.09.005.

[152] Umair MM, Zhang Y, Iqbal K, Zhang S, Tang B. Novel strategies and supporting materials applied to shape-stabilize organic phase change materials for thermal energy storage–A review. Appl Energy. 2019;235:846–73. doi: 10.1016/j.apenergy.2018.11.017.

[153] Hernández-Nava R, López-Malo A, Palou E, Ramírez-Corona N, Jiménez-Munguía MT. Encapsulation of oregano essential oil (Origanum vulgare) by complex coacervation between gelatin and chia mucilage and its properties after spray drying. Food Hydrocoll. 2020;109:106077. doi: 10.1016/j.foodhyd.2020.106077.

[154] Tian Q, Zhou W, Cai Q, Ma G, Lian G. Concepts, processing, and recent developments in encapsulating essential oils. Chin J Chem Eng. 2021;30:255–71. doi: 10.1016/j.cjche.2020.12.010.

[155] Hong W, Wang R, Li N, Gao L, Jiao T. Facile preparation and excellent ultraviolet shielding application of polyurethane-TiO2 composite microcapsules. Part Part Syst Charact. 2021;38(1):2000265. doi: 10.1002/ppsc.202000265.

[156] Cheng P, Wei K, Shi W, Shi J, Wang S, Ma B. Preparation and performance analysis of phase change microcapsule/epoxy resin composite phase change material. J Energy Storage. 2022;47:103581. doi: 10.1016/j.est.2021.103581.

[157] Wang X, Ma B, Wei K, Zhang W. Thermal stability and mechanical properties of epoxy resin/microcapsule composite phase change materials. Constr Build Mater. 2021;312:125392. doi: 10.1016/j.conbuildmat.2021.125392.

[158] Kim EY, Kim Hdo. Preparation and properties of microencapsulated octadecane with waterborne polyurethane. J Appl Polym Sci. 2005;96:1596–604. doi: 10.1002/app.21603.

[159] Qin L, Lin L, Fu F, Fan M. Micrographia microstructure and quantitative micromechanical analysis of wood cell – emulsion polymer isocyanate and urea – formaldehyde interphases. Microsc Microanal. 2017;23(3):687–95. doi: 10.1017/S1431927617000216.

[160] Wang X, Li C, Zhao T. Fabrication and characterization of poly(melamine-formaldehyde)/silicon carbide hybrid microencapsulated phase change materials with enhanced thermal conductivity and light-heat performance. Sol Energy Mater Sol Cells. 2018;183:82–91. doi: 10.1016/j.solmat.2018.03.019.

[161] Borreguero AM, Serrano A, Garrido I, Rodríguez JF, Carmona M. Polymeric-SiO2-PCMs for improving the thermal properties of gypsum applied in energy efficient buildings. Energy Convers Manag. 2014;87:138–44. doi: 10.1016/j.enconman.2014.07.027.

[162] Cao L, Tang F, Fang G. Synthesis and characterization of microencapsulated paraffin with titanium dioxide shell as shape-stabilized thermal energy storage materials in buildings. Energy Build. 2014;72:31–7. doi: 10.1016/j.enbuild.2013.12.028.

[163] Park S-J, Shin Y-S, Lee J-R. Preparation and characterization of microcapsules containing lemon oil. J Colloid Interface Sci. 2001;6:1243–51. doi: 10.1007/s12155-013-9327-2.

[164] Zhang XX, Tao XM, Yick KL, Fan YF. Expansion space and thermal stability of microencapsulated n-octadecane. J Appl Polym Sci. 2005;97:390–6. doi: 10.1002/app.21760.

[165] Su J, Ren L, Wang L. Preparation and mechanical properties of thermal energy storage microcapsules. Colloid Polym Sci. 2005;284:224–8. doi: 10.1007/s00396-005-1368-4.

[166] Su W, Darkwa J, Kokogiannakis G, Zhou T, Li Y. Preparation of microencapsulated phase change materials (MEPCM) for thermal energy storage. Energy Procedia. 2017;121:95–101. doi: 10.1016/j.egypro.2017.07.485.

[167] Fang G, Li H, Yang F, Liu X, Wu S. Preparation and characterization of nano-encapsulated n-tetradecane as phase change material for thermal energy storage. Chem Eng J. 2009;153:217–21. doi: 10.1016/j.cej.2009.06.019.

[168] Sari A, Alkan C, Karaipekli A. Preparation, characterization and thermal properties of PMMA/n-heptadecane microcapsules as novel solid–liquid microPCM for thermal energy storage. Appl Energy. 2010;87:1529–34. doi: 10.1016/j.apenergy.2009.10.011.

[169] Alkan C, Sari A, Karaipekli A. Preparation, thermal properties and thermal reliability of microencapsulated n-eicosane as novel phase change material for thermal energy storage. Energy Convers Manag. 2011;52:687–92. doi: 10.1016/j.enconman.2010.07.047.

[170] Qiu X, Lu L, Wang J, Tang G, Song G. Fabrication, thermal properties and thermal stabilities of microencapsulated n-alkane with poly(lauryl methacrylate) as shell. Thermochim Acta. 2015;620:10–7. doi: 10.1016/j.tca.2015.10.001v.

[171] Cho W, Kook JW, Lee SM, Koh WG, Kim JH. Modification of heat storage ability and adhesive properties of core/shell structured phase change material nanocapsules. Macromol Res. 2016;24:556–61. doi: 10.1007/s13233-016-4075-8.

[172] Fortuniak W, Slomkowski S, Chojnowski J, Kurjata J, Tracz A, Mizerska U. Synthesis of a paraffin phase change material microencapsulated in a siloxane polymer. Colloid Polym Sci. 2013;291:725–33. doi: 10.1007/s00396-012-2782-z.

[173] Deveci SS, Basal G. Preparation of PCM microcapsules by complex coacervation of silk fibroin and chitosan. Colloid Polym Sci. 2009;287:1455–67. doi: 10.1007/s00396-009-2115-z.

[174] Konuklu Y, Unal M, Paksoy HO. Microencapsulation of caprylic acid with different wall materials as phase change material for thermal energy storage. Sol Energy Mater Sol Cells. 2014;120:536–42. doi: 10.1016/j.solmat.2013.09.035.

[175] Lai WC, Cai YT, Cai YL. Novel green and sustainable shape-stabilized phase change materials for thermal energy storage. J Taiwan Inst Chem Eng. 2020;117:257–64. doi: 10.1016/j.jtice.2020.12.013.

[176] Nor Azlan AYH, Katas H, Mh Busra MF, Salleh NAM, Smandri A. Metal nanoparticles and biomaterials: The multipronged approach for potential diabetic wound therapy. Nanotechnol Rev. 2021;10:653–70. doi: 10.1515/ntrev-2021-0046.

[177] Ranu BC, Adak L, Ghosh T. Learning Green Chemistry and its principles from Nature's process and development of green procedures mimicking nature. Chem Teacher Int. 2021;12. doi: 10.1515/cti-2021-0023.

[178] Wijesena RN, Tissera ND, Rathnayaka VWSG, Rajapakse HD, de Silva RM, de Silva KMN. Shape-stabilization of polyethylene glycol phase change materials with chitin nanofibers for applications in "smart" windows. Carbohydr Polym. 2020;237:116132. doi: 10.1016/j.carbpol.2020.116132.

[179] Chen C, Liu W, Yang H, Zhao Y, Liu S. Synthesis of solid–solid phase change material for thermal energy storage by crosslinking of polyethylene glycol with poly (glycidyl methacrylate). Sol Energy. 2011;85:2679–85. doi: 10.1016/j.solener.2011.08.002.

[180] Fallahi A, Guldentops G, Tao M, Granados-Focil S, van Dessel S. Review on solid–solid phase change materials for thermal energy storage: Molecular structure and thermal properties. Appl Therm Eng. 2017;127:1427–41. doi: 10.1016/j.applthermaleng.2017.08.161.

[181] Li WD, Ding EY. Preparation and characterization of cross-linking PEG/MDI/PE copolymer as solid–solid phase change heat storage material. Sol Energy Mater Sol Cells. 2007;91:764–8. doi: 10.1016/j.solmat.2007.01.011.

[182] Ernest Ravindran RS, Subha V, Ilangovan R. Silver nanoparticles blended PEG/PVA nanocomposites synthesis and characterization for food packaging. Arabian J Chem. 2020;13:6056–60. doi: 10.1016/j.arabjc.2020.05.005.

[183] Sundararajan S, Samui AB, Kulkarni PS. Shape-stabilized poly (ethylene glycol) (PEG)-cellulose acetate blend preparation with superior PEG loading via microwave-assisted blending. Sol Energy. 2017;144:32–9. doi: 10.1016/j.solener.2016.12.056.

[184] Sundararajan S, Samui AB, Kulkarni PS. Synthesis and characterization of poly(ethylene glycol) (PEG) based hyperbranched polyurethanes as thermal energy storage materials. Thermochim Acta. 2017;650:114–22. doi: 10.1016/j.tca.2017.02.011.

[185] Karaman S, Karaipekli A, Sar A, Biçer A. Polyethylene glycol (PEG)/diatomite composite as a novel form-stable phase change material for thermal energy storage. Solar Energy Mat Solar Cells. 2011;95:1647–53. doi: 10.1016/j.solmat.2011.01.022.

[186] Meints T, Hansmann C, Gindl-Altmutter W. Suitability of different variants of polyethylene glycol impregnation for the dimensional stabilization of oak wood. Polymers (Basel). 2018;10(1):81. doi: 10. 10.3390/polym10010081.

[187] Strassburg S, Mayer K, Scheibel T. Functionalization of biopolymer fibers with magnetic nanoparticles. Phy Sci Rev. 2020;167–94. doi: 10.1515/psr-2019-0118.

[188] Seifert J, Koch K, Hess M, Schmidt AM. Magneto-mechanical coupling of single domain particles in soft matter systems. Phy Sci Rev. 2020;11:1237–61. doi: 10.1515/psr-2019-0092.

[189] Li Y, Li J, Deng Y, Guan W, Wang X, Qian T. Preparation of paraffin/porous TiO2 foams with enhanced thermal conductivity as PCM, by covering the TiO2 surface with a carbon layer. Appl Energy. 2016;171:37–45. doi: 10.1016/j.apenergy.2016.03.010.

[190] Liu Z, Zang C, Ju Z, Hu D, Zhang Y, Jiang J, et al. Consistent preparation, chemical stability and thermal properties of a shape-stabilized porous carbon/paraffin phase change materials. J Clean Prod. 2020;247. doi: 10.1016/j.jclepro.2019.119565

[191] Zhang C, Hu X, Xiao S, Luo W, Wang H, Jiang X. Enhanced thermal performance of phase-change material supported by nano-Ag coated eggplant-based biological porous carbon. J Energy Storage. 2021;43:103174. doi: 10.1016/j.est.2021.103174.

[192] Atinafu DG, Dong W, Huang X, Gao H, Wang G. Introduction of organic-organic eutectic PCM in mesoporous N-doped carbons for enhanced thermal conductivity and energy storage capacity. Appl Energy. 2018;211:1203–15. doi: 10.1016/j.apenergy.2017.12.025.

[193] Li J, Hu X, Zhang C, Luo W, Jiang X. Enhanced thermal performance of phase-change materials supported by mesoporous silica modified with polydopamine/nano-metal particles for

thermal energy storage. Renew Energy. 2021;178:118–27. doi: 10.1016/j.renene.2021.06.021.

[194] Liu P, Gao H, Chen X, Chen D, Lv J, Han M, et al. In situ one-step construction of monolithic silica aerogel-based composite phase change materials for thermal protection. Compos B Eng. 2020;195:108072. doi: 10.1016/j.compositesb.2020.108072.

[195] Li S, Kong L, Wang H, Xu H, Li J, Shi H. Thermal performance and shape-stabilization of comb-like polymeric phase change materials enhanced by octadecylamine-functionalized graphene oxide. Energy Convers Manag. 2018;168:119–27. doi: 10.1016/j.enconman.2018.05.014.

[196] Wen R, Jia P, Huang Z, Fang M, Liu Y, Wu X, et al. Thermal energy storage properties and thermal reliability of PEG/bone char composite as a form-stable phase change material. J Therm Anal Calorim. 2018;132:1753–61. doi: 10.1007/s10973-017-6934-8.

[197] Li Y, Wu M, Liu R, Huang Y. Cellulose-based solid–solid phase change materials synthesized in ionic liquid. Solar Energy Materials and Solar Cells. 2009;93:1321–8. doi: 10.1016/J.SOLMAT.2009.02.005.

[198] Qian T, Li J, Min X, Deng Y, Guan W, Ma H. Polyethylene glycol/mesoporous calcium silicate shape-stabilized composite phase change material: Preparation, characterization, and adjustable thermal property. Energy. 2015;82:333–40. doi: 10.1016/j.energy.2015.01.043.

[199] Jiang Y, Ding E, Li G. Study on transition characteristics of PEG/CDA solid–solid phase change materials. Polymer (Guildf). 2001;43:117–22. doi: 10.1016/S0032-3861(01)00613-9.

[200] Barreneche C, Vecstaudza J, Bajare D, Fernandez AI. PCM/wood composite to store thermal energy in passive building envelopes. IOP Conf Ser Mater Sci Eng. 2017;251:012111. doi: 10.1088/1757-899X/251/1/012111.

[201] Ding WD, Koubaa A, Chaala A, Belem T, Krause C. Relationship between wood porosity, wood density and methyl methacrylate impregnation rate. Wood Mater Sci Eng. 2008;3:62–70. doi: 10.1080/17480270802607947.

[202] Mathis D, Blanchet P, Landry V, Lagière P. Impregnation of wood with microencapsulated bio-based phase change materials for high thermal mass engineered wood flooring. Applied Sciences (Switzerland). 2018;8:2696. doi: 10.3390/app8122696.

[203] Nomura T, Okinaka N, Akiyama T. Impregnation of porous material with phase change material for thermal energy storage. Mater Chem Phys. 2009;115:846–50. doi: 10.1016/j.matchemphys.2009.02.045.

[204] Lee SY, Shin HK, Park M, Rhee KY, Park SJ. Thermal characterization of erythritol/expanded graphite composites for high thermal storage capacity. Carbon N Y. 2014;68:67–72. doi: 10.1016/j.carbon.2013.09.053.

[205] Jeong SG, Jeon J, Lee JH, Kim S. Optimal preparation of PCM/diatomite composites for enhancing thermal properties. Int J Heat Mass Transf. 2013;62:711–7. doi: 10.1016/j.ijheatmasstransfer.2013.03.043.

[206] Li X, Sanjayan JG, Wilson JL. Fabrication and stability of form-stable diatomite/paraffin phase change material composites. Energy Build. 2014;76:284–94. doi: 10.1016/j.enbuild.2014.02.082.

[207] Karaman S, Karaipekli A, Sar A, Biçer A. Polyethylene glycol (PEG)/diatomite composite as a novel form-stable phase change material for thermal energy storage. Solar Energy Materials and Solar Cells. 2011;95:1647–53. doi: 10.1016/j.solmat.2011.01.022.

[208] Sari A, Karaipekli A. Thermal conductivity and latent heat thermal energy storage characteristics of paraffin/expanded graphite composite as phase change material. Appl Therm Eng. 2007;27:1271–7. doi: 10.1016/j.applthermaleng.2006.11.004.

[209] Mehrali M, Latibari ST, Mehrali M, Metselaar HSC, Silakhori M. Shape-stabilized phase change materials with high thermal conductivity based on paraffin/graphene oxide composite. Energy Convers Manag. 2013;67:275–82. doi: 10.1016/j.enconman.2012.11.023.

[210] Sari A. Composites of polyethylene glycol (PEG600) with gypsum and natural clay as new kinds of building PCMs for low temperature-thermal energy storage. Energy Build. 2014;69:184–92. doi: 10.1016/j.enbuild.2013.10.034.

[211] Zhang Y, Zheng S, Zhu S, Ma J, Sun Z, Farid M. Evaluation of paraffin infiltrated in various porous silica matrices as shape-stabilized phase change materials for thermal energy storage. Energy Convers Manag. 2018;171:361–70. doi: 10.1016/j.enconman.2018.06.002.

[212] Kim YU, Park JH, Yun BY, Yang S, Wi S, Kim S. Mechanical and thermal properties of artificial stone finishing materials mixed with PCM impregnated lightweight aggregate and carbon material. Constr Build Mater. 2021;272:121882. doi: 10.1016/j.conbuildmat.2020.121882.

[213] Yang Y, Pang Y, Liu Y, Guo H. Preparation and thermal properties of polyethylene glycol/expanded graphite as novel form-stable phase change material for indoor energy saving. Mater Lett. 2018;216:220–3. doi: 10.1016/j.matlet.2018.01.025.

[214] Cheng P, Gao H, Chen X, Chen Y, Han M, Xing L, et al. Flexible monolithic phase change material based on carbon nanotubes/chitosan/poly(vinyl alcohol). Chem Eng J. 2020;397:125330. doi: 10.1016/j.cej.2020.125330.

[215] Liu X, Yang F, Li M, Sun C, Wu Y. Development of cost-effective PCM-carbon foam composites for thermal energy storage. Energy Rep. 2022;8:1696–703. doi: 10.1016/j.egyr.2021.12.065.

[216] Cabane E, Keplinger T, Merk V, Hass P, Burgert I. Renewable and functional wood materials by grafting polymerization within cell walls. ChemSusChem. 2014;7:1020–5. doi: 10.1002/cssc.201301107.

[217] Capanema NSV, Mansur AAP, de Jesus AC, Carvalho SM, de Oliveira LC, Mansur HS. Superabsorbent crosslinked carboxymethyl cellulose-PEG hydrogels for potential wound dressing applications. Int J Biol Macromol. 2018;106:1218–34. doi: 10.1016/j.ijbiomac.2017.08.124.

[218] Shi W, Xing J, Liu J, Lu S. Wet-driven shape-memory behaviors and thermal adaptability of cotton knitted fabrics containing crosslinked poly(ethylene glycol) moieties. J Appl Polym Sci. 2016;133:1–12. doi: 10.1002/app.43473

[219] Chen C, Wang L, Huang Y. Crosslinking of the electrospun polyethylene glycol/cellulose acetate composite fibers as shape-stabilized phase change materials. Mater Lett. 2009;63:569–71. doi: 10.1016/j.matlet.2008.11.033.

[220] Xi P, Gu X, Cheng B, Wang Y. Preparation and characterization of a novel polymeric based solid–solid phase change heat storage material. Energy Convers Manag. 2009;50:1522–8. doi: 10.1016/j.enconman.2009.02.013.

[221] Sarı A, Biçer A, Alkan C. Thermal energy storage characteristics of poly(styrene-co-maleic anhydride)-graft-PEG as polymeric solid–solid phase change materials. Solar Energy Materials and Solar Cells. 2017;161:219–25. doi: 10.1016/j.solmat.2016.12.001.

[222] Zhou L, Tang LS, Tao XF, Yang J, Yang MB, Yang W. Facile fabrication of shape-stabilized polyethylene glycol/cellulose nanocrystal phase change materials based on thiol-ene click chemistry and solvent exchange. Chem Eng J. 2020;396:125206. doi: 10.1016/j.cej.2020.125206.

[223] Zhou L, Shi F, Liu G, Ye JP, Han PS, Zhang G. Fabrication and characterization of in situ cross-linked electrospun Poly(vinyl alcohol)/phase change material nanofibers. Sol Energy. 2021;213:339–49. doi: 10.1016/j.solener.2020.11.039.

[224] Yin GZ, Díaz Palencia JL, Wang DY. Fully bio-based Poly (Glycerol-Itaconic acid) as supporter for PEG based form stable phase change materials. Comp Com. 2021;27:100893. doi: 10.1016/j.coco.2021.100893.

[225] Kuru A, Aksoy SA. Cellulose–PEG grafts from cotton waste in thermo-regulating textiles. Text Res J. 2014;84:337–46. doi: 10.1177/0040517513494251.

[226] Qin Y, Chen K, Zhang H, Luo X, Liang S, Tian C, et al. Structure-property correlation of poly(ethylene glycol) based form stable phase change materials with different crosslinking structure. Solar Energy Materials and Solar Cells. 2019;203:110192. doi: 10.1016/j.solmat.2019.110192.

[227] Abhat A. Low temperature latent heat thermal energy storage: heat storage materials. Sol Energy. 1983;30(4):313–32.

[228] Zhang H, Xing F, Cui HZ, Chen DZ, Ouyang X, Xu SZ, et al. A novel phase-change cement composite for thermal energy storage: Fabrication, thermal and mechanical properties. Appl Energy. 2016;170:130–9. doi: 10.1016/j.apenergy.2016.02.091.

[229] Serrano A, Borreguero AM, Garrido I, Rodríguez JF, Carmona M. Reducing heat loss through the building envelope by using polyurethane foams containing thermoregulating microcapsules. Appl Therm Eng. 2016;103:226–32. doi: 10.1016/j.applthermaleng.2016.04.098.

[230] Lai CM, Hokoi S. Thermal performance of an aluminum honeycomb wallboard incorporating microencapsulated PCM. Energy Build. 2014;73:37–47. doi: 10.1016/j.enbuild.2014.01.017.

[231] Liu F, Wang J, Qian X. Integrating phase change materials into concrete through microencapsulation using cenospheres. Cem Concr Compos. 2017;80:317–25. doi: 10.1016/j.cemconcomp.2017.04.001.

[232] Liu H, Wang X, Wu D, Ji S. Fabrication and applications of dual-responsive microencapsulated phase change material with enhanced solar energy-storage and solar photocatalytic effectiveness. Solar Ene Mater Solar Cells. 2019;193:184–97. doi: 10.1016/j.solmat.2019.01.012.

[233] Yu S, Wang X, Wu D. Microencapsulation of n-octadecane phase change material with calcium carbonate shell for enhancement of thermal conductivity and serving durability: Synthesis, microstructure, and performance evaluation. Appl Energy. 2014;114:632–43. doi: 10.1016/j.apenergy.2013.10.029.

[234] Kusama Y, Ishidoya Y. Thermal effects of a novel phase change material (PCM) plaster under different insulation and heating scenarios. Energy Build. 2017;141:226–37. doi: 10.1016/j.enbuild.2017.02.033.

[235] Lecompte T, le Bideau P, Glouannec P, Nortershauser D, le Masson S. Mechanical and thermo-physical behaviour of concretes and mortars containing phase change material. Energy Build. 2015;94:52–60. doi: 10.1016/j.enbuild.2015.02.044.

[236] Sarı A, Bicer A, Karaipekli A, Al-Sulaiman FA. Preparation, characterization and thermal regulation performance of cement

based-composite phase change material. Solar Energy Materials and Solar Cells. 2018;174:523–9. doi: 10.1016/j.solmat.2017.09.049.

[237] Cui H, Feng T, Yang H, Bao X, Tang W, Fu J. Experimental study of carbon fiber reinforced alkali-activated slag composites with micro-encapsulated PCM for energy storage. Constr Build Mater. 2018;161:442–51. doi: 10.1016/j.conbuildmat.2017.11.075.

[238] Arce P, Castellón C, Castell A, Cabeza LF. Use of microencapsulated PCM in buildings and the effect of adding awnings. Energy Build. 2012;44:88–93. doi: 10.1016/j.enbuild.2011.10.028.

[239] Mankel C, Caggiano A, Ukrainczyk N, Koenders E. Thermal energy storage characterization of cement-based systems containing microencapsulated-PCMs. Constr Build Mater. 2019;199:307–20. doi: 10.1016/j.conbuildmat.2018.11.195.

[240] Haurie L, Serrano S, Bosch M, Fernandez AI, Cabeza LF. Single layer mortars with microencapsulated PCM: Study of physical and thermal properties, and fire behaviour. Energy Build. 2016;111:393–400. doi: 10.1016/j.enbuild.2015.11.028.

[241] Jaworski M. Thermal performance of building element containing phase change material (PCM) integrated with ventilation system - An experimental study. Appl Therm Eng. 2014;70:665–74. doi: 10.1016/j.applthermaleng.2014.05.093.

[242] Guo X, Cao J, Peng Y, Liu R. Incorporation of microencapsulated dodecanol into wood flour/high-density polyethylene composite as a phase change material for thermal energy storage. Mater Des. 2016;89:1325–34. doi: 10.1016/j.matdes.2015.10.068.

[243] Jamil H, Alam M, Sanjayan J, Wilson J. Investigation of PCM as retrofitting option to enhance occupant thermal comfort in a modern residential building. Energy Build. 2016;133:217–29. doi: 10.1016/j.enbuild.2016.09.064.

[244] Wang C, Huang X, Deng S, Long E, Niu J. An experimental study on applying PCMs to disaster-relief prefabricated temporary houses for improving internal thermal environment in summer. Energy Build. 2018;179:301. doi: 10. 10.1016/j.enbuild.2018.09.028

[245] Kuznik F, Virgone J. Experimental assessment of a phase change material for wall building use. Appl Energy. 2009;86:2038–46. doi: 10.1016/j.apenergy.2009.01.004.

[246] Kim HB, Mae M, Choi Y, Kiyota T. Experimental analysis of thermal performance in buildings with shape-stabilized phase change materials. Energy Build. 2017;152:524–33. doi: 10.1016/j.enbuild.2017.07.076.

[247] Memon SA, Lo TY, Cui H, Barbhuiya S. Preparation, characterization and thermal properties of dodecanol/cement as novel form-stable composite phase change material. Energy Build. 2013;66:697–705. doi: 10.1016/j.enbuild.2013.07.083.

[248] Li M, Wu Z, Tan J. Heat storage properties of the cement mortar incorporated with composite phase change material. Appl Energy. 2013;103:393–9. doi: 10.1016/j.apenergy.2012.09.057.

[249] Zhao CY, Zhang GH. Review on microencapsulated phase change materials (MEPCMs): Fabrication, characterization and applications. Renewable Sustainable Energy Rev. 2011;15:3813–32. doi: 10.1016/j.rser.2011.07.019.

[250] Schossig P, Henning HM, Gschwander S, Haussmann T. Microencapsulated phase-change materials integrated into construction materials. Sol Energy Mater Sol Cells. 2005;89:297–306. doi: 10.1016/j.solmat.2005.01.017.

[251] Cabeza LF, Castellón C, Nogués M, Medrano M, Leppers R, Zubillaga O. Use of microencapsulated PCM in concrete walls for energy savings. Energy Build. 2007;39:113–9. doi: 10.1016/j.enbuild.2006.03.030.

[252] Lee SH, Yoon SJ, Kim YG, Choi YC, Kim JH, Lee JG. Development of building materials by using micro-encapsulated phase change material. Kor J Chem Eng. 2007;24:332–5.

[253] Zhang YP, Lin KP, Yang R, Di HF, Jiang Y. Preparation, thermal performance and application of shape-stabilized PCM in energy efficient buildings. Energy Build. 2006;38:1262–9. doi: 10.1016/j.enbuild.2006.02.009.

[254] Oliver A. Thermal characterization of gypsum boards with PCM included: Thermal energy storage in buildings through latent heat. Energy Build. 2012;48:1–7. doi: 10.1016/j.enbuild.2012.01.026.

[255] Barzin R, Chen JJJ, Young BR, Farid MM. Application of PCM energy storage in combination with night ventilation for space cooling. Appl Energy. 2015;158:412–21. doi: 10.1016/j.apenergy.2015.08.088.

[256] Borreguero AM, Carmona M, Sanchez ML, Valverde JL, Rodriguez JF. Improvement of the thermal behaviour of gypsum blocks by the incorporation of microcapsules containing PCMS obtained by suspension polymerization with an optimal core/coating mass ratio. Appl Therm Eng. 2010;30:1164–9. doi: 10.1016/j.applthermaleng.2010.01.032.

[257] Borreguero AM, Garrido I, Valverde JL, Rodríguez JF, Carmona M. Development of smart gypsum composites by incorporating thermoregulating microcapsules. Energy Build. 2014;76:631–9. doi: 10.1016/j.enbuild.2014.03.005.

[258] Entrop AG, Brouwers HJH, Reinders AHME. Experimental research on the use of micro-encapsulated phase change materials to store solar energy in concrete floors and to save energy in Dutch houses. Sol Energy. 2011;85:1007–20. doi: 10.1016/j.solener.2011.02.017.

[259] Jayalath A, San Nicolas R, Sofi M, Shanks R, Ngo T, Aye L, et al. Properties of cementitious mortar and concrete containing micro-encapsulated phase change materials. Constr Build Mater. 2016;120:408–17. doi: 10.1016/j.conbuildmat.2016.05.116.

[260] Dong Z, Cui H, Tang W, Chen D, Wen H. Development of hollow steel ball macro-encapsulated PCM for thermal energy storage concrete. Materials. 2016;9(1):59. doi: 10.3390/ma9010059.

[261] Cui H, Tang W, Qin Q, Xing F, Liao W, Wen H. Development of structural-functional integrated energy storage concrete with innovative macro-encapsulated PCM by hollow steel ball. Appl Energy. 2017;185:107–18. doi: 10.1016/j.apenergy.2016.10.072.

[262] Shi X, Park P, Rew Y, Huang K, Sim C. Constitutive behaviors of steel fiber reinforced concrete under uniaxial compression and tension. Constr Build Mater. 2020;233:117316. doi: 10.1016/j.conbuildmat.2019.117316.

[263] Cui H, Zou J, Gong Z, Zheng D, Bao X, Chen X. Study on the thermal and mechanical properties of steel fibre reinforced PCM-HSB concrete for high performance in energy piles. Constr Build Mater. 2022;350:128822. doi: 10.1016/j.conbuildmat.2022.128822.